

1-1-1977

## Polyoxymethylene ionomers and other trioxane polymers.

Lawrence P. Demejo  
*University of Massachusetts Amherst*

Follow this and additional works at: [https://scholarworks.umass.edu/dissertations\\_1](https://scholarworks.umass.edu/dissertations_1)

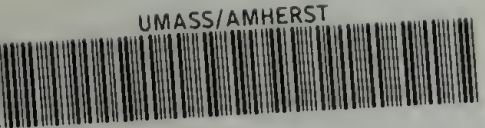
---

### Recommended Citation

Demejo, Lawrence P., "Polyoxymethylene ionomers and other trioxane polymers." (1977). *Doctoral Dissertations 1896 - February 2014*. 624.  
<https://doi.org/10.7275/r2ta-nt30> [https://scholarworks.umass.edu/dissertations\\_1/624](https://scholarworks.umass.edu/dissertations_1/624)

This Open Access Dissertation is brought to you for free and open access by ScholarWorks@UMass Amherst. It has been accepted for inclusion in Doctoral Dissertations 1896 - February 2014 by an authorized administrator of ScholarWorks@UMass Amherst. For more information, please contact [scholarworks@library.umass.edu](mailto:scholarworks@library.umass.edu).

UMASS/AMHERST



312066 0015 4660 6



POLYOXYMETHYLENE IONOMERS AND OTHER TRIOXANE POLYMERS

A Dissertation Presented

By

Lawrence Paul DeMejo

Submitted to the Graduate School of the  
University of Massachusetts in  
partial fulfillment of the requirements for the degree of

DOCTOR OF PHILOSOPHY

April

1977

Polymer Science and Engineering

3J✓

©

Lawrence Paul DeMejo

1977

All Rights Reserved

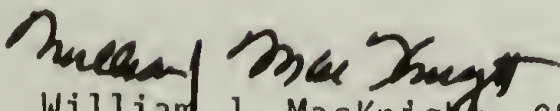
POLYOXYMETHYLENE IONOMERS AND OTHER TRIOXANE POLYMERS

A Dissertation

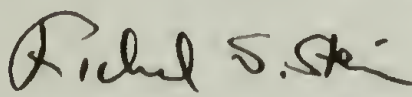
By

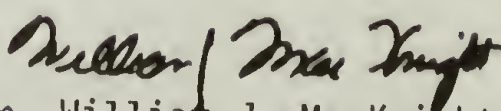
Lawrence Paul DeMejo

Approved as to style and content by:

  
Dr. William J. MacKnight, Chairman of Committee

  
Dr. Otto Vogl, Member

  
Dr. Richard S. Stein, Member

  
Dr. William J. MacKnight

Department Head

Polymer Science and Engineering

April 1977

## ACKNOWLEDGEMENTS

I would like to express my appreciation to my advisors, Dr. MacKnight and Dr. Vogl, for their enthusiastic support and invaluable technical advice throughout my graduate career at the University of Massachusetts. A special thanks, also, to my other committee member, Dr. Stein, for his helpful comments during the writeup of this dissertation.

I am deeply grateful to the other members of Dr. Vogl's research group and to the entire Department of Polymer Science and Engineering at the University of Massachusetts for contributing to a very valuable learning experience.

Finally, I would like to dedicate this work to my wife, Marguerite, who typed two drafts of this dissertation, including the final draft. It was her constant encouragement and understanding which kept me going despite the occasional frustrations associated with my graduate research.

Trust in the Lord with all your heart,  
and do not rely on your own insight.  
In all your ways acknowledge Him,  
and He will make straight your paths.

Proverbs 3.5

## ABSTRACT

## POLYOXYMETHYLENE IONOMERS AND OTHER TRIOXANE POLYMERS

Lawrence Paul DeMejo, B.S., Rochester Institute of Technology

M.S., Univ. of Massachusetts, Ph.D., Univ. of Massachusetts (May 1977)

Directed by : Professor William MacKnight and Professor Otto Vogl

Oxymethylene polymers were synthesized by various methods (gas phase, bulk and solution polymerization); the ionic and nonionic polymers were characterized by calorimetric, dynamic mechanical and dielectric techniques. Copolymers and terpolymers of trioxane with dioxolane and/or ethyl glycidate were prepared by cationic ring opening polymerization using either boron trifluoride or trifluoromethane sulfonic acid as the initiator. The polymers with ethyl glycidate were converted to the corresponding salts of monovalent cations and their free acid analogs. The calorimetric studies furnished evidence for the incorporation of oxyethylene units into the crystalline regions of the trioxane-dioxolane copolymers and for the presence of ionic clusters in the ionomers containing sodium thioglycolate side chains. Dynamic mechanical and dielectric relaxation spectra of the ionic and nonionic systems exhibited the three characteristic polyoxymethylene relaxations, labeled  $\alpha$ ,  $\beta$  and  $\gamma$  in order of decreasing temperature. Two additional peaks,  $\alpha'$  and  $\beta'$ , were ascribed, respectively, to motions within microphase segregated ionic clusters in the sodium thioglycolate copolymers and to motions of carbonyl ester side chains in the trioxane-ethyl glycidate-dioxolane terpolymers. The prominent  $\beta$  peak, mechanically active but dielectrically inactive in the trioxane-dioxolane copolymers, was assigned to flip-flop motions of rotational isomers containing the oxyethylene unit.



## T A B L E O F C O N T E N T S

ACKNOWLEDGEMENTS	iv
ABSTRACT	vi
LIST OF FIGURES	xi
LIST OF EQUATIONS	xiii
I. INTRODUCTION	
A. Oxymethylene Polymers	
1. General Background	1
2. Polymerization of Formaldehyde	
a. Anionic Polymerization	1
b. Cationic Polymerization	6
c. Gas Phase Polymerization	9
d. Polymerization in Hydroxylic Media	10
e. Copolymers Derived from Formaldehyde	11
3. Cationic Polymerization of Trioxane	12
4. Characterization of Oxymethylene Copolymers	
a. Physical and Chemical Properties	17
b. Analytical Methods	19
c. Crystalline and Amorphous Transitions	21
B. Organic Polymers Containing Polar Side Groups	
1. Ionomer as a Generic Term	26
2. Ionomers Based on Poly- $\alpha$ -Olefins	27
3. Ethylene-Phosphonic Acid Copolymers	29

4. Ionomers Based on Polypentenamers	30
5. Ionomers Based on Polyoxymethylene	31
II. EXPERIMENTAL PART	
A. Materials	
1. Monomers	33
2. Initiators	33
3. Reagents	33
4. Solvents	34
5. Polymer Solvents	34
6. Polymer Stabilizers	34
7. Polymer Samples	34
B. Measurements	35
C. Preparations	
1. Synthesis of Ethyl Glycidate	36
2. Gas Phase Polymerization	
a. Trioxane-Dioxolane Copolymer	38
b. Trioxane Homopolymer and Trioxane-Ethyl Glycidate Copolymer	40
c. Ionomers from Trioxane-Ethyl Glycidate Copolymer	42
d. Acid Derivative of Trioxane-Ethyl Glycidate Copolymer	43
3. Solution Polymerization	
a. Trioxane-Dioxolane Copolymers	44
b. Trioxane-Ethyl Glycidate Copolymers	47
c. Trioxane-Ethyl Glycidate-Dioxolane Terpolymers	48

d. Ionic Derivatives of the Terpolymers	51
e. Acid Derivatives of the Terpolymers	52
4. Bulk Polymerization	53
5. Addition of Stabilizers to the Copolymers and Terpolymers	54
6. Sample Preparation for the Structure and Property Testing	55
D. Structure and Property Testing	
1. Calorimetric Studies	57
2. Dynamic Mechanical Studies	59
3. Dielectric Studies	61
III. RESULTS AND DISCUSSION	
A. Preparations and Preliminary Characterization	
1. Synthesis of Ethyl Glycidate	65
2. Gas Phase Polymerization	
a. Trioxane-Dioxolane Copolymer	67
b. Trioxane Homopolymer and Trioxane- Ethyl Glycidate Copolymer	68
c. Ionomers and Acid Derivative from Trioxane- Ethyl Glycidate Copolymer	71
3. Solution Copolymers of Trioxane and Dioxolane	73
4. Solution and Bulk Copolymers and Terpolymers of Trioxane, Ethyl Glycidate and Dioxolane and Their Derivatives	80

B. Calorimetric Studies	
1. Trioxane-Dioxolane Copolymers	87
2. STG Copolymers	90
3. TED Terpolymers	92
C. Dynamic Mechanical Studies	
1. Trioxane-Dioxolane Copolymers	96
2. TED 5 Ester Terpolymer	103
3. STG Copolymers	106
D. Dielectric Studies	
1. Trioxane-Dioxolane Copolymers	109
2. TED Ester and Salt Terpolymers	116
IV. CONCLUSIONS	120
V. SUGGESTIONS FOR FURTHER WORK	124
REFERENCES	127
FIGURES	138
EQUATIONS	162



## L I S T   O F   F I G U R E S

FIGURE 1	PMR Spectrum of Ethyl Glycidate	138
FIGURE 2	Infrared Spectra of POM Derivatives	139
FIGURE 3	Infrared Spectra of POM Carboxylates	140
FIGURE 4	PMR Spectra of Trioxane Homopolymer and of Trioxane-Dioxolane Copolymers	141
FIGURE 5	Infrared Spectra of Trioxane-Dioxolane Copolymers	142
FIGURE 6	Infrared Spectra of POM Derivatives	143
FIGURE 7	Infrared Spectra of Fractions from Ethyl Glycidate Distillation	144
FIGURE 8	Infrared Spectra of Trioxane Homopolymer Before and After Endcapping	145
FIGURE 9	PMR Spectra of a POM Copolymer and a POM Terpolymer	146
FIGURE 10	Infrared Spectra of POM Acid Before and After Heat Treatment	147
FIGURE 11	Oxymethylene Copolymers and Terpolymers	148
FIGURE 12	DSC Crystallinity vs Oxyethylene Content	149
FIGURE 13	DSC Crystallinity vs STG Content	150
FIGURE 14	Melting and Crystallization of Ionic and Nonionic Copolymers	151

FIGURE 15	Onset of Crystallization in Ionic and Nonionic Copolymers	152
FIGURE 16	Dynamic Mechanical Relaxations of TD Copolymers at 110 Hz	153
FIGURE 17	Dynamic Mechanical Relaxations of a POM Terpolymer at 110 Hz	154
FIGURE 18	Mechanical Loss Maxima for the $\alpha$ Relaxation of TED Ester (0.9)	155
FIGURE 19	Dynamic Mechanical Relaxations of POM Ionomers at 110 Hz	156
FIGURE 20	Mechanical Loss Maxima for the $\alpha'$ Relaxation of STG 23	157
FIGURE 21	Dielectric Relaxations of TD Copolymers at 200 Hz	158
FIGURE 22	Dielectric Loss Maxima for $\gamma$ Relaxation of Oxymethylene Polymers	159
FIGURE 23	Dielectric Relaxations of POM Terpolymers at 200 Hz	160
FIGURE 24	Dielectric Relaxations of POM Ionomers at 200 Hz	161

## L I S T   O F   E Q U A T I O N S

EQUATION 1	Synthesis of Ethyl Glycidate	162
EQUATION 2	Vapor Phase Copolymerization of Trioxane with Ethyl Glycidate	163
EQUATION 3	Hydrolysis of Polymeric Ester to Sodium Salt	164
EQUATION 4	Exchange of Alkali Metal Cations	165
EQUATION 5	Conversion of Polymeric Salt to Free Acid	166
EQUATION 6	Solution Copolymerization of Trioxane with Dioxolane	167
EQUATION 7	Base Stabilization of Trioxane- Dioxolane Copolymers	168
EQUATION 8	Solution Polymerization of Trioxane with Ethyl Glycidate and Dioxolane	169
EQUATION 9	Hydrolysis of Polymeric Ester to Sodium Salt	170
EQUATION 10	Conversion of Polymeric Salt to Free Acid	171

## CHAPTER I

### INTRODUCTION

#### A. Oxymethylene Polymers

##### 1. General Background

Ionomers based on polyoxymethylene have been prepared by polymerizing trioxane with monomers containing ionizable functional groups.<sup>1-6</sup> The incorporation of ionic comonomer units into the crystallizable polyoxymethylene chain hindered the attainment of crystalline order in the polymers. This was attributed, in part, to the presence of the comonomer or branch units along the chain but also to the effects the ions exerted on the kinetics of the crystallization process.<sup>4</sup>

Polyoxymethylene has been prepared from formaldehyde, primarily, with anionic or cationic initiators. Formaldehyde polymerization was studied in the liquid state, in the gaseous state, in "solution" of aprotic solvents and in hydroxylic media. The homopolymer has also been obtained by ring opening polymerization of trioxane with cationic initiators in the solid, liquid and gaseous states or in solution. The discovery that anhydrous formaldehyde could be polymerized, with high molecular weight, by an anionic process and stabilized, by endcapping, to give a strong, tough polymer led to the decision by the Du Pont Company to commercialize polyoxymethylene.<sup>7-9</sup> A few years later, the Celanese Company commercialized copolymers based on trioxane.<sup>10</sup>

##### 2. Polymerization of Formaldehyde

###### a. Anionic Polymerization



Anionic initiators for anhydrous formaldehyde polymerization include acylates, most prominently tetraalkyl ammonium acetate, alkoxides or Lewis bases such as trialkyl or triaryl amines, arsines or phosphines.<sup>7-9</sup> Weaker nucleophiles such as chlorides are ineffective. An anionic mechanism has been established in which the alkoxide ion is the propagating species:



Termination of the polymerization usually takes place by reaction with chain transfer agents:



The active chain ends may also be occluded. Water, methanol and methyl formate are all good chain transfer agents in formaldehyde polymerization.<sup>11</sup> In the first two cases, a hydroxyl terminated polymer results and the polymerization is subsequently reinitiated by  $\text{HO}^{\ominus}$  or  $\text{CH}_3\text{O}^{\ominus}$ . With methyl formate, the formyl group is the terminating group and methoxide the reinitiating group.

A very important consideration in the initiation of aldehyde polymerization by cationic or anionic initiators is the relatively low molecular weight of aldehyde polymers as compared to the kinetic chain

length of polymerization. In other words, most initiation takes place via chain transfer. As a consequence, ten to a hundred chains of aldehyde polymer may be produced from one initiator fragment.

The efficiency of initiation of formaldehyde with acylates depends, primarily, on the nucleophilicity of the anion of the onium salt. The initiation mechanism involves the addition of the acylate anion to the carbonyl carbon:



Initiation with the acylate anion is slow and the overall rate of polymerization is dependent on the rate of termination by chain transfer to impurities.

Tertiary amines and phosphines are highly reactive initiators for formaldehyde polymerization. Primary and secondary amines are less active probably because the methylool compounds resulting from their reaction with formaldehyde are much less basic. In solution at  $-78^\circ\text{C}$ , branched amines ( $\alpha$ -carbon substituted) are less effective initiators than tertiary amines with *n*-alkyl substituents.<sup>12, 13</sup>

In the early forties, the Du Pont Company began work on the reaction of pure formaldehyde. One of the objectives was to prepare high molecular weight polymers. An anionic process for the preparation of formaldehyde polymers, that were tough, attractive and stable, was subsequently developed.<sup>7-9</sup> This work led, ultimately, to the commercialization of a polyoxymethylene homopolymer by the Du Pont Company under

the trademark of Delrin.

One of the essential conditions for the preparation of high molecular weight polymers was that the formaldehyde be purified and dried immediately prior to polymerization. This was accomplished by transforming a 60% formaldehyde solution into the hemiacetal of cyclohexanol or 2-ethylhexanol. The hemiacetal was separated, dehydrated and cracked thermally to the formaldehyde. The cooling system in the cracking process determined the level of impurity and, consequently, the ultimate molecular weight of the polymer. Lower temperatures of the partial condenser gave extension grade polyoxymethylene while somewhat higher cooling temperatures gave molding grade polyoxymethylene.

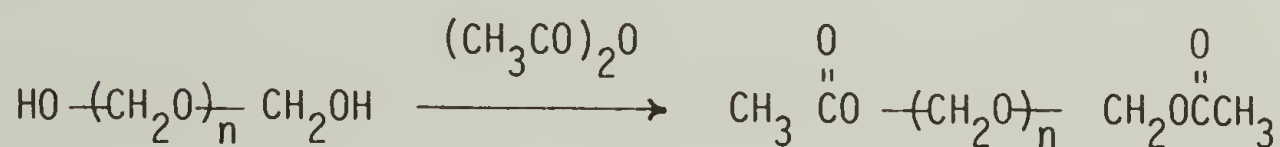
The Du Pont commercial process is a continuous process utilizing tetraalkyl ammonium acetate as the initiator. The monomer, purified and dried in the manner just described, is continuously swept at atmospheric pressure with  $N_2$  through a partial condenser and into the top of a reactor which contains a cyclohexane solution of the initiator. This type of reactor is generally useful for the continuous, exothermic polymerization of a gas in a liquid but is specifically applicable to formaldehyde polymerization.<sup>14</sup> The reactor may be operated continuously for days without excessive buildup of polymer on the metal parts of the equipment. The polymer is isolated from the slurry by filtration, washed with cyclohexane and acetone and dried under a stream of nitrogen.

Polyoxymethylenes, prepared from formaldehyde with cationic and anionic initiators or from trioxane with cationic initiators, contain thermally unstable hemiacetal groups. These groups are introduced by chain transfer reactions between the propagating polyoxymethylene

chains and water or other protic impurities. The thermally induced depropagation from chain ends (unzipping) in polyoxymethylene becomes significant at 90°C even though the ceiling temperature of the polymer is closer to 125°C. The mechanism of this reaction is ionic in nature. Successive monomer units are lost by rapid volatilization to yield only monomer and a lower weight, with little or no change in the overall polymer molecular weight:



In order to improve its thermal stability, polyoxymethylene is endcapped by reacting the polymer at elevated temperature with acetic anhydride:<sup>15</sup>



This reaction raises the temperature of noticeable degradation from 150°C to greater than 250°C. Also, the rate of degradation for endcapped polyoxymethylene is less than 0.01 %/min. at 222°C compared to 8%/min. for the untreated polymer.

Commercially, the dry polymer is vapor capped with acetic anhydride at 160°C.<sup>15, 16</sup> A gaseous mixture of acetic anhydride and nitrogen is passed slowly through a reaction vessel containing the powdered polymer. Reaction times range between one and five hours. The nitrogen stream is maintained while the reactor is cooled to room temperature.



The polymer is sparged with nitrogen, if desired, compounded, extruded and chopped into molding powder. Number average molecular weights are not appreciably changed by the acetylation treatment.

The endcapping reaction could also be carried out while the polyoxymethylene was dissolved in acetic anhydride at 160°C for times ranging from a half hour to two hours.<sup>15</sup> The same reaction has been performed on polyoxymethylene slurried in a hydrocarbon medium such as benzene or cyclohexane.<sup>15</sup> Other anhydrides and a variety of tertiary amines were utilized as endcapping agents and catalysts, respectively. This reaction was also run under a positive nitrogen pressure in a suitable reaction vessel.<sup>15</sup> In all cases, the endcapping reaction was only effective when carried out at temperatures above the  $\alpha$  crystal to crystal transition in polyoxymethylene (around 130°C).

#### b. Cationic Polymerization

Anhydrous formaldehyde may also be polymerized with three classes of cationic initiators: protonic or Bronsted acids, Lewis acids and stable ions.<sup>17-20</sup> In toluene, diethyl ether or methylene chloride and at -78°C, the protonic acids are the most active initiators while the activity of stable ions such as acetyl perchlorate is usually higher than that of Lewis acids, with the exception of the tin tetrahalides.<sup>21</sup>

Initiation with Lewis acids has been studied extensively. It is known that Lewis acids, by themselves, are not the actual initiators, but a reaction product of unknown structure formed either with the monomer or with impurities in the system.  $\text{SnCl}_4$  and  $\text{SnBr}_4$  are extremely active initiators, even at low concentrations, giving polyoxymethylenes

of similar molecular weight distributions and type of endgroups to the polymers obtained by anionic initiation.<sup>17</sup> However, polyoxymethylenes with a high content of formate and methoxy endgroups and broad molecular weight distributions are obtained when  $\text{AlBr}_3$  or  $\text{FeBr}_3$  are used.

Anionic initiators or anionically growing alkoxide chains can only grow or terminate, but cationic initiators or cationically growing chains may also cause acetal-interchange reactions (transacetalization) which rearrange the molecular weight distribution in homopolymers. Transacetalization reactions are responsible for the random incorporation of oxyethylene units into a polyoxymethylene prepared in the presence of cyclic ethers or cyclic formals, or of the polymers of cyclic formals.

The cationic polymerization of formaldehyde proceeds by a chain growth mechanism in which the electrophilic initiator is believed to add to the oxygen forming an oxonium ion:



The electrophile in Bronsted acids is the proton and in stable ions the cation, e.g. the acetyl group of acetyl perchlorate.

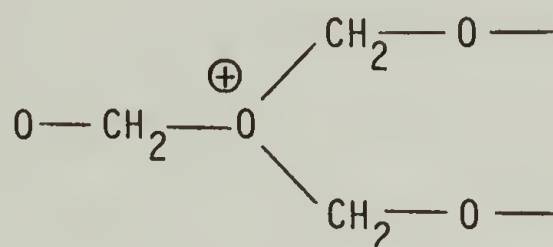
The oxonium ion is in resonance with the oxocarbenium ion:



The propagation step involves an electrophilic attack of the oxocarbenium carbon on the carbonyl oxygen of the highly polar formaldehyde:



Indirect evidence available from acid catalyzed random incorporation of oxyethylene units into polyoxymethylene (transacetalization) gives rise to a further refinement of this mechanism. Under certain conditions, it is possible for this oxocarbenium ion to be further solvated by an already formed polyoxymethylene chain to give



Termination occurs almost exclusively by chain transfer with protic species ( $R \equiv$  alkyl or H) such as water and alcohols:



or with chain transfer reagents such as acetals, esters and anhydrides:



where  $X \equiv -OR'$ ,  $-COOR'$  and  $-COOCOR'$  and  $R, R' \equiv$  alkyl.

Chain transfer is most pronounced in solvents of higher dielectric constant, where the polymerization rate is also high (methylene chloride, tetrahydrofuran and acetone), but is minimal in toluene and pentane (formaldehyde is only slightly soluble in the latter solvent).<sup>21</sup>

A series of excellent reviews on cationic polymerization of aldehydes and on the kinetics of aldehyde polymerization have appeared in literature in recent years.<sup>22, 23</sup>

Although solvents with high dielectric constants give higher rates of polymerization, the rate is not directly related to the polarity of the solvent. At low conversion, in non-polar solvents, formaldehyde, itself highly polar, strongly influences its own rate of polymerization. In solvents of very high dielectric constant, such as nitroethane, the growing polymer chain could be solvated by another polymer chain, as shown above, and also by a solvent molecule.<sup>21</sup> As a consequence, the effective local monomer concentration increased with respect to the overall monomer concentration in solution; monomer was depleted from the growing site and the rate of polymerization was decreased. Indeed, the observed rate at  $-78^{\circ}\text{C}$  and at  $-30^{\circ}\text{C}$  in nitroethane was slower than in methylene chloride or acetone, with  $\text{SnCl}_4$  as the initiator.<sup>21</sup>

### c. Gas Phase Polymerization

In the polymerization of formaldehyde from the gas phase, the rate of monomer disappearance can be followed, readily, manometrically.<sup>24, 25</sup>

This is a distinct advantage over polymerization in solution where one can only determine the "available" active cations by reacting the



growing ends with pentanol and quantitatively estimate the pentyloxy groups by pyrolysis chromatography.<sup>26,27</sup>

#### d. Polymerization in Hydroxylic Media

Polymerization of formaldehyde in hydroxylic media is, mechanistically, a step growth process but the polymer formed is an addition polymer.<sup>28,29</sup> Formaldehyde reacts with water in the form of methylene glycol and with methanol to give the hemiacetal. In dilute aqueous media, the main components are low molecular weight oligomers of polyoxymethylene glycols but a small amount of free formaldehyde is also present due to the instability of the methylene glycol. An increase in the formaldehyde concentration or a decrease in the temperature causes the precipitation of solid polyoxymethylene glycols. This occurs when the polyoxymethylene glycols attain a degree of polymerization of approximately ten and thereafter the polymerization continues in the heterogeneous crystalline phase.<sup>29</sup>

In principle, no catalyst is required for the reactions but, in order to work at reasonable rates, acid or base catalysis is used. Basic catalysts are actually preferred because acid catalysts are responsible for two undesirable side reactions: the formation of dimethyl formal, in methanolic media, which causes the disappearance of monomer and transacetalization which broadens the molecular weight distribution of the resulting polymer.

The limiting factors involved in this polymerization are the growth rate of the polymer crystals, the nucleation rate and the limiting molecular weight. The growth rate is nearly linear with formaldehyde

concentration going through the origin at the equilibrium concentration. The nucleation rate is insignificant until the supersaturation is high enough to cause spontaneous precipitation of polyoxymethylene. Then, it increases rapidly with increasing formaldehyde concentration until it crosses the growth rate, at which point only low molecular weight polymer is formed. As nucleation proceeds, the limiting molecular weight decreases and the molecular weight distribution broadens. The best formaldehyde concentration for polymerization is about four to eight percent above the equilibrium concentration of formaldehyde.<sup>29</sup> This is the region where the growth rate is already substantial, but the nucleation rate is still zero or low.

High molecular weight polyoxymethylene is obtained only if the medium is seeded with crystals of proper crystal habit (i.e. crystals, born by spontaneous nucleation, that can grow exclusively by addition to the chain ends which are aligned and available at the face of the polymer crystals). The molecular weight distributions of polyoxymethylene, prepared under these conditions, are near unity.

#### e. Copolymers Derived from Formaldehyde

Copolymers of formaldehyde have been prepared under anhydrous conditions with cationic and anionic initiators. Cationically, vinyl ethers have primarily been used as comonomers but also, less effectively, styrene, cyclic formals and cyclic ethers, cyclic anhydrides and carbon monoxide.<sup>30-36</sup> Isocyanates have been incorporated under anionic conditions.<sup>37</sup> Despite this versatility, formaldehyde does not copolymerize as readily and effectively with the above monomers to give uniform

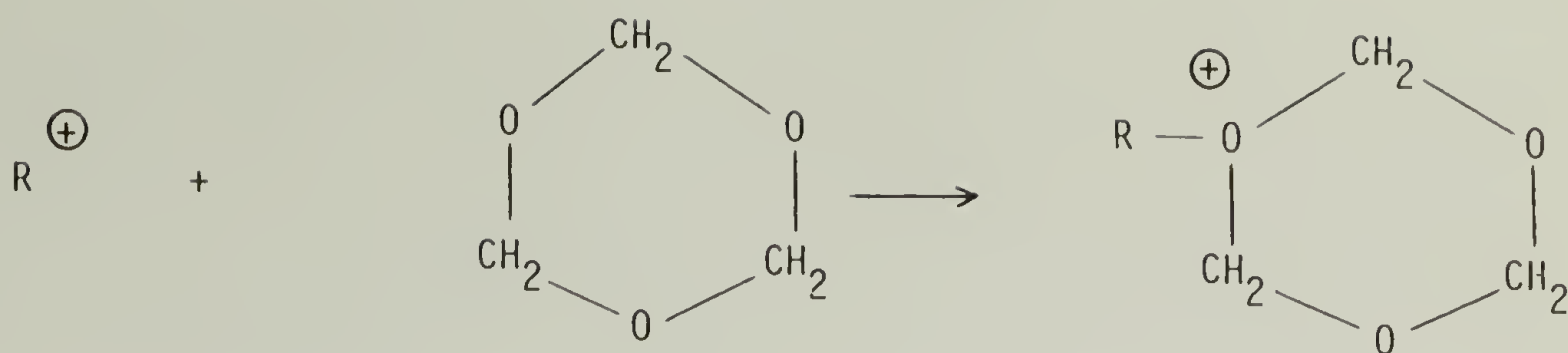
copolymers. Even when polymers are obtained the comonomer incorporation is poor and the yields, molecular weights and base stabilities of the resulting products are inadequate. As a consequence, copolymers derived from formaldehyde are still commercially unattractive.

### 3. Cationic Polymerization of Trioxane

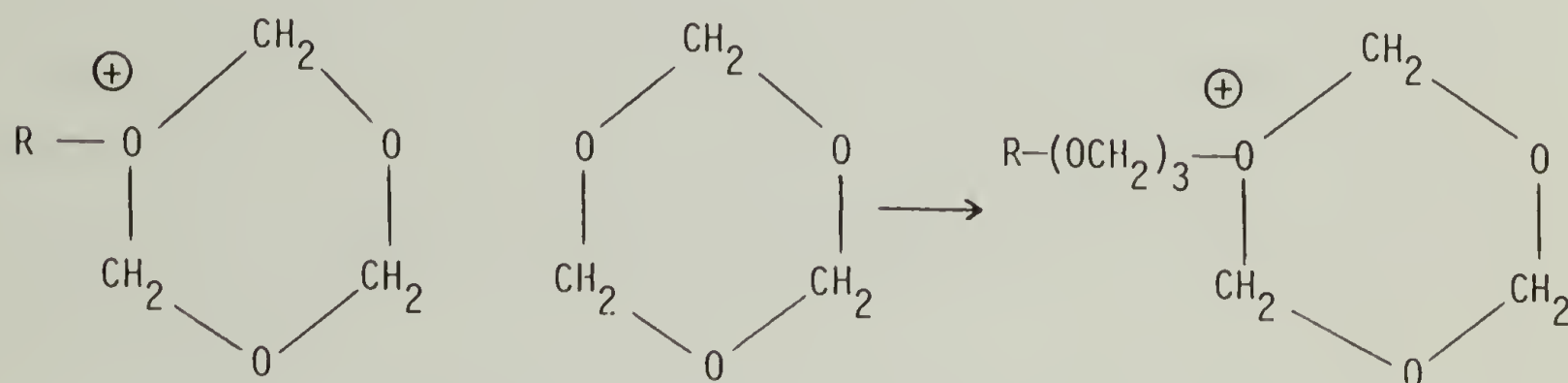
Polyoxymethylene can also be prepared by polymerization of trioxane, the cyclic trimer of formaldehyde. Actually, the transformation of formaldehyde into trioxane (which is equivalent to the hemiacetal of the formaldehyde process) is a convenient method of purifying the formaldehyde. Trioxane can be purified and dried for polymerization by recrystallization followed by distillation.

Trioxane is polymerized in the solid, liquid and gaseous states by ring opening polymerization with cationic initiators. Radiation induced polymerization of trioxane, postulated to be a cationic process, is also well known.<sup>38-40</sup> Again, like formaldehyde, the polymerization reaction may be conducted in bulk or in the presence of a solvent or dispersing medium. The same cationic initiators used in the polymerization of formaldehyde can be used to polymerize trioxane. Boron trifluoride, trifluoromethane sulfonic acid and methyl trifluoromethane sulfonate are efficient initiators for trioxane polymerization, but other Lewis and Bronsted acids and stable salts, capable of initiating cationic cyclic ether polymerization, are also effective.<sup>41-45</sup>

The mechanism of trioxane polymerization is similar to that advanced for the cationic polymerization of other cyclic ethers. An oxonium ion is formed by the addition of the electrophilic initiator to one of the ring oxygens in the monomer:



Such an oxonium ion attacks another monomer molecule in the propagation step:

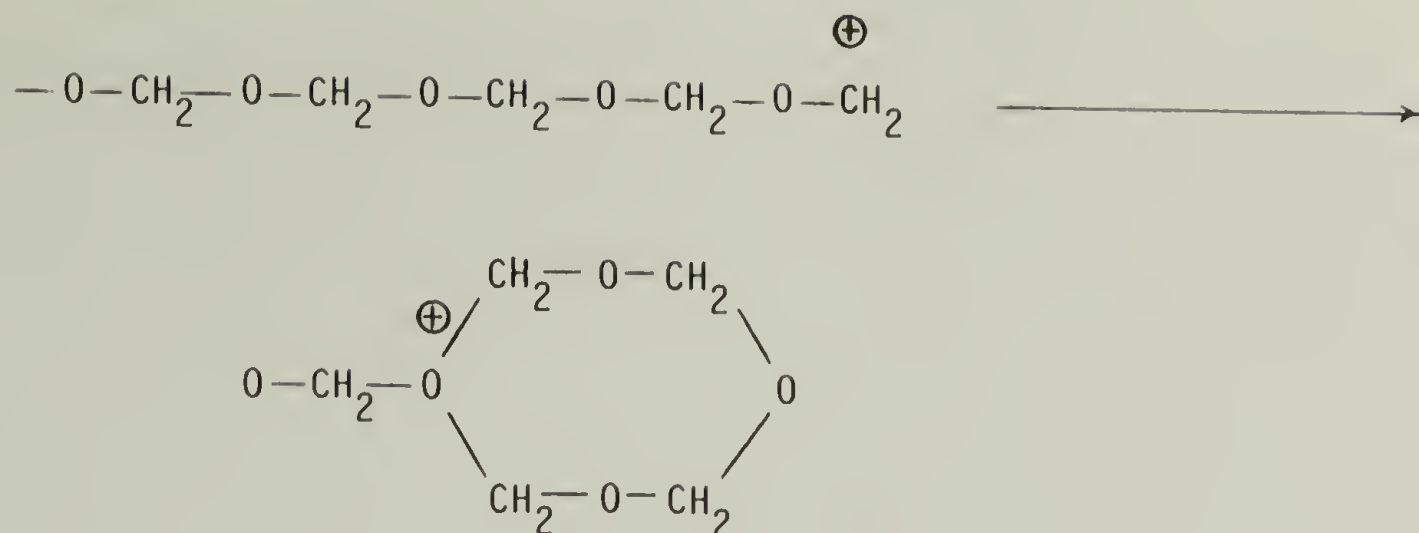


Again, "termination" of the chain is caused by chain transfer and the rate of polymerization is determined by the type of chain transfer agent that is present.

An induction period has often been observed both in bulk (melt) and solution polymerization of trioxane with different initiators.<sup>41, 46-49</sup> The cause of the induction period has been a continuous source of debate which has not been satisfactorily resolved.

Under certain reaction conditions tetraoxane is formed during the induction period.<sup>50, 51</sup> This side product results from intramolecular transacetalization or backbiting:





The precipitation of polyoxymethylene during the solution polymerization of trioxane is responsible for the acceleration of the rate of trioxane polymerization. Once the polymer begins to precipitate, the equilibrium is shifted in the direction of high polymer and the polymerization continues on the solid surface, independent of the polymerization in solution phase.

Cationic polymerization of trioxane has been extensively investigated in the solid state with Lewis acid type of initiators, such as  $BF_3$ , or by radiation induced polymerization.<sup>52-56</sup> This polymerization is best carried out a few degrees below the melting point of the monomer. After a high initial rate, the reaction proceeds to high conversion usually over an extended period of time.

Many cyclic monomers, capable of cationic polymerization, readily copolymerize with trioxane, in particular, 1,3 dioxolane, substituted dioxolanes, ethylene oxide and epichlorohydrin.<sup>5,6,10</sup> Other epoxides, such as propylene oxide, glycidyl ethers, glycidaldehyde, glycidonitrile, alkyl glycidates, allyl esters,  $\alpha$ -substituted styrenes, norbornadiene, acrylonitrile, alkyl acrylates and vinyl esters have also been claimed



to copolymerize with trioxane.<sup>1,2,57-61</sup>

During the copolymerization of trioxane with either ethylene oxide or dioxolane, the comonomer polymerizes preferentially in the early part of the reaction. At low comonomer content in the feed, all the ethylene oxide is present in the first five to ten percent of copolymer.<sup>62</sup> As polymerization proceeds, a continuous cleavage and recombination of polyoxymethylene chains takes place which ultimately leads to a completely random incorporation of the comonomer. Such a random distribution of comonomer units in the copolymer provides a zipper jammer close to the end of the polymer chain and gives a high base stable fraction. The amount of base degradable oxymethylene units at both ends of the copolymer chain is influenced by different types of initiators and increases, at constant comonomer content, with increasing comonomer sequence length, again assuming a random distribution of oxyethylene units along the chain.

Industrial research in trioxane homo- and copolymerization has been carried out extensively at Celanese and Farbwerke Hoechst.<sup>10,63</sup> A random copolymer based on trioxane is now produced under the trade name Celcon or Hostaform.

Schneider, at DuPont, first succeeded in preparing tough high molecular weight polyoxymethylenes from trioxane, under anhydrous conditions, in the presence of Lewis acid fluorides as initiators.<sup>64</sup> The resulting products could be molded and extruded. The pioneering work on the Celcon copolymer was accomplished by C. Walling, F. Brown and K. Bartz.<sup>10</sup> Ethylene oxide or dioxolane and boron trifluoride etherate were added to the trioxane, diluted with cyclohexane in a test tube, and the mixture was allowed to react in a bath for four hours at 67°C. The

polymer, recovered after work up, showed improved weight loss over homopolymer of trioxane.

Commercial base stabilization of oxymethylene copolymers is effected in solution at 160°C and 240 psi with triethylamine, in a mixture of isopropanol (or methanol) and water.<sup>65</sup> A stabilizer system, consisting of catalin CAO 5 antioxidant and cyanoguanidine, is incorporated into the base stable copolymer during workup. The stabilized product is then extruded and chopped into the molding powder.

A gas phase process was developed by O. Vogl<sup>1,2</sup> for the preparation of trioxane copolymers with functional groups. Comonomers were mixed with the boron trifluoride initiator in the vapor phase at 130°C. The vapors were condensed whereby the mixture polymerized to high conversion. Butadiene dioxide, glycidonitrile, ethyl glycidyl ether, ethyl glycidate, methyl glycidate, ethylene oxide and propylene oxide were employed as comonomers for the trioxane polymerization. The trioxane/comonomer molar feed ratio was varied from 27/1 to 700/1, the initiator flow rate from 2 to 15 cc/min and the polymerization time from 20 to 90 minutes depending on the type of comonomer and the amount of initiator used. The inherent viscosity of the endcapped product was as high as 1.62 while the base stability values for the uncapped product fluctuated between 15 and 90 percent by weight. In the case of copolymers incorporating up to 2 mole percent ethyl glycidate, the polymers exhibited an inherent viscosity of 1.0 when endcapped, but the uncapped products were only 30 percent base stable.

A homogeneous copolymer of trioxane and propylene oxide with a higher comonomer content and a markedly higher molecular weight was prepared, in this way, at a higher rate than by bulk polymerization

employing trioxane, propylene oxide and boron trifluoride in identical feed ratios. A propylene oxide content of 0.82 mole percent, an inherent viscosity of 1.04 and no induction time were observed in the gas phase process compared to a 0.67 mole percent incorporation of comonomer, a 0.52 inherent viscosity and a two minute induction period for the bulk reaction. In contrast to the gas phase technique, the bulk copolymerization produced inhomogeneous materials because it was difficult to distribute the initiator or the comonomer uniformly throughout the molten trioxane.

Polyoxymethylenes with functional side groups were molded and had a flexural modulus of 464,000 lbs./in.<sup>2</sup>, a tensile modulus of 474,000 lbs./in.<sup>2</sup>, a tensile strength of 8,910 lbs./in.<sup>2</sup>, an ultimate elongation of 4.6 percent, an Izod impact strength of 0.73 ft.lb./in. notch and a tensile impact strength of 65 ft. lb./in.<sup>3</sup>.

#### 4. Characterization of Oxymethylene Polymers

##### a. Physical and Chemical Properties

Delrin, Celcon and Hostaform are engineering plastics noted for their stiffness, fatigue resistance and creep resistance. Table 1 lists typical values for essential properties of such polymers.<sup>66, 67</sup> The copolymers are less crystalline and therefore have a lower density, hardness, tensile strength and flexural modulus. The main advantage claimed for the copolymers is improved processability with less degradation at processing temperatures.



Table 1  
Physical Properties of  
Delrin and Celcon

<u>Property</u>	<u>Delrin</u>	<u>Celcon</u>
Specific Gravity	1.425	1.410
Crystalline Melting Point (°C)	175	163
Crystallinity (%)	69	59
Tensile Strength (lbs./in. <sup>2</sup> )	10,000	8,500
Flexural Modulus (lbs./in. <sup>2</sup> )	410,000	360,000
Elongation at Break (%)	15	60
Impact Strength, (ft.lb./in. notch)	1.4	1.2
Hardness, Rockwell M	94	80

At room temperature, Delrin, Celcon and Hostaform are only soluble in hexafluoroacetone hydrate and 1,2-dichlorotetrafluoroacetone hydrate.<sup>68</sup> At elevated temperatures (between 60°C and 120°C) phenols such as p-chlorophenol and fluorinated alcohols such as octafluoropentanol are solvents.<sup>69, 70</sup>

Besides depropagation from chain ends or unzipping, polyoxymethylenes also degrade oxidatively in air by the action of ultraviolet light and/or elevated temperature. For these reasons, all acetal resins contain thermal stabilizers and antioxidants. Catalin CAO 5 antioxidant and cyanoguanidine are utilized commercially for oxymethylene copolymers. Di-β-naphtnyl-p-phenylene diamine (DNPD), Nylon 66/610/6 and phenols (such

as Santowhite powder) are effective antioxidants for acetate endcapped oxymethylene homopolymers.

#### b. Analytical Methods

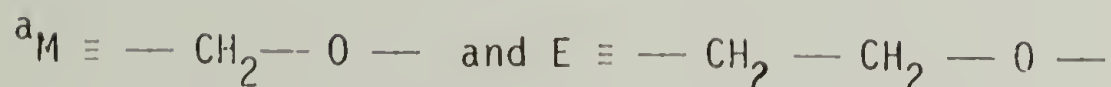
Composition of oxymethylene copolymers and the sequence distribution of comonomer units along the chain can be readily determined by inspection of the PMR spectrum. Considerable information is available in literature regarding this kind of analysis, specifically, on copolymers of trioxane and dioxolane.<sup>71-74</sup> At elevated temperature, in p-chlorophenol, a singlet corresponding to the  $\text{—O—CH}_2\text{—O—CH}_2\text{—O—CH}_2\text{—(MMM)}$  triad appears at approximately 4.9 ppm.<sup>71</sup> The presence of a small proportion of copolymerized oxyethylene units ( $\text{—O—CH}_2\text{—O—CH}_2\text{—CH}_2\text{—O—CH}_2\text{—(MEM)}$  triad) gives rise to an additional peak around 3.7 ppm thereby enabling quantities as low as one mole percent to be estimated.

Tris (dipivalomethano) europium complex, the corresponding praseodymium complex, and other lanthanide complex shift reagents were found to cause substantial chemical shift changes in the 60 MHz PMR spectra of dioxolane-trioxane copolymers and allowed to easily determine the structure and sequence distribution by PMR spectroscopy.<sup>74</sup> The formal segments were not as sensitive to the shift reagent as the ethylene oxide segments. In the 60 MHz PMR spectrum of a dioxolane/trioxane copolymer (with 63.1 mole percent dioxolane) in  $\text{CDCl}_3$  at room temperature in the presence of 6 mg. of  $\text{Pr (DPM)}_3$  three triads and three heptads could be distinguished. Their proton assignments and corresponding chemical shifts are listed in Table 2.



Table 2  
PMR of a Trioxane-Dioxolane Copolymer

<u>Chemical Shift ppm (<math>\delta</math>)</u>	<u>Proton Assignments</u>
1.7 - 1.9	MEMEMEM or MEMEMMM
2.7 - 2.9	EMMEMME or EMMEMMM
3.3	MMMEMMM
3.9 - 4.2	EME
4.4 - 4.5	EMM = MME
4.8 - 4.9	MMM



The presence of oxyethylene units in the copolymer is also characterized by the  $\text{---CH}_2\text{---}$  rocking vibration in the infrared at  $11.8 \mu$  for a carbon-carbon bond.<sup>72</sup> In addition, the backbone methylene torsion vibration ascribed to the  $\text{---O---CH}_2\text{---O---}$  unit appears at  $8.1 \mu$  whereas the one assigned to the  $\text{---O---CH}_2\text{---CH}_2\text{---O---}$  unit is found at  $7.8 \mu$ .

Infrared is a powerful technique for characterization of polyoxy-methylene homopolymers and copolymers. Composition studies of trioxane-dioxolane copolymers are only one example of its utility. I.R. is used to estimate the extent of base hydrolysis in trioxane and alkyl glycidate copolymers.<sup>1</sup> These copolymers were characterized by the presence of a band in the infrared spectrum at  $5.8 \mu$  due to the carbonyl band of the ester group. The ionomers resulting from the conversion of the ester to the sodium salt were identified by the same technique. The  $5.8 \mu$  band mentioned above was absent and was replaced by two bands at  $6.2 \mu$  and  $7.1 \mu$  due to the sodium salt group.

Infrared also provides a quantitative determination of the number average molecular weight of polyoxymethylene.<sup>15</sup> The oxymethylene content is measured in infrared absorbance units. By knowing the kind and the number of terminal groups on each polyoxymethylene chain, the infrared analysis permits a calculation of the number average molecular weight. The analysis is made in the region of 2 to 8 microns wavelength, the hydroxyl band (for unendcapped polyoxymethylene homopolymer) appearing at  $2.9\mu$  and the carbonyl band (for homopolymers endcapped with anhydride) at  $5.7\mu$ . Although the films obtained from various samples are not always exactly the same thickness, the variation in thickness can be standardized by expressing the hydroxyl and carbonyl values in relation to a standard absorbance of the same sample at a wavelength of  $4.3\mu$ . The absorbance at  $4.3\mu$  varies directly with the film thicknesses of different samples, but is essentially unaffected by the presence or absence of hydroxyl or acetate carbonyl in the samples.

### c. Crystalline and Amorphous Transitions

Crystallization in oxymethylene homopolymers and copolymers is an extremely important phenomenon since it not only bears a strong influence on the progress of the polymerization but also significantly affects the final polymer properties. The earliest report of highly crystalline polyoxymethylene is the work of Staudinger et. al. which treated the polymerization of formaldehyde or cyclic oligomers of formaldehyde in hydroxylic media.<sup>28</sup> Brown, later, showed that the additional driving force for this type of polymerization was provided by the crystallization of the polymer as it precipitated out of solution.<sup>29</sup> In hydroxylic polymerization, the polymer that is obtained is 100% crystalline

and presumably consists of extended chains. The common crystal form of polyoxymethylene is the hexagonal form. Upon molding, even the highly crystalline material with extended chains yields the normal 80 percent crystalline form of polyoxymethylene. An increase in the sequence length of the comonomer units in oxymethylene copolymers, increases the crystalline melting point of the copolymer.<sup>3</sup> Trioxane copolymers with varying dioxolane content (from 12 to 95%) show an unusual behavior with respect to density, specific volume and melting point as a function of composition.<sup>75</sup> This is believed to be caused by the formation of at least four different crystal structures in such copolymers. An orthorombic crystalline form (> 90% orthorombicity) of high molecular weight polyoxymethylene was formed when the polymerization of aqueous formaldehyde was carried out at 20°C to 30°C at pH > 10 in high salt concentrations (34 to 38 percent of HCOONa catalyst).<sup>76</sup>

Polymerization of trioxane in ethylene dichloride produced soluble low molecular weight polymer, during an induction period, and eventually formed crystal nuclei.<sup>77</sup> These initiated an accelerated reaction whose rate depended on the area of the crystal surface available for polymer deposition or formation. Kinetic arguments and microscopic evidence indicated a progressive increase in the size of the original crystals rather than a constant formation of fresh nuclei which strongly suggested that polymerization took place at the growing crystal surface.

Solid state cationic polymerization of trioxane with Lewis acid initiators was found to start on the surface of the monomer crystal.<sup>55</sup> The resulting polymer had excellent three-dimensional order and showed



fiber diagrams in which the amorphous scattering was completely absent.

Geil and O'Leary suggested that the reversible change they observed in the long spacing in small angle X-ray scattering with temperature for both bulk and drawn polyoxymethylenes could only be reconciled by using thermodynamic equilibrium theory to account for lamellar thickening in polyoxymethylene or by arguing that the long spacing could not be equated by Bragg's law to a periodicity in the sample, such as lamellar thickness.<sup>78, 79</sup> Two phase model considerations were also used to explain the slight increase in the long spacing and the pronounced decrease in the small angle X-ray intensity above 120°C for well-annealed melt crystallized polyoxymethylene samples.<sup>80</sup>

Recently, extended chain crystals of oxymethylene homopolymers and copolymers (containing up to a mole fraction of  $X_{\text{CH}_2\text{CH}_2\text{O}} = 0.1$ ) were obtained again, this time, by cationic polymerization of trioxane alone or with 1,3 dioxolane in nitrobenzene.<sup>81, 82</sup> In the copolymers, the comonomer units were distributed at random throughout the lattice of oxymethylene units. Nevertheless, comparison of the dependence of lattice parameters on mole fraction for the extended chain crystals and melt or solution crystallized copolymers indicated that in the semicrystalline samples the comonomer units are not distributed at random between amorphous and crystalline phases but, not surprisingly, the comonomer units are enriched in the amorphous phase.

The concept of a glass transition is only valid for amorphous polymers or polymers having a fairly low degree of crystallinity. For highly crystalline polymers, such as polyethylene and polyoxymethylene, attempts to assign a  $T_g$  must inevitably lead to some confusion. Various

authors have found that the glass transition which occurs within inter-crystalline layers of polyoxymethylene, polyethylene and polybutene -1 can be established by measuring the temperature dependence of the small angle X-ray intensity at low temperatures.<sup>80, 83-85</sup> Arguing on the basis of a two phase model, consisting of alternating crystalline and amorphous layers, these authors proposed that a density difference between crystalline and amorphous layers gives rise to the small angle X-ray scattering. Aoki and co-workers assigned the change of the thermal expansion coefficient in the amorphous layer (in the vicinity of -75°C) to the glass transition in the polymer.<sup>80</sup> Further evidence in favor of this interpretation was provided by heat capacity measurements and by brittle point and internal friction data which indicated the presence of a glass transition in this region.<sup>86, 87</sup> The fact that the change in the thermal expansion coefficient was not affected by annealing and  $\gamma$ -irradiation confirmed the observations of Vonk and co-workers and of Fisher and co-workers that the amorphous layer between lamellar crystals of polyoxymethylene is fully amorphous and almost independent of the crystalline regions.<sup>85, 88</sup>

In addition to small angle X-ray scattering, two other variable temperature techniques have been used extensively to detect crystalline and amorphous transitions in oxymethylene polymers, dynamic mechanical viscoelasticity and solid state dielectrics. Three characteristic relaxations have been observed in polyoxymethylene both dielectrically and mechanically. It is generally accepted that the high temperature  $\alpha$  relaxation is associated with the crystalline phase involving translational



motions along the chain axis.<sup>89-91</sup> There is still controversy over the question of assigning either the intermediate temperature  $\beta$  relaxation or the low temperature  $\gamma$  relaxation to the glass transition in the polymer. McCrum and Bohn, independently, have reported that the magnitude of the mechanical  $\gamma$  peak located between  $-10^{\circ}\text{C}$  and  $30^{\circ}\text{C}$  depends both on the thermal history of the sample and on comonomer content in the polymer.<sup>90,92</sup> The  $\beta$  relaxation has also been shown to be moisture sensitive.<sup>90</sup> On the other hand, the magnitude of this relaxation relative to that of the other two relaxations is low and only very weak  $\beta$  peaks have been observed dielectrically.<sup>93,94</sup> The  $\gamma$  relaxation has been shown to be sensitive to changes in the thermal history of the polymer and also to be affected by the addition of plasticizers to polyoxymethylene but the mechanical  $\gamma$  transition was found to be rather insensitive to increases in comonomer content in at least two instances.<sup>90-92,95</sup> Aoki's small angle X-ray evidence coupled with Miki's dynamic mechanical results suggest that the  $\gamma$  relaxation at  $-75^{\circ}\text{C}$  reflects a change in the thermal expansion coefficient of the amorphous layer in a semicrystalline polyoxymethylene.<sup>80,96</sup> If this assignment is correct, then the temperature dependent coefficient of thermal expansion of one hundred percent crystalline polyoxymethylene should not be affected in the low temperature region below  $-20^{\circ}\text{C}$ .

The dynamic mechanical behavior of oxymethylene homopolymers, copolymers with ethylene oxide (0 to 5.1%) and terpolymers with ethylene oxide and a small amount of a rigid non-crystallizable termonomer was investigated at 100 cps in the temperature range from  $-150^{\circ}\text{C}$  to the

crystalline melting point.<sup>95</sup> Density variations in the polymers were introduced either by changing the chemical structure of the polymer or by varying its thermal history. The  $\gamma$  relaxation located at  $-60^{\circ}\text{C}$  remained unaffected by such variations. Nevertheless, the tendency for test specimens to yield and cold draw upon elongation at  $-40^{\circ}\text{C}$  was explained on the basis of a cooperative rotational motion of the chain associated with a brittle-ductile  $\gamma$  transition. The magnitude of the  $\beta$  relaxation was observed to increase as the density decreased. In addition, the  $\beta$  loss temperature increased with increasing density or by incorporation of a rigid non-crystallizable chemical unit. The location of this peak ranged in temperature between 0 and  $40^{\circ}\text{C}$ . Polymer ductility improved with the occurrence of the relaxation. These effects suggested that the long-range chain motions (of micro-Brownian type) in the inter-crystalline regions of the polymer were responsible for the  $\beta$  relaxation. The  $130^{\circ}\text{C}$   $\alpha$  relaxation became more prominent with an increase in crystallite size and perfection consistent with the interpretation that the relaxation was due to motion of the molecular helix within the crystalline phase.

## B. Organic Polymers Containing Polar Side Groups

### 1. Ionomer as a Generic Term

Dynamic mechanical and dielectric relaxations also arise as a result of strong ionic interchain forces in polymers containing pendant ionic groups. These polymers, commonly referred to as "ionomers", exhibit a polar or non-polar backbone and contain a relatively low concentration of carboxyl, sulfonyl or phosphonyl groups associated with free metallic

cations, mainly from Group I or II of the Periodic Table.

## 2. Ionomers Based on Poly- $\alpha$ -olefins

Historically, ionomers based on  $\alpha$ -olefins were introduced before the advent of polyoxymethylene ionomers. Rees and Vaughan, whose early pioneering work, led, ultimately, to the commercialization of the  $\alpha$ -olefin ionomers by the DuPont company under the "Surlyn" trademark, were the first to recognize that strong ionic interchain forces play the dominant role in controlling the mechanical, electrical, rheological, optical and solution properties of this class of polymers.<sup>97-99</sup> The interchain ionic forces are responsible for the reduction of visible crystalline structure but also for the increase in the tensile strength, resilience and chain rigidity. The ionomers are insoluble in all conventional solvents at room temperature and are characterized by unusual oil resistance. Electrical insulating characteristics and resistance to breakdown at high voltages are very satisfactory. Also, due to their excellent melt strength and unusually high activation energy of viscous flow, these thermoplastics are particularly well adapted for high-speed extrusion processes.<sup>99</sup>

The dynamic mechanical behavior of the ionomer at room temperature and above resembles more that of conventional polyethylene than that of its parent ethylene-methacrylic acid copolymer.<sup>98</sup> While the acid copolymer exhibits a room temperature relaxation, the ionomer and polyethylene, both undergo mechanical transitions at  $-10^{\circ}\text{C}$  and at  $62^{\circ}\text{C}$ . Rees and Vaughan attributed the  $-10^{\circ}\text{C}$  relaxation in the ionomer to an interlamellar transition, like in conventional polyethylene. The  $25^{\circ}\text{C}$  loss peak in the acid was argued as being evidence for the onset of mobility in chain segments held rigid at lower temperatures by hydrogen bonding.



The 62°C transition, which in polyethylene represents a crystalline disordering transition, was instead assigned to the ionic bonding in the ionomer which, being less labile than hydrogen bonding-type interactions, would be effective at higher temperatures.

Exactly, how the ionic interactions affected the morphology of these materials on a molecular scale remained an unsolved problem for some time until MacKnight and co-workers carried out a series of investigations in order to elucidate the possibility of microphase separation in organic polymers containing acid or ionic side groups.<sup>100-115</sup> A variety of analytical techniques were utilized to conduct these studies. These included dynamic mechanical viscoelasticity, dielectrics, dynamic and steady-shear melt rheology, X-ray scattering (both wide angle and low angle), birefringence, scanning electron microscopy, infrared dichroism, thermogravimetric analysis, infrared analysis and differential scanning calorimetry.

The first of three systems investigated by MacKnight et.al. consisted of copolymers of ethylene and either methacrylic or acrylic acid neutralized to form various salts.<sup>100-109</sup> The acid groups in the acid copolymers were found to exist largely in the form of hydrogen bonded dimers below the glass transition temperature of the material. Strong inverse dependence of crystallinity on acid content indicated that such dimers could not be accommodated in the crystal phase.<sup>109</sup> The dielectric behavior of both the acid copolymers and their salts paralleled their dynamic mechanical behavior as reported by Rees and Vaughan.<sup>98</sup> The high temperature  $\alpha$  peak was shown to arise from microphase separated ionic clusters dispersed in the hydrocarbon matrix.<sup>103, 108, 109</sup> McKenna

argued that a three phase model consisting of ionic domains and ill-developed crystalline regions dispersed in a polyethylene-like amorphous matrix explained the mechanical relaxation and crystallization behavior of these systems.<sup>102</sup> He found that the extent of this phase segregation increased with ionization and annealing. Also, since the nature of the crystalline regions was affected by ionization, he concluded that ionic phase segregation influences both development of crystallinity and lamellar structure. A combined low angle and wide angle X-ray scattering investigation of the unionized copolymers and salts (mainly the cesium salt) of ethylene-methacrylic acid and ethylene-acrylic acid (2.1 to 6.3 mole % acid) confirmed the existence of microphase segregated domains in these materials.<sup>108,109</sup> The ionic groups of cesium salts were found to range in size from atomic dimensions to about 20 Å in diameter. The larger regions resulted, therefore, from the aggregation of ions into spherical clusters composed of 50-100 ionic groups. The low angle maximum in the scattering pattern of the dry salts was shown to be an interference peak resulting from short range ordering of ionic groups around larger ionic clusters.<sup>109</sup> Melt rheology studies indicated that the ionic domains retained their integrity in the melt to high temperatures.<sup>104</sup>

### 3. Ethylene-Phosphonic Acid Copolymers

In a series of random ethylene-phosphonic acid copolymers, prepared by chlorophosphorylation of polyethylene followed by hydrolysis, new mechanical and dielectric relaxation peaks occurred in the copolymer containing 7.4 mole percent of phosphonic acid groups. This behavior was interpreted as arising due to the presence of clusters of phosphonic acid groups stabilized by hydrogen bonding.<sup>110-113</sup> Recently, several phos-



phosphonates of low density polyethylene were prepared and characterized.<sup>114</sup> The properties of the materials containing low molecular weight substituent groups such as dimethyl phosphonate could be adequately explained by random copolymer theory. On the other hand, phosphonates of higher molecular weight and polarity (polyethylene oxide-phosphonate ester grafts) were found to exhibit microphase separation although dynamic mechanical results indicated that complete phase segregation may not have occurred.

#### 4. Ionomers Based on Polypentenamers

A third class of organic polymers containing acid or ionic side groups is represented by a completely hydrogenated polypentenamer modified by the random incorporation of pendant thioglycolate groups which are capable of being hydrolyzed to various salts or the free acid of the corresponding ester.<sup>115</sup> The resulting materials, unlike the  $\alpha$ -olefin derivatives, exhibit a uniform molecular weight and molecular weight distribution as a function of composition as well as a random distribution of acid or ionic groups along the polymer chain. Furthermore, due to the unique polypentenamer structure of the unhydrogenated precursor, both the ionized and unionized hydrogenated polymers are completely free of alkyl chain branching. Pendant group content affects the glass transition temperatures and melting points of these polymers, as expected, but no major difference in calorimetric properties is observed between polymers in which the pendant groups are in the salt form as compared to those in the corresponding carboxylic acid form. In addition, the thermal stability of ionomers bearing divalent ions, particularly the calcium

ion, is markedly lower than that of the monovalent salt derivatives.<sup>115</sup>

#### 5. Ionomers Based on Polyoxymethylene

A new dimension was added to the study of ionomers and their unionized precursors when polyoxymethylene was selected as the linear crystallizable backbone on which pendant ester, acid or ionic groups could be incorporated. Polyoxymethylenes with ester groups were obtained by copolymerizing trioxane with the ethyl or methyl ester of glycidic acid,<sup>1, 2</sup> with p-glycidoxybenzoic acid esters<sup>3</sup> or with ethoxy-carbonyl-1,3-dioxolane.<sup>6</sup> In all cases, base hydrolysis led to polyoxymethylenes with free carboxyl groups. The sodium salts could also be obtained by copolymerization of trioxane with epichlorohydrin followed by a coupling reaction with disodium thioglycolate.<sup>4, 5</sup> The corresponding free acid or salts of different cations have been produced by treatment of the polymeric sodium salt with a dilute solution of acetic acid in a dioxane/water mixed solvent or with an excess of the chloride of the appropriate cation in aqueous medium, respectively.<sup>116</sup>

The tensile, calorimetric and flow properties and water sensitivity of oxymethylene copolymers containing pendant ionic groups have been investigated by Wissbrun and co-workers.<sup>4</sup> The ionomers were obtained by reaction of disodium thioglycolate with a copolymer of trioxane and epichlorohydrin. The lithium, sodium and potassium monovalent cations and the magnesium, calcium and strontium divalent cations were incorporated. A major drawback of this particular system was exemplified by a decrease in the molecular weight of the copolymers with increasing epichlorohydrin content (since larger amounts of initiator were required

to cause polymerization). As a consequence, a direct comparison of properties could only be made over a narrow range of compositions. On the other hand, a comparison of the properties of the ionomers versus those of the corresponding unionized copolymers at a given copolymer composition was justifiable. The ionic copolymers were found to differ from the non-ionic copolymers in that the crystalline order was poorer, which resulted in increased transparency and ductility and in decreased stiffness and strength. At least in part, this was believed to be a consequence of the effects the ions exerted on the kinetics of the crystallization process. Melt viscosity and the temperature dependence of the melt viscosity of the ionic copolymers was higher than those of the non-ionic copolymers. Introduction of ionic groups also increased water sensitivity to a degree determined by the nature of the cation and by the polarity of the polymer. Ionomers neutralized with divalent cations showed some unusual aging effects.

The present dissertation describes the preparation and characterization of oxymethylene polymers.

## EXPERIMENTAL PART

## A. Materials

## 1. Monomers

Trioxane (Celanese Research Co.) was recrystallized from dichloromethane and distilled from sodium, in the presence of a small amount of benzophenone, immediately before use (Karl Fischer analysis:  $\leq 60$  ppm  $H_2O$ ). 1,3 Dioxolane (Eastman Organic Chemicals) was distilled from lithium aluminum hydride before use (Karl Fischer analysis:  $\leq 28$  ppm  $H_2O$ ).

## 2. Initiators

Gaseous boron trifluoride (Matheson Products) was used as supplied. Boron trifluoride diethyl etherate (Aldrich Chemical Co.), antimony pentachloride (Alfa Products) (b.p.  $86^\circ C$ , 30 mm) and trifluoromethane sulfonic acid (Aldrich Chemical Co.) (b.p.  $76^\circ C$ , 30 mm) were distilled through a Vigreux column and stored in the refrigerator, in tightly capped bottles, before use.

## 3. Reagents

Ethyl acrylate (Aldrich Chemical Co.), propionic anhydride (Aldrich Chemical Co.) (b.p.  $68^\circ C$ , 25 mm) and triethylamine (Eastman Organic Chemicals) were distilled before use. Trifluoroacetic anhydride (Aldrich Chemical Co.), 90 percent hydrogen peroxide (FMC Corp.), glacial acetic acid (Fisher Scientific Co.), d,l- $\alpha$ -pinene (Aldrich Chemical Co.) and tributylamine (Aldrich Chemical Co.) were used without further purification. All solid reagents, including the metal halides, bases, buffers and drying agents, were obtained from the Fisher Scientific Company or Alfa Products and were used as supplied.



#### 4. Solvents

1,2 Dichloroethane (Aldrich Chemical Co.), dichloromethane (Fischer Scientific Co.) and dioxane (Mallinckrodt Chemical Works) were distilled from lithium aluminum hydride before use (Karl Fisher analysis (1,2 dichloroethane):  $< 40$  ppm  $H_2O$ ). When dry methanol and ethanol were required, these solvents were refluxed over calcium oxide for 48 hours, distilled from sodium and stored over molecular sieves. Ninety-nine percent pure dimethylformamide and benzyl alcohol (Aldrich Chemical Co.) were stored in the refrigerator and used as supplied.

#### 5. Polymer Solvents

p-Chlorophenol (m.p.  $38 - 40^{\circ}C$ ) (Eastman Organic Chemicals) was distilled at reduced pressure (b.p.  $94^{\circ}C$ , 8 mm). For viscosity measurements, two percent by weight of d,l- $\alpha$ -pinene was added to the p-chlorophenol. Deuterated and undeuterated, hexafluoroisopropanol (Aldrich Chemical Co.), hexfluoroacetone sesquihydrate (Aldrich Chemical Co.) and octafluoro-1-pentanol (Pfaltz and Bauer Inc.) were used without further purification. Hexafluoroacetone sesquihydrate was buffered with triethylamine (one percent by weight) before use.

#### 6. Polymer Stabilizers

Cyanoguanidine (Aldrich Chemical Co.) and di- $\beta$ -naphthyl phenylene diamine antioxidant were used as supplied.

#### 7. Polymer Samples

Films of five copolymers of trioxane, containing different amounts of sodium thioglycolate substituted oxyethylene units randomly distributed along the polymer chain, were obtained from the Celanese

Research Company. Their preparation and characterization are described in literature.<sup>4, 5</sup> These copolymers will, hereafter, be referred to as STG copolymers to differentiate them from the copolymers and terpolymers prepared in our laboratories.

## B. Measurements

Most infrared spectra were recorded on a Perkin Elmer 727 Spectrophotometer. Some polymer spectra were recorded on a Perkin Elmer 283 Spectrophotometer. Solid samples were measured as thin films ( $\sim 1$  mil thick) or as pressed pellets and liquid samples were measured between sodium chloride plates. The peak assignments were made to the nearest 0.1 micron.

Gas chromatograms on liquid samples were recorded on a Varian 920 Aerograph. Helium was used as the carrier gas.

The PMR spectra of low molecular weight compounds were measured on a 60 MHz R-24 Hitachi Perkin Elmer Spectrometer. Polymer spectra were recorded, at room temperature, in deuterated hexafluoroacetone sesquihydrate on a 90 MHz R-32 Perkin Elmer Spectrometer.

The thermal properties of the polymers were determined on a Perkin Elmer DSC-1B Differential Scanning Calorimeter, at a scanning rate of 20°C/min. The instrument was calibrated against salicylic acid, benzoic acid and indium.

Dielectric properties were measured on a General Radio 1615-A Capacitance Bridge consisting of a 1620-A Capacitance Measuring Assembly and a 1311-A Audio Oscillator generating frequencies ranging

from 50 Hz to 10 kHz. Film samples were placed between circular capacitor plates, 53 mm in diameter, mounted on a Balsbaugh Laboratories cell. Temperatures were monitored with a Leeds and Northrup potentiometer.

The dynamic mechanical properties measurements were carried out on a Toyo DDV-II-B Rheovibron Dynamic Viscoelastometer. A Toyo pyrometer recorded temperatures from liquid nitrogen to about 150°C. Readings were taken at a constant frequency of either 3.5, 11 or 110 Hz.

All calorimetric, mechanical and dielectric experiments were carried out under a dry nitrogen atmosphere. Polymer films were compression molded, under nitrogen, between platens on a Pasadena press.

## C. Preparations

### 1. Synthesis of Ethyl Glycidate

A solution of peroxytrifluoroacetic acid was prepared by adding, with stirring over a five minute period, trifluoroacetic anhydride (76.5 ml, 0.54 moles) to a 250 ml beaker containing a suspension of 90 percent hydrogen peroxide (12.5 ml, 0.45 moles) in ethylene dichloride (50 ml) cooled in an ice bath.

The resulting colorless solution was carefully transferred to an additional funnel fitted to a 1000 ml three-necked round bottom flask that was also equipped with a reflux condenser and a motor stirring unit. The flask contained a mixture of ethylene dichloride (250 ml), disodium hydrogen phosphate (204 g, 1.44 moles) and ethyl acrylate (22.9 g, 0.23 moles) maintained under a nitrogen blanket, with efficient stirring.



The contents of the flask were allowed to come to reflux by immersing the flask in an oil bath set at 100°C. The solution in the addition funnel was then added dropwise, over a 30 minute period, to the boiling mixture. The resulting slurry was stirred vigorously, at reflux, for an additional 30 minutes.

The reaction was stopped first by removing the heat source and immersing the flask into an ice bath and then by adding approximately 500 ml of water, through the addition funnel, while the stirring and nitrogen flow were still being maintained. The water dissolved most of the salts. The contents of the flask were subsequently transferred to a 10 l beaker and stirred with an additional 500 ml of water to complete the dissolution of salts. Two colorless layers resulted. The bottom (organic) layer was separated and the aqueous layer extracted with three 100 ml portions of methylene chloride. The combined organic extracts were washed with 100 ml of a five percent sodium bicarbonate solution and dried over magnesium sulfate.

Most of the solvent was evaporated at reduced pressure at a temperature not exceeding 40°C. The residual liquid was then fractionated, through a Vigreux column, to yield 11.8 g (51.7%) of ethyl glycidate (b.p. 73-77°C, 30 mm) (lit. 88-90°C, 60 mm, lit. 60-64°C, 23 mm).<sup>117, 118</sup>

The infrared spectrum (liquid film) showed absorptions at 5.8  $\mu$  (C=O ester stretching), 8.0  $\mu$  and 11.0 - 13.0  $\mu$  (deformation vibrations of the epoxy group) and no absorption at 6.0 to 6.1  $\mu$  (indicating the absence of C=C).<sup>119</sup> The PMR spectrum (CCl<sub>4</sub>) showed



$\delta$  : 1.30 ( $\text{COOCH}_2\text{CH}_3$ , 3) ; 2.88 ( $-\overset{|}{\text{CH}}_2$ , 2) ; 3.35 ( $-\overset{|}{\text{CH}}-$ , 1) ; 4.22 ( $\text{COOCH}_2\text{CH}_3$ , 2). (Figure 1).

## 2. Gas Phase Polymerization

### a. Trioxane - Dioxolane Copolymer

Trioxane (81.8 g, 0.91 moles) and 1,3 dioxolane (17.0 g, 0.23 moles) were introduced in separate nitrogen gas streams into the top of a stainless steel cylindrical mixer along with the boron trifluoride initiator, also in a nitrogen carrier. The reactor had a diameter of approximately three inches and a length of twelve inches and was jacketed with a standard heating tape to control the temperature in the mixing device.

Immediately prior to polymerization, an amount slightly in excess of the indicated weight of trioxane was distilled from sodium directly into a three necked round bottom glass vaporizer. The heating tapes surrounding the flow lines for the trioxane and the dioxolane and those surrounding the cylindrical mixer were then set to achieve a temperature of approximately  $140^\circ\text{C}$  in each of the lines and within the mixer. Two oil baths, one adjusted to  $120^\circ\text{C}$  and the other to  $80^\circ\text{C}$ , were utilized to heat up the two monomers to approximately  $5^\circ\text{C}$  below their respective boiling points.

Nitrogen was passed through the trioxane and dioxolane and, at approximately the same instant, a gaseous mixture of five moles of nitrogen per mole of boron trifluoride were introduced in the upper area of the reactor at a rate of 5 cc/min. The mixed vapors from the upper stage of the reactor were quenched in the lower portion of a

large filter flask which was immersed in a dry ice-isopropanol mixture. Nitrogen gas was bled off through an exhaust port in the neck of the collection vessel.

The polymerization reaction was allowed to proceed for one hour. The amount of each monomer, used up in the polymerization, was determined by weighing each vaporizer flask before and after the run.

A chalky white solid was collected in the filter flask, washed with water, aqueous sodium bicarbonate, again water and methanol and finally dried at 65°C (30 mm) for 16 hours to give 85.3 g (87% yield) of polymer. The polymer was insoluble in most common organic solvents but swelled in water and in acetone.

Base unstable segments were removed by reacting 20 g of crude polymer with 5.0 g of potassium hydroxide in 300 ml of benzyl alcohol at 160°C for one hour. The mixture was held under a nitrogen blanket during the reaction. The solid which precipitated upon cooling was filtered, washed with water and methanol and dried at 80°C (30 mm) for 16 hours to give 12.2 g (61% yield) of polymer.

The inherent viscosity of a 0.1% solution of the base stable copolymer in 98/2 p-chlorophenol/  $\alpha$ -pinene at 60°C was 0.83. The PMR spectrum (deuterated hexafluoroacetone sesquihydrate, 35°C) showed  $\delta$  : 4.8 to 5.2 ( $\text{CH}_2\text{O}$ , 2) ; 3.7 to 4.0 ( $\text{CH}_2\text{CH}_2\text{O}$ , 4). According to the PMR analysis, the copolymer consisted of approximately seven mole percent of oxyethylene units, as judged by the relative

integrated signal intensities of the oxyethylene protons and oxymethylene protons of the main chain repeat units.

b. Trioxane Homopolymer and Trioxane - Ethyl Glycidate Copolymer

Trioxane (117.2 g, 1.30 moles) and boron trifluoride initiator were introduced in separate nitrogen gas streams into the top of the reactor, following the same procedure described above. The comonomer flow line was temporarily shut off by means of a three-way Teflon stopcock. The same reaction conditions, described in the previous section, were maintained for this experiment.

During the one hour reaction, a fluffy white solid was collected in the filter flask; afterwards, it was worked up with water, aqueous sodium bicarbonate, again water and acetone and then dried in a vacuum oven at 65°C, for 16 hours, to give 99.2 g (85% yield) of polymer.

At the end of the first hour, the stopcock was opened to allow the mixture of ethyl glycidate (8.0 g, 0.07 moles) and nitrogen gas to flow into the top of the reactor along with the trioxane (117.2 g, 1.30 moles) and the boron trifluoride, also in nitrogen carriers. The ethyl glycidate vapor was obtained by heating the liquid monomer with a silicone oil bath set at 190°C. A chalky white solid was collected in the filter flask, during the next hour. After the run, the same workup and drying procedures were followed to give 105.1 g (84% yield) of polymer.

The flow rates of the trioxane/nitrogen mixture and of the boron trifluoride/nitrogen mixture were maintained constant for the entire duration of both reactions. The total amount of each monomer utilized in the combined runs was again determined by weighing each



vaporizer flask before and after the two reactions. Approximately one half of the total amount of trioxane was used up in the one hour homopolymerization reaction and the other half was consumed during the one hour copolymerization reaction.

The thermally unstable homopolymer was capped with ester endgroups by dissolving 10 g of the polymer in a mixture containing 1000 ml of dimethylformamide, 400 ml of pure propionic anhydride and 80 ml of tributyl amine at 160°C, under nitrogen. After dissolution occurred, the mixture was stirred under reflux at 155°C for an additional 30 minutes. 9.4 g (94% yield) of the polymer, which precipitated upon cooling, were recovered after workup. The presence of the propionate endcaps was verified by infrared spectroscopy. A new moderately weak absorption at approximately  $5.8\ \mu$ , due to the ester carbonyl, replaced a broad absorption between  $2.7\ \mu$  and  $3.0\ \mu$ , due to the hydroxyl endgroups.

The base stability of the trioxane-ethyl glycidate copolymer (i.e. the amount of polymer recovered after high temperature exposure to potassium hydroxide) was 35 percent.

3.1 g (62% yield) of heat treated ester copolymer were obtained by heating 5.0 g of the crude trioxane-ethyl glycidate copolymer in 750 ml of dimethylformamide until a clear light gold solution resulted (at approximately 160°C). The gel which precipitated upon cooling was then washed with methanol and finally dried under vacuum.

The inherent viscosity of a 0.1% solution of the heat treated ester copolymer in 98/2 p-chlorophenol/  $\alpha$ -pinene at 60°C was 0.35 while that of the endcapped homopolymer was 1.35. The DSC melting points of



the same homopolymer and copolymer were 168°C and 161°C, respectively. The copolymer exhibited a strong infrared absorption at  $5.8\mu$  due to the ethyl ester carbonyl on the side chains. The PMR spectrum of the same (deuterated hexafluoroacetone sesquihydrate, 35°C) showed  $\delta$ : 4.8 to 5.2 ( $\text{CH}_2\text{O}$ ); 1.2 to 1.4 ( $\text{COOCH}_2\text{CH}_3$ , 3). According to the PMR analysis, the copolymer consisted of approximately two mole percent 1-carboethoxy oxyethylene units as judged by the relative integrated signal intensity of the ethyl ester methyl protons to that of the oxymethylene protons.

#### c. Ionomers from Trioxane-Ethyl Glycidate Copolymer

40 g of crude trioxane-ethyl glycidate copolymer were slurried with 30 g (0.75 moles) of sodium hydroxide in a dioxane/water mixture (1600 ml/400ml) for one hour at 85°C, under nitrogen. The solid product, separated from the mixture, after the slurry was cooled to room temperature, was washed with methanol and dried under vacuum (30 mm) at 60°C for 16 hours, to give 18.5 g (45% yield) of polymer.

The infrared spectrum of this polymer (Figure 2) showed two new absorptions between  $6.2\mu$  and  $6.3\mu$  and between  $7.0\mu$  and  $7.1\mu$  due to the carboxylate anion but retained a weak shoulder at  $5.8\mu$  due to the polymeric salt. The inherent viscosity of a 0.1 % solution of the ionomer in 98/2 p-chlorophenol/ $\alpha$ -pinene at 60°C was 0.33. 1.1 % sodium, found in the polymer, corresponded to approximately 1.4 mole % of comonomer units.

Two 100 ml round bottom flasks were each charged with 5 g of the sodium salt of the trioxane-ethyl glycidate copolymer, 35 ml of

deionized water and with 1.9 g (0.05 moles) of lithium chloride or 3.8 g (0.02 moles) of cesium chloride, respectively. The flasks were then equipped with a magnetic stirring bar and fitted with a condenser. The reactants were stirred vigorously at room temperature, under nitrogen. The pH of the metal chloride aqueous solutions, during the lithium and cesium exchange reactions, changed from 6.1 to 6.6 and from 4.8 to 6.6, respectively. After one hour, the solids were recovered by filtration, washed extensively with deionized water to remove salt impurities and methanol and finally dried over phosphorous pentoxide, for 16 hours at 60°C (30 mm). The yields for both reactions were quantitative.

Analysis of the polymeric cesium salt for sodium (0.2% Na) indicated that approximately 0.3 mole percent of the comonomer units in the polymer had not exchanged. The analyses of the polymeric lithium salt (Li : 0.3%, Na : 0.04%) showed that approximately 1.3 mole % of the comonomer units in the polymer had exchanged. The inherent viscosities of 0.1% solutions of the polymeric salts in 98/2 p-chlorophenol/ $\alpha$ -pinene at 60°C were 0.32 for the lithium salt and 0.34 for the cesium salt. Infrared absorptions, due to the carboxylate anion in the lithium and cesium ionomers, were found at 6.2  $\mu$  and 7.0  $\mu$  and at 6.3  $\mu$  and 7.1  $\mu$ , respectively. In both cases, the shoulder at 5.8  $\mu$ , due to the ester carbonyl, was still present (Figure 3).

#### d. Acid Derivative of Trioxane-Ethyl Glycidate Copolymer

The sodium salt of the trioxane-ethyl glycidate copolymer (5g) and 5 ml of glacial acetic acid were stirred vigorously in 200 ml of dioxane and 45 ml of deionized water for three hours at room

temperature, under nitrogen. The filtered solid was washed repeatedly with water, then with methanol and finally dried under vacuum, at 60°C for 16 hours, to give 4.2 g (84% yield) of polymer.

The infrared spectrum of the polymeric acid exhibited the characteristic broad carboxylic acid carbonyl absorption at  $5.8\mu$  (Figure 2). Its inherent viscosity in 98/2 p-chlorophenol/ $\alpha$ -pinene (0.1% solution) at 60°C was 0.36. The presence of less than 0.05% sodium in the polymer indicated that the hydrolysis reaction had essentially gone to completion.

### 3. Solution Polymerization

#### a. Trioxane-Dioxolane Copolymers

Trioxane (102.5 g, 1.14 moles) was distilled from sodium directly into a three-necked round bottom flask equipped with a glass stopper and a stirring rod and shaft unit. At the end of the distillation, a rubber septum was rapidly fitted around the neck through which the trioxane had been introduced and the entire assembly was transferred to a dry box. Next, freshly distilled, dry 1,2 dichloroethane (241 ml) was added to the trioxane. The flask was shaken until all the trioxane appeared to have dissolved. 11.2 g (0.15 moles) of dioxolane were then introduced into the polymerization flask and the septum was quickly fitted into place.

The initiator solution was prepared fresh by syringing 0.1 ml ( $1.3 \times 10^{-3}$  moles) of trifluoromethane sulfonic acid, through a rubber septum, into a vial containing 14 ml of 1,2 dichloroethane. Dry nitrogen was bubbled into the light gold solution during the addition of the acid.



Next, the polymerization flask, containing the monomers and the solvent, was rapidly transferred out of the dry box and immersed into an oil bath at 40°C. Thereafter, rapid stirring was initiated as a slow stream of dry nitrogen was being bled in and out of the flask. Nine ml of the initiator solution were added through the septum and into the flask over a period of one minute. Two additional minutes elapsed before the first visible appearance of cloudiness in the reaction medium. Polymer crystals continued to precipitate for some time. The reaction was allowed to proceed for three hours.

A very fine white polymer powder was filtered, washed with a five percent sodium bicarbonate solution, water and finally with methanol. It was dried at 65°C (30 mm) for 16 hours to give 111.1 g (97% yield) of polymer. This polymer was labeled TD-10.

Thirty grams of the crude copolymer were reacted with 7.5 g of potassium hydroxide in 450 ml of benzyl alcohol at 160°C to remove the base unstable segments. Nitrogen was slowly bubbled into the reaction mixture to minimize oxidative degradation during the one hour reaction. Twenty-five grams (83% yield) of a fine white solid were recovered after workup.

Copolymers TD-20 and TD-30, each incorporating increasingly higher levels of dioxolane, were prepared and stabilized in the same manner. Thus, 90.0 g (1 mole) of trioxane and 18.5 g (0.25 moles) of dioxolane, dissolved in 250 ml of dichloroethane, were polymerized in the presence of 0.06 ml ( $8.5 \times 10^{-4}$  moles) of trifluoromethane sulfonic acid to give 104.16 g (96% yield) of TD-20. The induction period for this polymeriza-



tion was five minutes. A 95% base stable copolymer was recovered after high temperature exposure to potassium hydroxide.

TD-30 was obtained in 67% yield by reacting 42.2 g (0.47 moles) of trioxane with 14.8 g (0.20 moles) of dioxolane after 0.03 ml ( $4.6 \times 10^{-4}$  moles) of trifluoromethane sulfonic acid were added to the two monomers dissolved in 125 ml of 1,2 dichloroethane. A fifteen minute induction period was observed for this reaction. The base stability of TD-30 was 87%.

The intrinsic viscosities of the base stable copolymers were measured at room temperature in a hexafluoroacetone-water mixed solvent (mole ratio 1/1.5). These values are reported in Table 3 along with the corresponding values for the weight average molecular weight calculated using the expressions derived by Stockmayer and Chan.<sup>68</sup>

The PMR spectra of the three copolymers (deuterated hexafluoroacetone sesquihydrate, 35°C) showed  $\delta$  : 4.8 to 5.2 ( $\text{CH}_2\text{O}$ , 2) ; 3.7 to 4.0 ( $\text{CH}_2\text{CH}_2\text{O}$ , 4). The mole percent of oxyethylene units determined from the integrated PMR signals, is also listed in Table 3.

Table 3  
Characterization of Trioxane-Dioxolane Copolymers

<u>Sample Designation</u>	<u>TD-10</u>	<u>TD-20</u>	<u>TD-30</u>
Intrinsic Viscosity (dl/g)	2.3	1.9	3.2
Weight Average Molecular Weight	$9.8 \times 10^4$	$7.2 \times 10^4$	$1.6 \times 10^5$
CH <sub>2</sub> CH <sub>2</sub> O units/100 CH <sub>2</sub> O units based on PMR	2.2	3.2	4.2

The PMR peak assignments in the copolymers are confirmed by a comparison of the spectrum for TD-30 (Figure 4a) with those for a gas phase trioxane homopolymer (Figure 4b) and a polydioxolane prepared in bulk using antimony pentachloride as the cationic initiator (Figure 4c).

The ratio of the  $7.8 \mu$  absorbance (backbone ethylene torsion vibration) to the standard  $4.3 \mu$  absorbance, in the infrared, remained unchanged at 1.7 for samples TD-10 and TD-20 but increased to 2.0 for TD-30 (Figure 5). A relatively weak hydroxyl absorption ( $2.7 \mu - 3.0 \mu$ ) was observed in all three cases.

#### b. Trioxane-Ethyl Glycidate Copolymers

An attempt was made to prepare a trioxane-ethyl glycidate copolymer in solution. Thus, 1.5 g ( $1.7 \times 10^{-2}$  moles) of trioxane and 0.25 g ( $2.1 \times 10^{-3}$  moles) of ethyl glycidate were dissolved in 3.3 ml of 1,2 dichloroethane and reacted with 0.001 ml ( $1.5 \times 10^{-5}$  moles) of trifluoromethanesulfonic acid for three hours at 40°C. No polymer was recovered from the reaction mixture. The same amount of trioxane, dissolved in 3.3 ml of 1,2 dichloroethane at 40°C, gave an 80% yield of homopolymer, five minutes after the addition of 0.001 ml of the initiator.

High yields of copolymer could be obtained by adding less comonomer, more initiator and by adjusting the reaction temperature close to the melting point of trioxane. In a representative example, 11.4 g ( $1.3 \times 10^{-1}$  moles) of trioxane, 0.75 g ( $6.5 \times 10^{-3}$  moles) of ethyl glycidate and 0.006 ml ( $9.3 \times 10^{-5}$  moles) of trifluoromethane sulfonic acid were reacted in 25 ml of 1,2 dichloroethane for three hours at 60°C to give a 93% yield of copolymer. Its base stability was 19%.

c. Trioxane-Ethyl Glycidate-Dioxolane Terpolymers

In a series of experiments, ethylene oxide units were introduced randomly along the backbone of polymer chains containing methylene oxide units and 1-carboethoxy oxyethylene units. The purpose of these experiments was to obtain ionizable polymers, in moderate yields, that exhibited high base stabilities. All reactions, except one, were carried out in 25 ml of 1,2 dichloroethane for three hours at 60°C. The results of these preliminary experiments are summarized on the next page (Table 4).

Table 4

## Solution Polymerization of Trioxane, Ethyl Glycidate and Dioxolane

<u>Trioxane</u>	<u>Ethyl Glycidate</u>	<u>Dioxolane</u>	<u>Initiator</u>	<u>Yield</u>	<u>Base Stability<sup>a</sup></u>
(mole %)	(mole %)	(mole %)	(mole %)	(%)	(%)
95	5	0	0.07 <sup>b</sup>	93	19.0
85	5	10	0.10 <sup>b</sup>	28	-
85	5	10	0.07 <sup>c</sup>	62	85.5
85	5	10	0.07 <sup>c</sup>	62	95.0
90	5	5	0.05 <sup>c</sup>	90	41.5
75	15	10	0.06 <sup>c</sup>	40 <sup>d</sup>	69.5
75	10	15	0.12 <sup>c</sup>	52	78.5

<sup>a</sup>Polymer recovered after high temperature exposure to potassium hydroxide.

<sup>b</sup>Trifluoromethane sulfonic acid.

<sup>c</sup>Boron trifluoride diethyl etherate.

<sup>d</sup>Thirty minutes at 60°C in 15 ml of 1,2 dichloroethane.

In the course of three scale-up procedures, the amount of ethyl glycidate in the feed was varied from 5 to 15 mole percent while the amount of dioxolane was maintained constant (10 mole percent). The resulting terpolymers were labeled TED 5, TED 10 and TED 15, respectively. The trioxane and dioxolane monomers, dissolved in dichloroethane, were stirred vigorously in a three-necked round bottom flask, immersed in an oil bath at 65°C. The boron trifluoride diethyl etherate initiator was added as a solution in dichloroethane. This solution was added through a rubber



septum directly into the reaction medium. After approximately 15 minutes, the solution in the polymerization flask became cloudy. At this point, the ethyl glycidate was rapidly added to the reaction mixture through an addition funnel. The reaction was allowed to proceed for a specified period of time after which the stirring was discontinued and the flask was removed from the oil bath.

The workup and drying procedures were the same as used for the recovery of copolymers TD-10, TD-20 and TD-30. The recipes, reaction conditions and yields for these experiments are listed in Table 5

Table 5

#### Synthesis of Trioxane-Ethyl Glycidate-Dioxolane Copolymers

<u>Sample Designation</u>	<u>TED 5</u>	<u>TED 10</u>	<u>TED 15</u>
Trioxane, g (moles)	184.0 (2.04)	161.9 (1.80)	178.5 (1.98)
Ethyl Glycidate, g (moles)	12.4 (0.11)	26.1 (0.23)	45.9 (0.40)
Dioxolane, g (moles)	16.8 (0.23)	16.6 (0.23)	19.5 (0.26)
Initiator, ml (moles)	0.20 ( $1.6 \times 10^{-3}$ )	0.18 ( $1.5 \times 10^{-3}$ )	0.22 ( $1.8 \times 10^{-3}$ )
Solvent, ml	426	403	403
Conditions	2.0 hrs at 65°C	2.5 hrs at 65°C	3.0 hrs at 65°C
Yield, Percent	63	63	50

A Parr reactor was charged with 15 g of crude terpolymer (TED 5) and 322 ml of ethanol. The reactor was flushed with nitrogen and then pressurized with nitrogen to approximately 40 psi. The contents of the reactor were heated to 160°C and stirred at that temperature for one hour. The purpose of this experiment was to thermally unzip any trioxane homo-

polymer that might have been present and also remove thermally unstable hemiacetal endgroups on the terpolymer. At the end of the reaction, the autoclave was lifted out of the variac heating unit and immersed in a bucket of ice-water, causing the thermally stabilized terpolymer to rapidly precipitate out of solution. The solid was washed several times with methanol and dried at 60°C (30 mm) for 16 hours. The entire procedure was repeated for TED 10 and TED 15. The yields of heat treated TED 5, TED 10 and TED 15 were 91%, 96% and 95%, respectively.

#### d. Ionic Derivatives of the Terpolymers

Thirty g of crude trioxane-ethyl glycidate-dioxolane terpolymer (TED 5) were reacted with 4.5 g (0.11 moles) of sodium hydroxide in a methanol/water mixture (386 ml/257 ml) for one hour at 160°C. The reaction was carried out in a Parr reactor at approximately 240 psi. Before heating the reactants to 160°C, the reactor was pressurized with a slight positive nitrogen pressure. At the end of the reaction, the contents of the Parr reactor were rapidly cooled back down to room temperature by immersing the stainless steel reaction vessel into a bucket of ice-water. The solid precipitate was filtered, washed with water and with methanol and finally dried at 60°C (30 mm) for 15 hours. The sodium salts of TED 10 and TED 15 were prepared in exactly the same way. The yields of the TED 5, TED 10 and TED 15 sodium salts were 93%, 83% and 88%, respectively. Their intrinsic viscosities (at 110°C in octafluoropentanol) and respective weight average molecular weights are reported in Table 6. The mole percent of 1-sodium carboxylate oxyethylene in the sodium salts are also reported in Table 6.

Table 6  
Characterization of the Ionic Derivatives of  
Trioxane-Ethyl Glycidate-Dioxolane Terpolymers

<u>Sample Designation</u>	<u>TED 5 (Salt)</u>	<u>TED 10 (Salt)</u>	<u>TED 15 (Salt)</u>
Intrinsic Viscosity (dl/g)	0.30	0.28	0.27
Weight Average Molecular Weight <sup>a</sup>	$1.50 \times 10^4$	$1.40 \times 10^4$	$1.40 \times 10^4$
Mole % $\text{CH}_2\text{CH}(\text{COO}^-\text{Na}^+)_0$ Based on Na	0.9	1.7	2.0

<sup>a</sup>Based on the expression derived by Wagner and Wissbrun.<sup>69</sup>

#### e. Acid Derivatives of the Terpolymers

Five g of each salt of the three terpolymers were stirred vigorously, in separate round bottom flasks, with 5 ml of glacial acetic acid, 45 ml of deionized water and 200 ml of dioxane for three hours, at room temperature, under nitrogen. The filtered solids were washed repeatedly with water, then with methanol and dried under vacuum for 16 hours at 60°C. The yields of the corresponding polymeric acids were 90 percent or higher (taking into account the replacement of a sodium atom with a hydrogen atom during the reaction). The intrinsic viscosity (at 110°C in octafluoropentanol) was 0.3 for all three acids (unchanged from that of the three salt precursors).

Figure 6 shows the infrared spectra of the heat treated ester, the sodium salt and the acid derivatives of TED 5. Two new absorptions between  $6.2\mu$  and  $6.3\mu$  and between  $7.0\mu$  and  $7.1\mu$ , due to the carboxy-



late anion in the salt, are seen to replace the  $5.8\mu$  absorption due to the ester carbonyl. The spectrum of the polymeric acid shows a new absorption at  $5.8\mu$  and a weak absorption at  $6.2\mu$  possibly due to the carboxylate anion of the salt precursor.

Table 7 shows the results of the sodium analyses of the salt and acid derivatives of TED 5, TED 10 and TED 15.

Table 7  
Sodium Content in the Derivatives of  
Trioxane-Ethyl Glycidate-Dioxolane Terpolymers

<u>Sample Designation</u>	<u>TED 5</u>	<u>TED 10</u>	<u>TED 15</u>
Wt % Na in the Salts	0.55	1.01	1.22
Wt % Na in the Acids	0.10	0.10	0.10

#### 4. Bulk Polymerization

Bulk polymerization reactions to prepare trioxane-ethyl glycidate copolymers were also investigated. In one attempt, 1.5 g ( $1.7 \times 10^{-2}$  moles) of trioxane, 0.25 g ( $2.1 \times 10^{-3}$  moles) of ethyl glycidate and 0.001 ml ( $1.5 \times 10^{-5}$  moles) of trifluoromethane sulfonic acid (added as a solution in 0.1 ml of 1,2 dichloroethane) were utilized, and the reaction was allowed to proceed for two hours at  $70^{\circ}\text{C}$ . A 24 percent yield of polymer was obtained. Eleven percent of it was recovered after high temperature exposure to potassium hydroxide. However, when 1.5 g of trioxane was reacted with 0.001 ml of trifluoromethane sulfonic acid (added as a solution in 0.1 ml of 1,2 dichloroethane) at  $70^{\circ}\text{C}$ , gel



formation occurred within three minutes and an 85% yield of homopolymer could be isolated.

Additional attempts to copolymerize ethyl glycidate with trioxane, in the presence of higher levels of trifluoromethane sulfonic acid, gave mediocre yields of products with high content of base unstable fraction. These results are summarized in Table 8.

Table 8

## Bulk Polymerization of Trioxane and Ethyl Glycidate

<u>Trioxane</u>	<u>Ethyl Glycidate</u>	<u>Initiator</u>	<u>Conditions</u>	<u>Yield</u>	<u>Base Stability</u>
(Mole %)	(Mole %)	(Mole %)		(%)	(%)
95	5	15.9	15 min @ 70°C	58	33
90	10	26.0	15 min @ 70°C	32	36
85	15	9.3	15 min @ 70°C	44	5

## 5. Addition of Stabilizers to the Copolymers and Terpolymers

Antioxidant and thermal stabilizers were added, in the final methanol wash, to the base stable TD copolymers and to the heat treated terpolymers, during workup. Thus, a portion of each polymer was slurried in a methanol solution of 0.2 wt % (based on the weight of polymer) of di- $\beta$ -naphthyl phenylene diamine antioxidant and 0.5 wt % (based on the weight of polymer) of cyanoguanidine stabilizer, for one hour at room temperature. Subsequently, the methanol was evaporated off and the solids were, first, air dried for about four hours and then dried at 60°C (30 mm) for 15 hours.

A small portion of each polymer was not treated with stabilizers. This portion was used for the calorimetric studies on polymer powders.

#### 6. Sample Preparation for the Structure and Property Testing

The polymers were dried at  $110^{\circ}\text{C}$  in a vacuum oven for 15 hours and were molded between Ferro-type backed polyester sheets at  $160^{\circ}\text{C}$ , using a 45 second pre-heat period without pressure and a 60 second molding period at 20,000 psi. The Carver press was equipped with a water cooling system. Thus, the films were cooled back down to ambient temperature at approximately  $9^{\circ}\text{C}$  per minute. Films of the TD copolymers all exhibited excellent mechanical strength when molded between Teflon coated aluminum sheets (using a 10 or 20 mil spacer), whereas, the films based on the TED terpolymers, due to their low molecular weight and low inherent mechanical strength, cracked during the cooling cycle. As a result, the dynamic mechanical experiment could be carried out only on one member of the heat treated TED ester series. The TED acid series exhibited some anhydride formation, during the molding procedure, so it was not included in the subsequent dynamic mechanical and dielectric studies.

In order to carry out dielectric relaxation experiments on the TED esters and salts, the samples had to be prepared in a special way. One of the Teflon coated aluminum sheets was replaced with an aluminum sheet during the molding step. The cracked film adhered to the aluminum sheet, upon cooling, and a circular sample with an aluminum backing could be cut out for the dielectric experiment. The error in the dielectric measurements due to air gaps (cracks) in the sample was minimized by the

fact that the sample was relatively thick (between 15 and 30 mils) and the cracks were very narrow.

The STG copolymers were received from the Celanese Research Company in film form with thermal stabilizers and antioxidants already incorporated in them. The films were at least six years old and had aged in air most of that time. The samples, as received, appeared flexible but after being dried at 110°C (30 mm) for 16 hours, they became too brittle to cut. In order to circumvent this problem, the films were stored in a large empty dessicator and exposed to 100% relative humidity at room temperature for a period of a week. After this treatment, the films were flexible enough to be cut smoothly with a razor blade into samples with the proper dimensions for the calorimetric, dynamic mechanical and dielectric experiments. Once the samples were cut, they were dried to constant weight, at 110°C (30 mm). The observed weight loss in the copolymers, during this annealing period, as a function of salt content is reported in Table 9.

Table 9

Weight Loss During Annealing in the STG Copolymers

Sample Designation #	7	2	9	23
Moles % Comonomer <sup>a</sup>	1.3	2.9	4.5	6.5
Weight Before Annealing, g	0.6666	0.8767	0.7562	1.0854
Weight After Annealing, g	0.6631	0.8612	0.7355	1.0493
Percent Weight Loss	0.5	1.8	2.7	3.3

<sup>a</sup>Based on sodium and sulfur analyses.

## D. Structure and Property Testing

### 1. Calorimetric Studies

Measurements of crystallinity were carried out on a Perkin-Elmer DSC-1B Differential Scanning Calorimeter. The instrument and the technique of measuring heats of crystallization have been described in detail.<sup>120, 121</sup> The dried samples, in film form or in powder form (1 to 8 mg), were weighed accurately on a micro-analytical balance to  $10^{-5}$  g and the cover sealed with a crimping device. The samples were then heated in a nitrogen atmosphere from 37°C to 177°C at 20°C/min., held for two minutes at this temperature and finally cooled back down to ambient temperature at 20°C/min.

The freezing curves were well defined, with a horizontal baseline in the melt region and a more or less sharply delineated onset of crystallization. After the peak, there was considerable tailing which caused the end of crystallization to be somewhat indefinite. An estimate of the heat of crystallization was obtained by measuring the area between the exotherm and a baseline extrapolated from the horizontal portion of the low temperature (solid region) baseline. The area was converted to calorie units by calibration with indium. This standard was run at the same range and heating and cooling rate settings as the polymer samples. The following equation was developed for these calculations.



$$\Delta H_c^{\text{sample}} = \frac{\Delta H_c^{\text{indium}} (A_{\text{sample}}) (W_{\text{indium}})}{(A_{\text{indium}}) (W_{\text{sample}})}$$

Where, W is the weight of the material in mg,

$\Delta H_c$  is the heat of crystallization in mcal/mg, and

A is the area under the crystallization curve, respectively.

$\Delta H_c^{\text{indium}}$  was taken as 6.8 mcal/mg.<sup>122</sup> The  $\Delta H_c$  of 100% crystalline polyoxymethylene was assumed to be 50 mcal/mg.<sup>4</sup> The following equation was used to determine percent crystallinity.

$$\% \text{ Crystallinity} = \frac{\Delta H_c^{\text{sample}} (100)}{50}$$

The temperature scale was calibrated, for a given set of instrument settings, using three Fisher Calorimeter Standards, in the temperature range of interest. All temperatures reported are corrected according to the calibration.

The onset of melting was too gradual to permit estimation of the heat of fusion. Melting points were determined by the initial slope method. Occasionally multiple endotherms were observed. Also, the melting endotherms of the TD and TED polymers, after one complete melting-recrystallization cycle, were so undefined that the samples had to be remelted at the same heating rate in order to measure sharper melting points and record sharper melting peak temperatures. In those instances when multiple endotherms were observed, this multiplicity persisted even after two and a half melting-recrystallization cycles. No multiple

crystallization exotherms were observed in any of the samples.

Melting points and melting peak temperatures were also determined for the Vibron and dielectric samples (in film form) of the TD and TED-polymers, after a single melting run at 20°C/min from 37°C to 177°C. This experiment was necessary in order to detect any gross change in the crystallinity of the Vibron or dielectric films due to sample preparation.

## 2. Dynamic Mechanical Studies

A Vibron Dynamic Viscoelastometer (Toyo Measuring Instrument Co.) Model DDV-II was used for this work. The temperature range for these measurements was from liquid nitrogen temperature (about 150°C) to the temperature at which the dynamic force exceeded the value of 1000 at an amplitude factor setting of 30 decibels. The temperatures were measured with a calibrated pyrometer that was provided with the instrument. Measurements were made at a constant frequency of either 3.5, 11 or 110 Hz. This provided a check on the data recorded at a single frequency. In addition, three points could be extracted from the data at three frequencies for a log frequency vs.  $1/T_{\max}$  plot ( $T_{\max}$  being the temperature at which the maximum in a given relaxation process occurs) to give a rough calculation of the activation energy for that mechanical relaxation process.

The Vibron measures the complex tensile or Young's modulus

$$E^* = E' + iE''$$

Where,  $E'$  is the elastic modulus, and

$E''$  is the loss modulus.

The damping function,  $\tan \delta$ , is simply:

$$\tan \delta = \frac{E''}{E'}$$

The  $\tan \delta$  is read directly from the Vibron. The imaginary part of the complex modulus is extracted from the experimental parameters in the following way:

$$E'' \times 10^{-7} = \sin \delta (200/A) ((L + 0.001\Delta L)/D)$$

Where,  $\sin \delta = \tan \delta$  at  $\tan \delta \leq 0.5$  ( $\tan \delta = 2 \sin (\delta/2)$ ).

$A$  = sample thickness (in mils) x sample width (in cm) x  $2.54 \times 10^{-3}$ .

$L$  is the sample length between clamps (in cm).

$\Delta L$  is the change in the sample length from the original length,  $L$ , at a given temperature, and

$D$  is the dynamic force.

Knowing the damping function and the loss modulus, one can solve for the third unknown, the elastic modulus.

Vibron samples of the TD polymers, the Delrin standard and of one TED heat treated ester terpolymer were molded using a 10 mil spacer (1 mil =  $10^{-3}$  in.). The STG Vibron samples were cut from films of the required thickness. The variation in the thickness of each sample was  $\pm 0.5$  mils. Typical sample dimensions are listed in Table 10.

Table 10

## Range of Sample Dimensions for the Vibron Experiment

Sample Thickness (mils)	4 - 10
Sample Width (cm)	0.15 - 0.20
Sample Length (cm)	2 - 5

## 3. Dielectric Studies

Dielectric measurements were carried out using a General Radio Capacitance Measuring Assembly of the transformer ratio arm bridge type (Model 1620 A). Capacitance and  $\tan \delta_\epsilon$  measurements were carried out at 0.2, 0.5, 1, 5 and 10 kHz, over the temperature range -160 to 100°C. Measurements from -160°C to room temperature were made using a three terminal cell (Balsbaugh Type LD-3) with 53 mm, diameter electrodes. Temperature variation in this range was achieved by regulating the flow of dry nitrogen gas through a copper coil immersed in liquid nitrogen and control to  $\pm 0.5^\circ\text{C}$  was achieved. Measurements from room temperature to 100°C were made using a specially constructed two terminal stainless steel cell with 53 mm diameter electrodes and Teflon insulation. Temperature variation, in this range, was achieved by surrounding the dielectric cell with two large heating mantles regulated by two variable current controls. Temperatures were monitored with a Leeds and Northrup potentiometer.

A General Radio Megohmmeter (Type 1862-A) was used to measure d.c. resistance in the range  $10^6$  - 1 Megohms. The data could, in turn, be used to correct the dielectric loss data for d.c. conductivity.

The experimental setup allows one to regard the sample as equivalent to a capacitance in series with a resistance.<sup>123</sup> The di-



electric constant, in an equivalent series circuit, is related to experimental parameters in the following way:

$$\epsilon'_{\text{exp}} = C / C_0 (1 + (\tan^2 \delta_{\epsilon})_{\text{exp}})$$

Where,  $C$  is the measured capacitance in picofarads.

$C_0$ , the capacitance of the capacitor, is related to cell dimensions and sample thickness by

$$C_0 = (565 / \text{sample thickness (in mils)}) + 9, \text{ and}$$

$\tan \delta_{\epsilon}$  is the measured dielectric loss tangent.

The dielectric loss,  $\epsilon''$ , is in turn related to the dielectric constant by a relationship analogous to the mechanical dependence of the loss modulus on the storage modulus.

$$\epsilon''_{\text{exp}} = \epsilon'_{\text{exp}} \tan \delta_{\epsilon} \text{ exp}$$

Porter and Boyd have demonstrated that for both polyoxymethylene and polyethylene oxide the loss behavior in the frequency range from 20 Hz to  $10^7$  Hz cannot be interpreted by a simple series resistor and capacitor model or by a simple parallel resistor and capacitor model.<sup>123, 124, 125</sup>

The same models predict a dielectric constant that is independent of frequency.<sup>123</sup> In contrast, Porter and Boyd found an enormous increase in dielectric constant at low frequency (61 at 20 Hz, 50°C). This same phenomenon has also been observed in the present work and in the dielectric studies of hydrogenated and unhydrogenated cyano-substituted poly-pentenamers.<sup>126</sup> This increase is much too large to be ascribed to a dipole-orientation dispersion. The dominant cause for this effect is

believed to be the relaxation of an impurity ion double layer.<sup>126</sup>

Furthermore, when comparing measured loss data for polyoxymethylene with loss data calculated from the measured d.c. conductivity, it is seen that the calculated loss lies well below the measured loss and a dipole peak would not result from the subtraction of the two curves.<sup>124</sup> Although electrode polarization effects could possibly obviate the legitimacy of using the measured d.c. resistance, it is apparent that it is not possible to extract an  $\alpha$  dipole relaxation peak from the data.

In light of the previous discussion and its obvious relevance to the present work, the cited investigators and this investigator conclude that even if an  $\alpha$  dielectric dispersion does exist, it cannot be resolved from the loss data collected in the 0.2 to 10 kHz frequency range. As a result, the data that showed ionic conductance effects was not analyzed. Unfortunately, in the ionomer samples, these effects may have masked a peak or peaks reflecting orientational relaxations occurring in the ionic domains as well.

The capacitance of the STG samples was observed to decrease steadily, at all frequencies, with a corresponding increase in temperature over the entire temperature range. One would expect the opposite trend. Indeed, the correct trend was observed in the data for the TED, TD and Delrin systems. A major drawback with the STG samples was that they were too thin for the dielectric analysis and there was not enough specimen available to repeat the analysis on thicker samples. The thickness of

all the STG samples was between 4 and 6.5 mils, whereas the recommended size for the analysis is between 10 and 30 mils. Due to the highly questionable nature of these results, the dielectric data collected for the STG samples was not analyzed.

Dielectric samples of the TED polymers, TD polymers and of the Delrin standard were molded using a 20 mil circular spacer. The variation in the thickness of each sample was  $\pm 1$  mil. Typical sample dimensions are listed in Table 11.

Table 11

Sample Dimensions for the Dielectric Experiments

Range of Sample Thicknesses (mils)	16 - 27
Sample Diameter (mm)	60

Due to the high affinity of the TED and STG samples to moisture, all Vibron and dielectric samples were dried to constant weight in a vacuum oven (30 mm) and stored in a dessicator under vacuum prior to analysis.

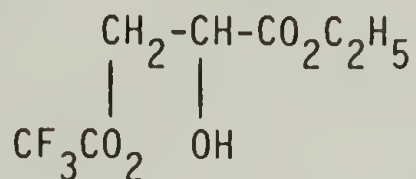
## C H A P T E R I I I

### RESULTS AND DISCUSSION

#### A. Preparations and Preliminary Characterization

##### 1. Synthesis of Ethyl Glycidate

Emmons and Pagano and Aboul-Enein described the preparation of ethyl glycidate by epoxidation of ethyl acrylate with peroxytrifluoroacetic acid (Equation 1) in similar yields to that obtained in the present work, 54% and 50%, respectively.<sup>117, 118</sup> Aboul-Enein also isolated a major by-product in 48% yield. This compound, which boiled at 95 - 99°C (40 mm) was identified spectroscopically to be ethyl (2-hydroxy-3-trifluoroacetoxy)-propionate. It has the following structure:



The substituted propionate could be converted to ethyl glycidate by refluxing with an equimolar amount of sodium hydride in benzene to provide ethyl glycidate in total yield of 84%.<sup>118</sup>

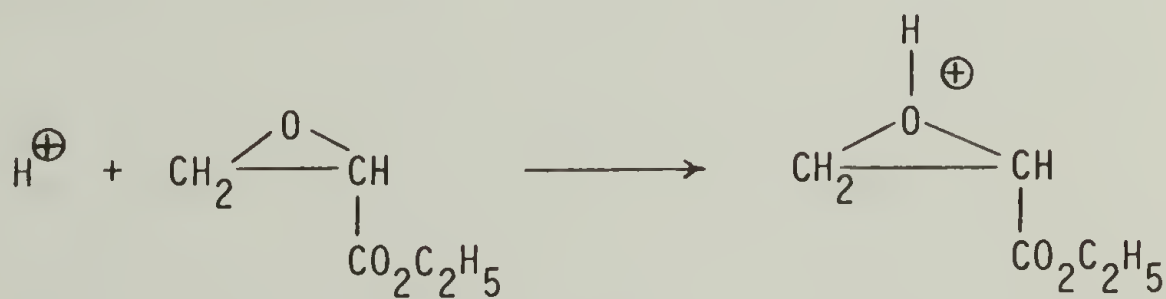
A higher boiling fraction 4 (b.p. 90 - 95°C at 30 mm) was also isolated in the present work in about 40% yield. The infrared spectrum (liquid film) of this fraction (Spectrum D in Figure 7) shows clearly the presence of new absorptions at 2.9 $\mu$  and at 5.6 $\mu$  due to the OH stretch and the C=O trifluoroacetyl stretch, respectively, in addition to the 5.8 $\mu$  (C=O ester stretch) and 8.0 $\mu$  and 11.0 - 13.0 $\mu$  (deformation vibrations

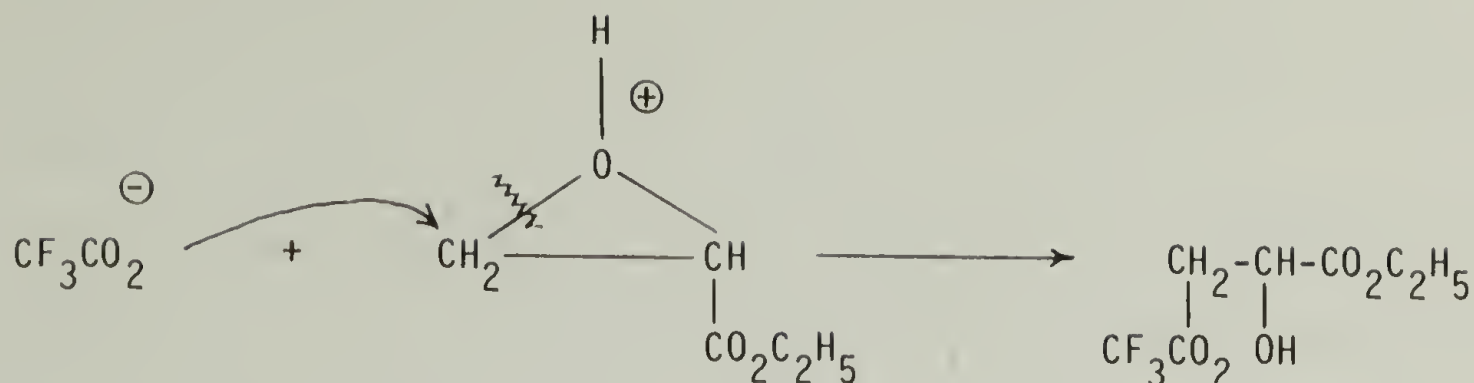


of the epoxy group). The infrared analysis suggests that fraction 4 is a mixture of ethyl glycidate and ethyl (2-hydroxy-3-trifluoroacetoxy)-propionate rather than a pure fraction of the substituted propionate. Spectrums A through C in Figure 7 are the infrared spectra of fractions 1 through 3 from the distillation. Spectrum B corresponds to fraction 2, which is believed to be pure ethyl glycidate.

The PMR spectra ( $\text{CCl}_4$ ) of fractions 2 and 4, measured on a 60 MHz instrument, are essentially indistinguishable. One way to detect the presence of the substituted propionate and quantitatively determine its presence in the mixture with ethyl glycidate, by PMR, would be to dope fraction 4 with a slight amount of  $\text{D}_2\text{O}$ , look for the singlet at  $\delta: 3.27$  due to the OH proton which exchanged with  $\text{D}_2\text{O}$ , and then compare its integral with that of  $\delta: 1.30$  ( $\text{COOCH}_2\text{CH}_3$ , 3).

The relevance of the above discussion to the scope of this work is the fact that it sheds some light on the mechanism of ring opening of the ethyl glycidate in the presence of cationic species. The substituted propionate is formed by the reaction of the trifluoroacetic acid side product with ethyl glycidate:





The above mechanism indicates that the major by-product, isolated according to the particular reaction conditions used in the synthesis of ethyl glycidate, results from the attack of the nucleophile on the unsubstituted carbon in the epoxy ring. This result will be utilized later in the discussion of the cationic ring opening polymerization of cyclic acetals with ethyl glycidate.

## 2. Gas Phase Polymerization

### a. Trioxane-Dioxolane Copolymer

This copolymer was obtained with a 61 percent base stable fraction. A higher percent of trioxane homopolymer may have been formed during the gas phase reaction which upon base treatment completely unzipped to monomer. The tendency of the two monomers to homopolymerize or copolymerize by cationic ring opening polymerization in the gas phase could be significantly different from their behavior in bulk or in solution in the presence of the same type of initiators.

Another important consideration is the difference in the vapor pressure of the two comonomers close to their respective boiling points.

Perhaps more trioxane may have been carried off with the nitrogen stream than dioxolane, even though the same flow rate of nitrogen into the vaporizer flasks was maintained throughout the reaction.

Finally, there is also the possibility that randomization reactions, i.e. transacetalization, may occur at a slower rate than chain propagation reactions in the gas phase. As a result, a truly random copolymer of trioxane and dioxolane may not be obtained by this process. It would be very useful to find out how important a role transacetalization reactions really play during the continuous polymerization of trioxane and dioxolane in the gas phase.

b. Trioxane Homopolymer and Trioxane - Ethyl Glycidate Copolymer

Relatively high yields (84 and 85%) of homopolymer and copolymer were obtained by this procedure (Equation 2). These yields are comparable to those obtained by Vogl and Martin.<sup>1,2</sup>

The homopolymer was endcapped only partially as shown by the presence of both the propionate ester carbonyl absorption at  $5.8\mu$  and the hydroxyl absorption between  $2.7\mu$  and  $3.0\mu$  in infrared spectrum B (Figure 8). Spectrum A refers to the homopolymer prior to endcapping.

The inherent viscosity of the endcapped homopolymer (1.35) was as high as that of various endcapped copolymers synthesized previously by the same process.<sup>1,2</sup> This high inherent viscosity value indicates that water, a typical chain transfer agent for these systems, was not present in any appreciable amount during the homopolymerization and co-

polymerization reactions. On the other hand, the low intrinsic viscosity of the copolymer might be indicative of the decreased tendency on the part of the epoxide to copolymerize with trioxane. This point will be further elucidated in a subsequent discussion of the solution and bulk polymerization of cyclic acetals with ethyl glycidate.

The reason why the intrinsic viscosities of the trioxane-ethyl glycidate copolymers, cited in references one and two, are so high (1.06 and 0.98) is because the crude copolymers were immediately endcapped with acetic anhydride. In the present work, the crude copolymer, instead of being endcapped, was dissolved in hot DMF. During this reaction, the majority of unstable segments and homopolymer chains unzipped causing a drastic decrease in the overall molecular weight of the untreated polymer. Only 60 percent of the heat treated trioxane-ethyl glycidate copolymer was recovered. If the crude copolymer had indeed been endcapped, then its intrinsic viscosity would probably have been considerably higher (in the range of useful mechanical properties).

The base stability of the uncapped trioxane-ethyl glycidate copolymer prepared in this work compares well with the base stability of trioxane-alkyl glycidate copolymers, of roughly the same composition, prepared previously by the same process (Table 12).



Table 12

Base Stability of Trioxane-Alkyl Glycidate Copolymers Prepared in the Gas Phase

<u>Alkyl Glycidate/Trioxane Molar Feed Ratio<sup>1</sup></u>	<u>Base Stability of the Uncapped Product (Wt %)</u>
1/27 <sup>a</sup>	44
1/30 <sup>a</sup>	53
1/50 <sup>a</sup>	57
1/19 <sup>b</sup>	35 <sup>c</sup>
1/40 <sup>b</sup>	34
1/93 <sup>b</sup>	30

<sup>a</sup>Methyl Glycidate.

<sup>b</sup>Ethyl Glycidate.

<sup>c</sup>This Work.

The reaction times and initiator flow rates for the preparation of the copolymers listed in Table 12 were 60 minutes and  $5 \pm 1.5$  cc/min, respectively.

The methyl glycidate copolymers exhibit slightly higher base stability values in the same composition range than the corresponding ethyl glycidate copolymers. The methyl esters also show a trend toward higher base stabilities when less comonomer is fed into the reactor. The base stability of the ethyl glycidate copolymers is essentially unchanged over the entire composition range reported in Table 12. These trends may be indicative of a reluctance on the part of the glycidic esters to copolymerize with trioxane, under these conditions, or an inhibition of transacetalization reactions during the polymerization

due to the presence of carboalkoxy oxyethylene units along the chain.

c. Ionomers and Acid Derivative from Trioxane-Ethyl Glycidate Copolymer

Figure 2 furnishes spectral information on the heat treated ester, sodium salt and acid derivatives of the trioxane-ethyl glycidate copolymer prepared in the gas phase. A moderately strong absorption at  $5.8\mu$ , due to the ester or acid carbonyl is still retained after base hydrolysis. This result is indicative of the inefficiency of the slurry hydrolysis technique (Equation 3). Since the polymeric ester only partially swells in the dioxane/water-sodium hydroxide solution, it never really has a chance to come in intimate contact with the base to cause the salt formation. A variety of reaction times, reaction temperatures, amounts of base and different relative volumes of dioxane to water were tried, but the best results were obtained using the conditions reported specifically in the experimental part of this work. Higher relative amounts of sodium hydroxide to polymer than the reported weight ratio of 3 to 4 did not decrease the magnitude of the  $5.8\mu$  shoulder but resulted in colored products. The inherent viscosity of the polymeric salt, reported in this work, was essentially unchanged from that of its ester precursor. A better base hydrolysis technique for this system will be discussed in a later section.

The OH absorption between  $2.7\mu$  and  $3.3\mu$  is very strong in all three derivatives of the polyoxymethylene copolymer but sharper in the case of the heat treated ester than in the case of the corresponding

polymeric salt and polymeric acid (Figure 2). The strength of the absorption is indicative of the low molecular weight of the polymers (high hydroxyl group content). It appears broader in the salt and in the acid due to the presence of hydrogen bonded carboxylic acid hydroxyl groups and also due to the presence of bound water. The acid and salt derivatives of organic polymers, especially those based on polyoxymethylene, are expected to exhibit high affinity toward water. This phenomenon has already been observed in a variety of ionomers.<sup>4, 107, 127</sup>

The change in the pH of the metal chloride aqueous solutions and its convergence to the same value ( $\text{pH} = 6.6$ ), during the reaction of the sodium salt with lithium chloride and with cesium chloride, was an indication that the exchange reaction had taken place (Equation 4). The exchange of polyoxymethylene ionic salts with the chlorides of different cations was first described by Wissbrun and co-workers<sup>5</sup> but the preparation of a cesium salt of a polyoxymethylene derivative has never been described.

A slight shift of the infrared carbonyl absorptions, due to the carboxylate anions, to higher wavelength (the asymmetrical stretching band moving from  $6.2\mu$  to  $6.3\mu$  and the symmetrical stretching band moving from  $7.0\mu$  to  $7.1\mu$ ) was observed as the size of the cation increased from lithium to cesium (Figure 3). The carboxylate anion has two strongly coupled carbon to oxygen bonds with bond strengths intermediate between  $\text{C}=\text{O}$  and  $\text{C}-\text{O}$ . Apparently, this bond strength shifted even further toward the  $\text{C}-\text{O}$  bond strength as the size of the cation increased. A similar effect was reported by Wissbrun and Hannon who studied the interaction



of inorganic salts with polar polymers.<sup>128</sup> They observed a slight but real shift of the ester carbonyl from 5.8 to 5.9 in going from a 1:1 "solution" of  $\text{Ca}(\text{NO}_3)_2$  in poly(methyl acrylate) to one containing  $\text{Zn}(\text{NO}_3)_2$  in the same proportions and finally to one in which cadmium replaced the zinc cation in the nitrate salt. Their observations were interpreted in terms of complex formation between the polymer and the salts in the solid state. The structure of this complex allowed for an analogous interaction between the cation on the salt and the carbonyl group on the polymer chain to what is observed in the ionic salts prepared in this work.

The technique for the conversion of the polymeric sodium salt to the corresponding acid was developed by this author (Equation 5). Mild reaction conditions were maintained to prevent acid catalyzed degradation of the polymer backbone. The inherent viscosity of the product was unchanged from that of its precursor. Conversion to the acid form was essentially complete within three hours as indicated by analysis for sodium in the polymeric acid. Unreacted carboxylate groups on the polymer chain or a small amount of sodium acetate impurity may have been retained in the product as indicated by the presence of a weak absorption at 6.2  $\mu$ , due to the carboxylate anion, in the infrared spectrum of the acid (Figure 2).

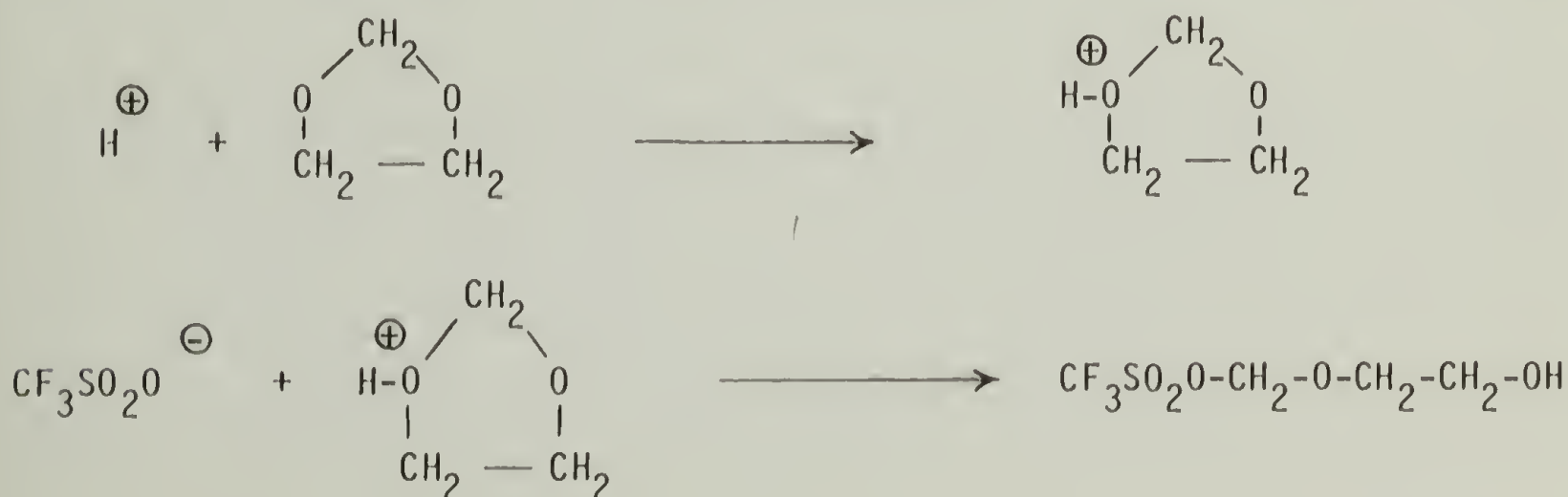
### 3. Solution Copolymers of Trioxane and Dioxolane

Penczek and co-workers have shown that the best results, i.e., short induction periods, high polymerization rates, high polymerization degrees and a content of unstable fraction comparable with other systems have been obtained in the polymerization of trioxane with dioxolane.

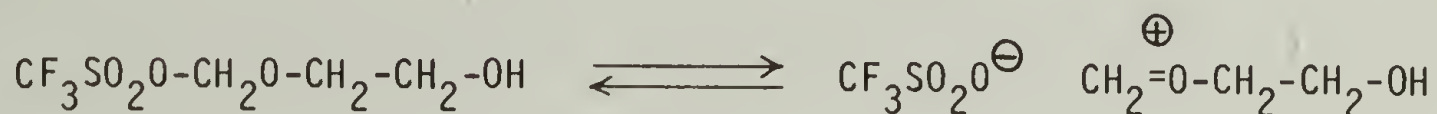


in the presence of the ester or anhydride derivatives of trifluoromethane sulfonic acid.<sup>45</sup> The excellent performance of these systems as cationic initiators was ascribed to the low nucleophilicity and high stability of the  $\text{CF}_3\text{SO}_2\text{O}^\ominus$  anion. The occurrence of transacetalization reactions in the solution polymerization of cyclic acetals initiated by cationic species is well established.<sup>129, 130</sup> In view of these facts, the trifluoromethane sulfonic acid initiating system was selected in an attempt to prepare random copolymers in high yield which exhibited relatively high molecular weights and base stabilities (Equation 6). The results of the present work show that these attempts proved successful.

When trifluoromethane sulfonic acid is used as the initiator for trioxane-dioxolane copolymerization, initiation can be described as an  $\text{S}_\text{N}2$  reaction at the carbon atom; it is known that  $\text{CF}_3\text{SO}_2\text{O}^\ominus$  is one of the best leaving groups.<sup>45</sup> Penczek and co-workers have also shown that, in the copolymerization of trioxane with dioxolane, catalyzed by cationic species, trioxane is more reluctant to participate in the initiation step.<sup>131, 132</sup> On the basis of this finding, a very probable initiation step, in the present work, is the reaction of trifluoromethane sulfonic acid with dioxolane:

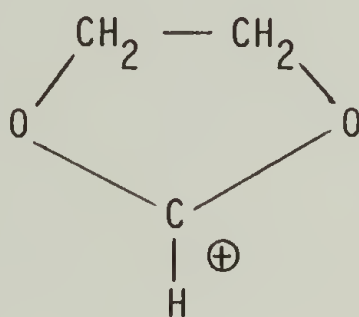


On the basis of the most recent investigations of polyether polymerizations in the presence of superacid catalysts, a macroester  $\rightleftharpoons$  macroion equilibrium is also believed to occur in the polymerization of cyclic acetals with initiators bearing anions able to form covalent bonds:<sup>45, 133, 134</sup>



This species probably cationates trioxane and/or dioxolane starting in this way chain growth.

Two phenomena are characteristic of cyclic acetal polymerizations initiated with the anhydride of trifluoromethane sulfonic acid.<sup>45</sup> Shorter induction periods are observed at comparable conditions than with triphenyl methylum salts ( $\text{AsF}_6^\ominus$  or  $\text{SbF}_6^\ominus$  anions), and much lower concentrations of the superacid anhydride are needed to achieve the same polymerization reactions by the triphenylmethylum cation to form this relatively stable carbenium ion



are avoided when using the superacid anhydride as the initiating species.<sup>131</sup>

Table 13 draws a comparison between the results for the copolymerization of trioxane with dioxolane in the presence of trifluoromethane sulfonic acid, its anhydride or other types of cationic initiators. The copolymeriza-

tions that apply to reference 45 were conducted at 60°C in cyclohexane as the solvent and in the presence of two weight percent of polyethylene oxide with  $\bar{M}_n = 40,000$ . All copolymerizations listed in Table 13 were carried out for three hours except for the one initiated with the triphenyl methylium salt ( $\text{AsF}_6^\ominus$  anion) which lasted for two and a half hours.

Table 13

## Cationic Ring Opening Copolymerization of Trioxane with Dioxolane

Initiator	Initiator Conc. (Moles/liter)	Comonomer Conc. Trioxane+Dioxolane (Mole/liter)	Induction Period (Sec)	Mol. Wt. <sup>a</sup>
$(\text{CF}_3\text{SO}_2)_2\text{O}^b$	$8 \times 10^{-4}$	$7.0 \pm 0.4$	240	$1.4 \times 10^5$
$(\text{CF}_3\text{SO}_2)_2\text{O}^b$	$1 \times 10^{-3}$	$7.0 \pm 0.4$	120	$1.4 \times 10^5$
$\text{CF}_3\text{SO}_2\text{OH}^c$	$5 \times 10^{-3}$	$4.6 \pm 0.6$	120	$9.8 \times 10^4$
$\text{CF}_3\text{SO}_2\text{OH}^c$	$3 \times 10^{-3}$	$4.0 \pm 1.0$	300	$7.2 \times 10^4$
$\text{CF}_3\text{SO}_2\text{OH}^c$	$4 \times 10^{-3}$	$4.0 \pm 1.6$	900	$1.6 \times 10^5$
$\text{BF}_3\text{O}(\text{C}_4\text{H}_9)_2^b$	$4 \times 10^{-2}$	$7.3 \pm 0.4$	120	$8.8 \times 10^4$
$(\text{C}_6\text{H}_5)_3\text{C}^\oplus \text{AsF}_6^\ominus^b$	$6 \times 10^{-3}$	$6.5 \pm 0.3$	200	$8.6 \times 10^4$

## % Yield

Stable Fraction	Unstable Fraction
74	6
82	7
81	16
91	5
58	9
75	6
78	6

<sup>a</sup>In reference 45, Molecular Weight =  $\bar{M}_n$ ; in this work, Molecular Weight =  $\bar{M}_w$ .

<sup>b</sup>Reference 45.

<sup>c</sup>This work.

The base stabilization of the copolymers investigated in Reference 45 was carried out in benzyl alcohol at 150°C in the presence of tri-n-butyl amine for 30 minutes. The base stabilization of the other copolymers is described in Part 3a, Section C, Chapter II of this work (Equation 7).

The overall performance of the systems initiated with trifluoromethane sulfonic acid or its anhydride is better than those initiated with other types of cationic initiators both in terms of molecular weight of the final product and amount of initiator needed to achieve the same polymerization rates, same amount of base unstable fraction and final yields. The induction period is seen to increase dramatically in the systems studied in the present work when the amount of dioxolane in the feed is increased from 12 to 30 mole% (based on moles trioxane + moles dioxolane) at approximately the same level of initiator in the feed.

The presence of a larger amount of dioxolane apparently shifts the macroester  $\rightleftharpoons$  macroion equilibrium toward the slower propagating macroester, causing a longer induction period. Indeed, preliminary measurements of the second order rate constants of propagation ( $\bar{k}_p$ ) in the homopolymerization of dioxolane showed that  $\bar{k}_p$  found for the  $\text{CF}_3\text{SO}_2\text{O}^\ominus$  anion is actually lower than that measured for the  $\text{AsF}_6^\ominus$  and  $\text{SbF}_6^\ominus$  anions.<sup>136</sup>



On the other hand, less of the trifluoromethane sulfonic acid or its anhydride is needed to produce the same or better results, in the copolymerization of trioxane with relatively small amounts of dioxolane, than the initiating systems bearing the complex anions such as  $\text{AsF}_6^-$  (see Table 13).

The moderate yield and high molecular weight obtained for the copolymer with 30 mole% of dioxolane (based on moles trioxane + moles dioxolane) in the feed (TD-30) may be due to the fact that the polymerization was stopped at a relatively low % conversion (when copolymer rich in dioxolane was still present). This dioxolane rich copolymer was still soluble in dichloroethane and was therefore removed during the isolation of the insoluble copolymer.

Spectrum A in Figure 9 shows a PMR spectrum of a trioxane-dioxolane copolymer (deuterated hexafluoroacetone sesquihydrate, 35°C). The major peak ( $\delta$  : 4.8 to 5.2) corresponds to the two oxymethylene protons and the minor singlet ( $\delta$  : 3.7 to 4.0) corresponds to the four oxyethylene protons. Spectra such as these were used to determine the compositions of copolymers TD-10, TD-20, and TD-30 as well as the trioxane-dioxolane copolymer prepared in the gas phase.

On the basis of PMR compositions and assuming that all ester end-groups were "killed" during workup, the following structures are proposed for random copolymers of TD-10, TD-20, and TD-30 after base stabilization:

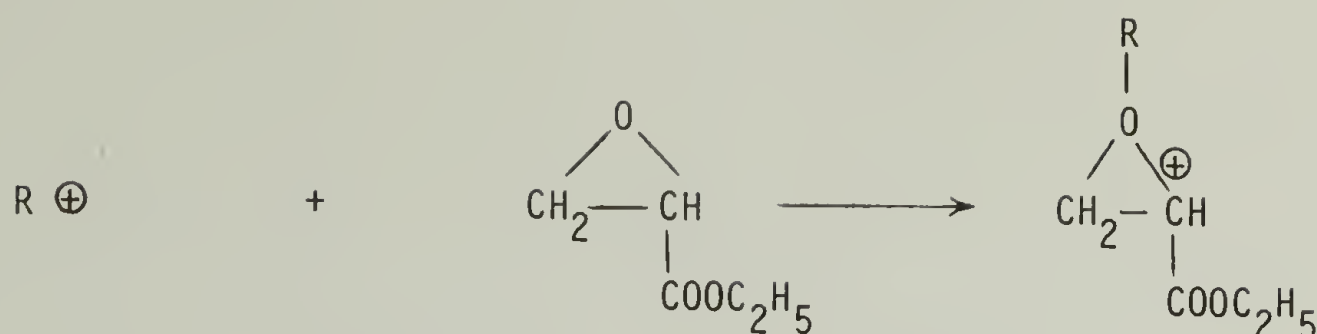


#### 4. Solution and Bulk Copolymers and Terpolymers of Trioxane, Ethyl Glycidate and Dioxolane and Their Derivatives

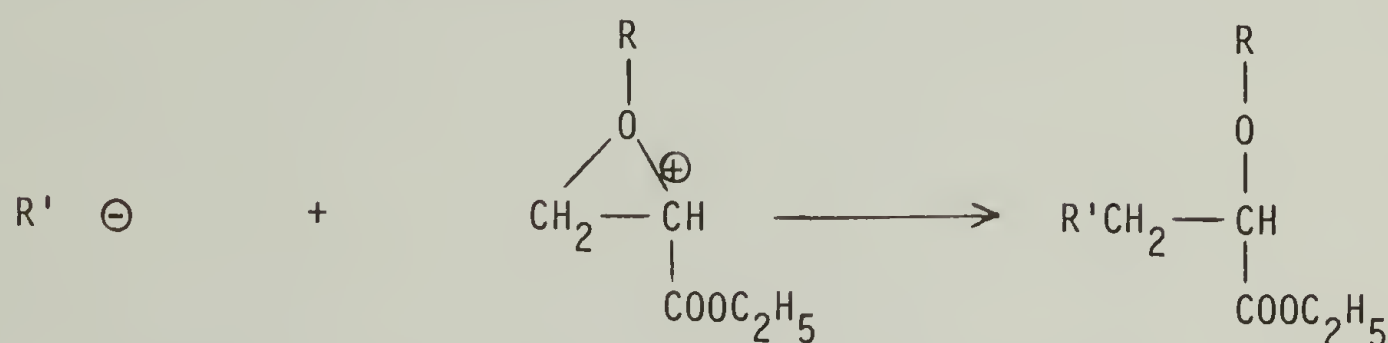
Many of the preparations of trioxane-ethyl glycidate copolymers and trioxane-ethyl glycidate-dioxolane terpolymers were run concurrently with blank runs utilizing the same experimental conditions but replacing either the two monomers or the three monomers with trioxane alone. These blank runs were necessary in order to insure that the effects observed were not due to the presence of impurities such as moisture. Nevertheless, care was taken to purify and dry all reagents according to standard procedures. The purification procedures are described in Chapter II of this work.

The low yields, high contents of base unstable fraction and low molecular weights observed in the products obtained from the solution and bulk polymerizations of trioxane with ethyl glycidate are evidence of the fact that trioxane does not copolymerize as readily and effectively with ethyl glycidate to give uniform copolymers under conditions in which high yields and high molecular weights of trioxane homopolymer and high yields, low content of base unstable fraction and high molecular weights of trioxane-dioxolane copolymers are usually observed.

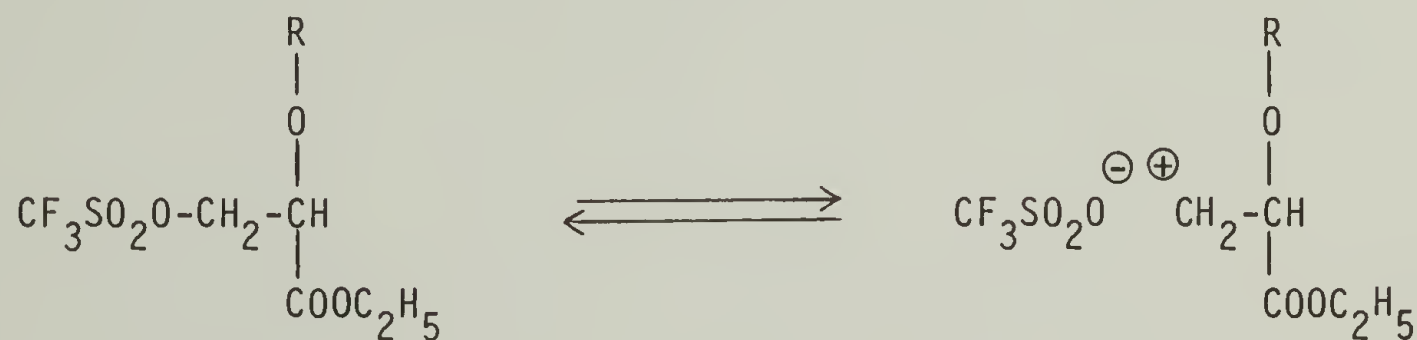
Based on the mechanism proposed for the formation of ethyl-2-hydroxy 3-trifluoroacetoxy propionate from ethyl glycidate (see Chapter III (A), Section 1), the ring opening step is believed to be the following:



The unsubstituted carbon on this cyclic oxonium ion is then attacked by a nucleophile to form a propagating species:

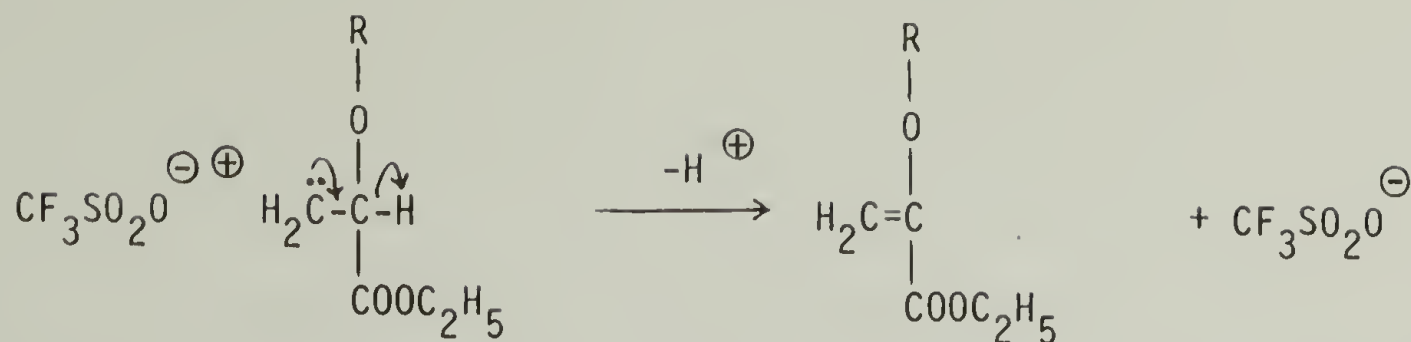


Depending on the nature of the nucleophile, this species may propagate or may be transformed into an inactive species. If  $R^{\oplus} = H^{\oplus}$ , a monomeric oxonium ion or an oxonium ion attached to the propagating chain and  $R'^{\ominus} = \text{CF}_3\text{SO}_2\text{O}^{\ominus}$  (which is applicable to some of the systems investigated in the present work), then an equilibrium should exist between:

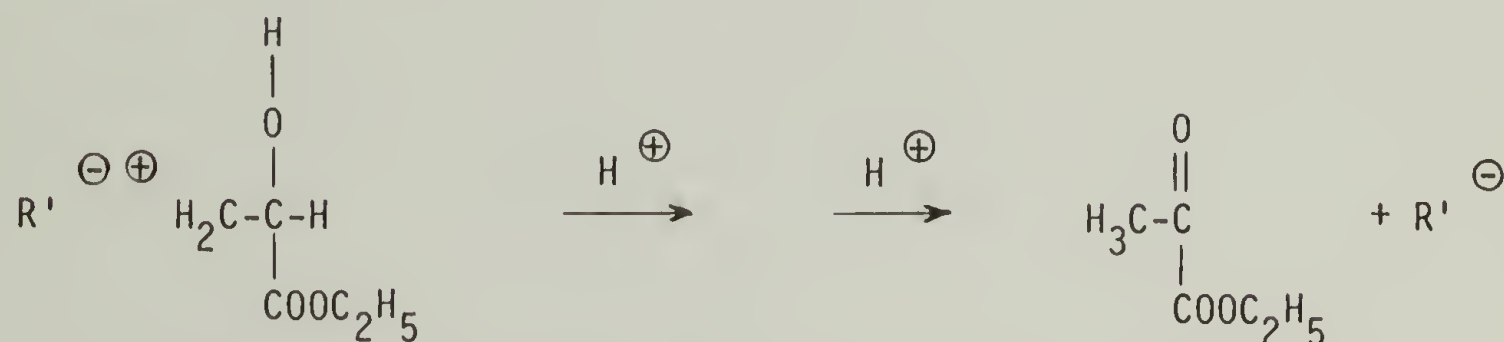


The ester or the ionic form may react with trioxane and/or dioxolane and/or another ethyl glycidate monomer. On the other hand, since the  $\text{CF}_3\text{SO}_2\text{O}^{\ominus}$  anion is a very good leaving group, the ionic form of the addition product may be transformed, via the elimination of an  $\alpha$ -hydrogen, into a vinyl compound:

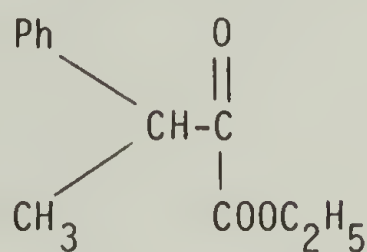




In addition, if  $\text{R}=\text{H}$ , the carbenium ion may rearrange, by a proton shift followed by the elimination of an  $\alpha$ -hydrogen, to give the corresponding  $\alpha$ -keto ester:



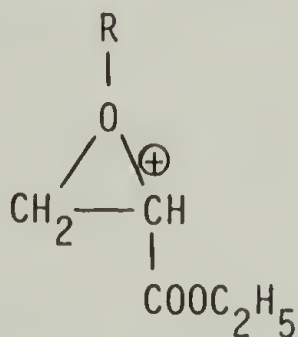
Indeed, 3,3 substituted alkyl glycidates, in the presence of Lewis acids show preference toward this rearrangement reaction rather than polymerize.<sup>137</sup> An additional example is the isolation of:



as a by-product during the synthesis of ethyl (3-methyl-3-phenyl) glycidate with peracids.<sup>138</sup> Assuming, the ester form of the addition product is a slower propagating species than the ionic form, then, depending on the reaction conditions, one of the chain termination reactions described above may be more or less favorable.

It would be desirable to analyze and identify all by-products of the polymerization reaction to see if any of these predicted side-products are in fact present. This was not done in the present work. The main objective of this work was to obtain polymers with ionizable side chains, in order to characterize some of their physical properties. A more in-depth study of the actual synthesis of these polymers (with model compounds, etc.) was not carried out.

The above reactions point out as to why the rate of propagation of



may be much slower than that of the addition product between  $\text{R}^{\oplus}$  and dioxolane and/or trioxane. In addition, the ether oxonium ion itself may be more reluctant to react with another monomer than the corresponding acetal oxonium ions of dioxolane and of trioxane in analogy to the effect of low molecular weight ethers or polyethers on trioxane homopolymerization and on trioxane-dioxolane copolymerization.<sup>135, 139</sup> The rate is lowered in the presence of the low molecular weight ethers or polyethers.

Due to the influence of the ester substituent on the  $\alpha$  carbon atom, ring opening of the epoxide occurs preferentially between the  $\beta$  carbon atom and the ring oxygen. In view of this observation, electrophilic attack on the oxygen next to the  $\alpha$  carbon atom on the polymer chain with subsequent chain cleavage of the  $\alpha$  carbon-oxygen bond is less likely, during

transacetalization, than attack on the oxygen next to the  $\beta$  carbon atom with subsequent chain cleavage. Electrophilic addition to the carbonyl oxygen (which is a reversible reaction) may also occur. Both of these events would hinder the randomization process and produce copolymers of trioxane and ethyl glycidate with a higher content of unstable fraction than that of copolymers of trioxane with dioxolane (or ethylene oxide).

Another observation was made during the preliminary experiments on the synthesis of trioxane-ethyl glycidate-dioxolane terpolymers with  $\text{BF}_3\text{O}(\text{C}_2\text{H}_5)_2$ , (Equation 8). If the initiator was added to a solution of the three monomers in dichloroethane, the yields were the same or lower and the base stabilities were lower than those of a product obtained by first adding the initiator to a solution of trioxane and dioxolane in dichloroethane and waiting for the polymer particles to precipitate out of solution before adding the ethyl glycidate monomer (Table 4 - Examples 3 and 4). The same argument used to explain the higher content of base unstable fraction observed in copolymers of trioxane and ethyl glycidate than that observed in copolymers of trioxane and dioxolane could be invoked to account for this experimental observation.

The PMR spectra of the heat treated polymeric esters of TED 5, TED 10 and TED 15 (deuterated hexafluoroacetone sesquihydrate,  $35^\circ\text{C}$ ) showed  $\delta$  : 4.8 to 5.2 ( $\text{CH}_2\text{O}$ , 2): 3.7 to 4.0 ( $\text{CH}_2\text{CH}_2\text{O}$ , 4 and  $\text{CH}_2\text{CHO}$ , 2): 1.2 to 1.4 ( $\text{COOCH}_2\text{CH}_3$ , 3) (Figure 9 , Spectrum B). The PMR spectra of the corresponding sodium salts and acids showed the same absorptions except those for protons on the methyl group of the ethyl ester. Due to the

relatively small amount of 1-carboethoxy oxyethylene units incorporated on the polymer chain, the acid protons in the polymeric acids could not be characterized properly.

The number of 1-carboethoxy oxyethylene units/100 oxymethylene units was determined by comparing the integrated peak intensities of  $\delta$  : 1.2 to 1.4 ( $\text{COOCH}_2\text{CH}_3$ , 3) with  $\delta$  : 4.8 to 5.2 ( $\text{CH}_2\text{O}$ , 2). Dividing the value corresponding to  $\delta$  : 1.2 to 1.4 ( $\text{COOCH}_2\text{CH}_3$ , 3) by three gave the fraction of the peak intensity due to one proton. This number was then multiplied by two and subtracted from the integrated peak intensity of  $\delta$  : 3.7 to 4.0 ( $\text{CH}_2\text{CH}_2\text{O}$ , 4 and  $\text{CH}_2\text{CHO}$ , 2) to calculate the contribution by the  $\beta$  protons in the carboethoxy oxyethylene units. The remainder was then used to determine the mole% of oxyethylene units along the polymer chain.

The compositions of the polymeric esters, salts and acids, calculated by this method agreed very well internally and also surprisingly well with the compositions based on the results of sodium analysis on the polymeric salts considering the error involved in both the PMR analysis and the atomic absorption analysis for metals. The results are shown in Table 15.



Table 15

Composition of Trioxane-Ethyl Glycidate-Dioxolane Terpolymers<sup>a</sup>

<u>Sample Designation</u>	<u>TED 5</u>	<u>TED 10</u>	<u>TED 15</u>
Mole% of 1-Carboethoxy Oxyethylene Units (Based on PMR of the Ester)	1.0	1.8	2.0
Moles% of 1-Carboethoxy Oxyethylene Units (Based on Na analysis of the Salt)	0.9	1.7	2.0
Moles% of Oxyethylene Units (Based on PMR of the Ester)	1.2	1.3	1.2
Moles% of Oxyethylene Units (Based on PMR of the Salt)	1.2	1.3	1.2
Moles% of Oxyethylene Units (Based on PMR of the Acid)	1.2	1.3	1.2

<sup>a</sup>All compositions are based on 100 moles CH<sub>2</sub>O

An improved base hydrolysis technique was utilized in this work to convert the crude polymeric ester terpolymer to the corresponding polymeric salt. The advantage of this "solution" technique (Equation 9) over the slurry technique (Equation 3) is apparent from infrared analysis of the product (Figure 6). Only a fifth of the amount of sodium hydroxide, used in the slurry technique, was necessary to replace all of the ester carbonyl groups with the corresponding sodium carboxylate groups (in this case, the 5.8 $\mu$  absorption, due to the ester carbonyl, has disappeared).

Infrared analyses were carried out on thin films of the acid derivative of TED 5 (Equation 10), prepared in a KBr pelletizer at room temperature. After subjecting these films to a five-minute heat treat-

ment at 160°C (in a Carver press) followed by fast cooling back to room temperature, a new peak at 5.6 $\mu$  was observed to grow in the infrared spectrum of this "heat treated" acid (Figure 10). This peak was regarded as evidence for the presence of anhydride in the sample.<sup>140</sup> 0.02g of the "heat treated" acid were still soluble in 0.1 ml of hexafluoroisopropanol, indicating that extensive crosslinking reactions had not occurred during the heat treatment. These results were also obtained for the acid derivatives of TED 10 and TED 15 terpolymers.

Various structures may be postulated on the basis of these results. The formation of a seven-membered cyclic anhydride would suggest the presence of short blocks of substituted oxyethylene units along the chain, whereas, a linear anhydride could only result from mild crosslinking reactions or from chain extension reactions between substituents on end-groups.

## B. Calorimetric Studies

The structures of the repeat units of polymers, whose calorimetric, dynamic mechanical and dielectric properties were investigated in this work, are shown in Figure 11.

### 1. Trioxane - Dioxolane Copolymers

Table 16 summarizes the results of calorimetric studies carried out on base stable trioxane-dioxolane powders as a function of composition.

Table 16

## Calorimetric Studies of Trioxane-Dioxolane Copolymers (Powders)

<u>Sample Designation</u>	<u>TD-10</u>	<u>TD-20</u>	<u>TD-30</u>
Moles % Oxyethylene Units <sup>a</sup>	2.2	3.2	4.2
Melting Point (°C)	155	147	143
Melting Peak Temperature (°C)	159	153	149
Freezing Onset Temperature (°C)	144	139	135
Freezing Peak Temperature (°C)	136	131	128
Heat of Crystallization (cal/g)	28.4	26.7	22.3
Crystallinity (%)	57	53	45

<sup>a</sup>Based on 100 moles CH<sub>2</sub>O

The degree of crystallinity estimated by DSC decreased as comonomer content increased. This variation is not linear, as shown in Figure 12. A % crystallinity of Celcon M-90 (~1.4 mole % CH<sub>2</sub>CH<sub>2</sub>O) reported in Reference 4 is plotted along with the % crystallinities of the TD copolymers. This and future comparisons in this section are justified by the fact that the same DSC melting-recrystallization procedure, that was described in Reference 4 was also carried out in this work.

One way to explain the non-linear dependence of % crystallinity on the concentration of oxyethylene units, at low levels of comonomer incorporated, is to assume that some of the oxyethylene units, which do not contain long bulky side chains, actually incorporate into the crystalline regions of the polymer. This phenomenon has been known for some time and

was again recently verified by Wegner and co-workers.<sup>82</sup> They found that crystals of trioxane-dioxolane copolymers behaved like an ideal solution of  $\text{CH}_2\text{CH}_2\text{O}$  units in the crystal of  $\text{CH}_2\text{O}$  units, up to 10 mole % of  $\text{CH}_2\text{CH}_2\text{O}$  units. These copolymers were unique in the sense that one could measure the variations in the thermodynamic properties of the copolymer crystal which were solely dependent on disturbances created by the oxyethylene units inside the crystal.

Wegner and co-workers also showed that the fraction of oxyethylene units which actually incorporates into the crystalline phase of melt crystallized copolymers (like the ones prepared in this work) is small compared to the fraction which segregates into the amorphous phase.<sup>82</sup> Therefore, a linear dependence of % crystallinity on the concentration of oxyethylene units may be observed at higher levels of comonomer incorporation.

The melting points and melting peak temperatures of the trioxane-dioxolane film samples for the vibron and dielectric experiments are collected in Table 17.



Table 17

## Endotherm Parameters of Trioxane-Dioxolane Film Samples

## Recrystallized in the Mold

<u>Sample Designation</u>	<u>Melting Point (°C)</u>	<u>Melting Peak Temperature (°C)</u>
TD-10 (Vibron)	154	158
TD-20 (Vibron)	147	152
TD-30 (Vibron)	143	147
TD-10 (Dielectric)	154	159
TD-20 (Dielectric)	147	154
TD-30 (Dielectric)	143	149

The endotherm parameters are the same for the DSC recrystallized films and for the mold recrystallized films (Table 16 vs. Table 17).

The powders were recrystallized as thin films at 20°C/min. The Vibron and dielectric film samples were compression molded and cooled back down to room temperature at 10°C/min. The same heating rate was used to re-melt the DSC and mold recrystallized films. Previous arguments indicate that the oxyethylene units, when present in relatively low concentration, are less effective in hindering the formation of polymer crystallites. Therefore, one might expect very little difference between the endotherm parameters for the DSC and mold recrystallized samples.

## 2. STG Copolymers

Two endotherms were observed in the STG films when the samples were heated in the DSC oven at 20°C/min. The minor endotherm, which ap-

peared at a lower temperature, grew in size and shifted to higher temperatures as the content of ionic comonomer in the copolymer increased. Upon cooling the samples back down to room temperature, a single recrystallization exotherm was observed in every case. The samples were not remelted after the first recrystallization to see if the temperature and/or magnitude of the minor endotherm had been affected by the thermal history of the sample. It is difficult to speculate on the origin or the minor endotherm without further calorimetric evidence.

The DSC data for the STG films is tabulated in Table 18. Only the melting points and melting peak temperatures of the major endotherms are reported.

Table 18

Calorimetric Studies of Polyoxymethylene Ionomers (Films) (Sodium Salts)

<u>Sample Designation</u>	<u>STG 7</u>	<u>STG 2</u>	<u>STG 9</u>	<u>STG 23</u>
Moles % Comonomer	1.3	2.9	4.5	6.5
Melting Point (°C)	157	150	144	131
Melting Peak Temperature (°C)	163	157	151	143
Freezing Onset Temperature (°C)	142	136	129	121
Freezing Peak Temperature (°C)	137	127	120	109
Heat of Crystallization (Cal/g)	26.7	23.7	19.1	14.3
Crystallinity (%)	53	47	38	29

The % crystallinity is inversely proportional to the ionic comonomer content but, in this case, the dependence is also linear (Figure 13). The STG unit is probably only incorporated into the amorphous

regions of the polymer. This unit, in contrast to the oxyethylene unit, contains a long bulky side chain so it is hard to visualize how it would incorporate into the polyoxymethylene crystal.

Another interesting DSC result is illustrated in Figure 14. The top curve shows that the melting peak temperatures of all the polymers, ionic and non-ionic, fall on the same curve, independent of the nature of the comonomer. This behavior has been observed previously by Wissbrun and Inoue, independently, for a number of non-ionic acetal copolymers.<sup>4, 141</sup> The crystallization behavior of the polymers, on the other hand, depends on whether the comonomer units are ionic or not. This was also demonstrated by Wissbrun.<sup>4</sup> The peak freezing temperatures of the STG polymers fall considerably below those of the trioxane-dioxolane or trioxane-epichlorohydrin polymers, as shown in the bottom curves of Figure 14. Figure 15 demonstrates that the onset of crystallization is essentially independent of the nature of the comonomer, so the shift of the freezing peak is indicative of a broadening of the crystallization peak (i.e. the rate of crystallization is slowed down by the presence of the ionic groups).

### 3. TED Terpolymers

The calorimetric properties of the heat treated esters, sodium salts and acids are summarized in Table 19 - 21, respectively. The values in parentheses refer to the minor endotherms observed after two melting-recrystallization cycles. The multiple endotherms may be indicative of the blocky nature of these polymers. Alternatively, some of these systems may actually be mixtures of dioxolane rich terpolymers and trioxane

rich terpolymers, the latter exhibiting a higher temperature endotherm. The presence of a copolymer impurity is also possible. Finally, the melting-recrystallization-remelting phenomena may reflect a reorganization of polymer chains into more perfect arrays within the crystals.

Table 19

Calorimetric Studies of Polyoxymethylene Derivatives (Powder)  
(Esters)

<u>Sample Designation</u>	<u>TED 5</u>	<u>TED 10</u>	<u>TED 15</u>
Moles % E <sup>a</sup>	0.9	1.7	2.0
Moles % D <sup>b</sup>	1.2	1.2	1.2
Melting Point (°C)	155 (158)	149 (154)	(148) 153
Melting Peak Temperature (°C)	157 (159)	152 (156)	(153) 155
Freezing Onset Temperature (°C)	142	138	136
Freezing Peak Temperature (°C)	137	133	132
Heat of Crystallization (Cal/g)	30.7	29.1	27.5
Crystallinity (%)	61	58	55

Table 20

Calorimetric Studies of Polyoxymethylene Derivatives (Powders)  
(Sodium Salts)

<u>Sample Designation</u>	<u>TED 5</u>	<u>TED 10</u>	<u>TED 15</u>
Moles % E <sup>a</sup>	0.9	1.7	2.0
Moles % D <sup>b</sup>	1.2	1.2	1.2
Melting Point (°C)	156	154	152
Melting Peak Temperature (°C)	140	158	155



Table 20, continued

<u>Sample Designation</u>	<u>TED 5</u>	<u>TED 10</u>	<u>TED 15</u>
Freezing Onset Temperature (°C)	140	138	136
Freezing Peak Temperature (°C)	134	132	130
Heat of Crystallization (Cal/g)	29.8	28.8	27.5
Crystallinity (%)	60	58	55

Table 21

## Calorimetric Studies of Polyoxymethylene Derivatives (Powders)

(Acids)

<u>Sample Designation</u>	<u>TED 5</u>	<u>TED 10</u>	<u>TED 15</u>
Moles % E <sup>a</sup>	0.9	1.7	2.0
Moles % D <sup>b</sup>	1.2	1.2	1.2
Melting Point (°C)	156	153 (156)	(149) 155
Melting Peak Temperature (°C)	159	156 (158)	(152) 157
Freezing Onset Temperature (°C)	143	140	137
Freezing Peak Temperature (°C)	136	134	132
Heat of Crystallization (Cal/g)	28.2	26.5	25.4
Crystallinity (%)	56	53	51

<sup>a</sup>Moles  $\text{CH}_2\text{CH}(\text{COOR})\text{O}/100$  moles  $\text{CH}_2\text{O}$ , where  $\text{R} = \text{C}_2\text{H}_5$ , Na or H.

<sup>b</sup>Moles  $\text{CH}_2\text{CH}_2\text{O}/100$  moles  $\text{CH}_2\text{O}$ .

In general, no significant differences were observed in the calorimetric properties in going from the unionized esters to the corresponding ionized salts. The % crystallinity of all the samples was calculated on the basis of the original weight of the sample. In the

acid series, a sample weight loss was recorded at the end of the DSC run. This weight loss may have been due to the evolution of water vapor during the formation of anhydrides at high temperature and/or the evolution of formaldehyde as a result of acid catalyzed degradation of the polymer chain also at high temperatures. The net result of this weight loss was an artifact, i.e., the % crystallinities in the acid series appeared lower than the % crystallinities of the ester series even though the melting and crystallization parameters of the two series were practically identical.

The melting points and melting peak temperatures of the TED ester and TED salt film samples for the dielectric experiment are shown in Table 22.

Table 22

Endotherm Parameters of TED Film Samples Recrystallized in the Mold

<u>Sample Designation</u>	<u>Melting Point (°C)</u>	<u>Melting Peak Temperature (°C)</u>
TED 5 Ester (Dielectric)	155	161
TED 10 Ester (Dielectric)	155	158
TED 15 Ester (Dielectric)	(149) 153	(154) 158
TED 5 Salt (Dielectric)	(151) 157	(159) 164
TED 10 Salt (Dielectric)	154	163
TED 15 Salt (Dielectric)	150 (156)	158 (161)

The values in parentheses refer to minor endotherms. The endotherm parameters for the mold recrystallized films are all slightly higher than those of the corresponding DSC recrystallized films. Also, the endotherms in the salt series appear broader. The crystallization in these systems

is hindered both by the presence of unsubstituted oxyethylene units and by the presence of substituted (branched) oxyethylene units. As a result, in this case, even a relatively small decrease in the rate of crystallization (from 20°C/min to 10°C/min) may have been responsible for the observed increase in the endotherm parameters. Furthermore, the presence of ionic groups in the salt series probably slowed down this rate even further, causing a broadening of the endotherms.

### C. Dynamic Mechanical Studies

#### 1. Trioxane-Dioxolane Copolymers

The dynamic mechanical behavior of the three trioxane-dioxolane copolymers (TD-10, TD-20, and TD-30) measured at a frequency of 110 Hz is illustrated in Figure 16. The 110 Hz frequency measurements are shown so they may be compared with the dielectric relaxation studies at 200 Hz. In addition, the  $\tan \delta$ 's are plotted rather than the loss modulus,  $E''$ , because of the greater resolution in  $T_{\max}$  from  $\tan \delta$  compared to  $E''$ . The  $\tan \delta$ 's will also be used for the calculations of  $T_{\max}$ .

Figure 16 shows three relaxation regions occurring in these copolymers, labeled  $\alpha$ ,  $\beta$ , and  $\gamma$  in order of decreasing temperature, while two relaxation regions, labeled  $\beta$  and  $\gamma$  in order of decreasing temperature occur in the polyoxymethylene homopolymer (Delrin).

Read and Williams observed a rapid broadening of the  $\gamma$  mechanical and dielectric relaxation spectra of polyoxymethylene with decreasing temperature.<sup>91</sup> They attributed the marked asymmetry of the  $\gamma$  peak to these phenomena and showed that the determination of the average relaxation

times ( $\tau_{AV} = (2\pi f_{\max})^{-1}$ ), and hence the activation energy could only be performed from the  $f_{\max}$  curve. Indeed, a divergence between the  $f_{\max}$  and  $T_{\max}$  curves was observed in both mechanical and dielectric determinations of  $\delta$  at temperatures lower than  $-40^{\circ}\text{C}$ .<sup>123</sup> It is clear that an apparent activation energy derived erroneously from the  $T_{\max}$  curve will be larger than the correct value at low temperatures and will appear to vary with temperature.

The correct method to analyze the data, collected in this work, for the mechanical and dielectric  $\delta$  relaxations is, therefore, to extract  $\tan \delta$  values for different frequencies at the same temperature from a plot of  $\tan \delta$  vs. temperature. Next, plot these  $\tan \delta$  values as a function of frequency and determine the frequency at which a maximum occurs,  $f_{\max}$ . Finally, plot  $\log f_{\max}$  vs.  $1/T$  and obtain the activation energy from the slope.

In this work, it was only possible to analyze the  $\delta$  dielectric data, collected at five frequencies, by the above method. The  $\delta$  mechanical data was taken at only three frequencies and therefore  $f_{\max}$  could not be determined with any degree of accuracy. Thus, only  $T_{\max}$  values are reported. Table 23 summarizes these values for the TD copolymers and the Delrin standard.



Table 23

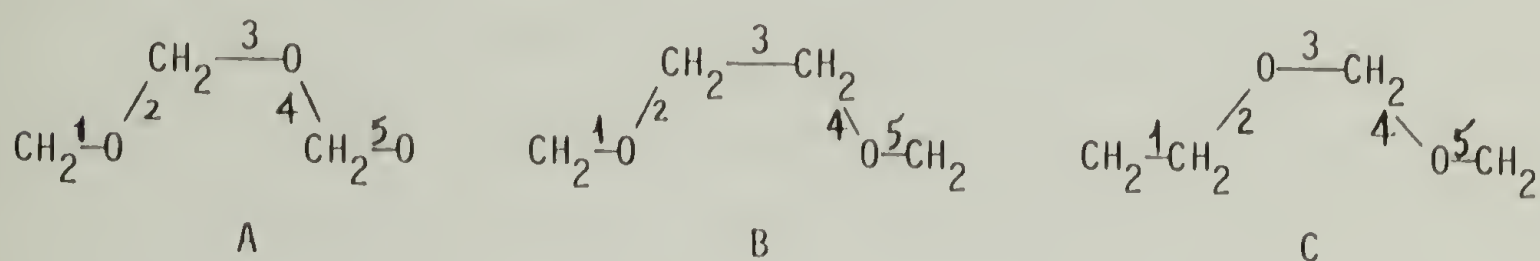
$T_{\max}$  for the  $\gamma$  ( $\tan \delta$ ) Relaxation of  
Trioxane-Dioxolane Copolymers and Delrin

Sample Designation	Moles $\text{CH}_2\text{CH}_2\text{O}/$ 100 Moles $\text{CH}_2\text{O}$	$T_{\max}$ (110 Hz) (°C)	$T_{\max}$ (11 Hz) (°C)	$T_{\max}$ (3.5 Hz) (°C)
Delrin	0	-60	-65	-71
TD-10	2.2	-60	-65	-71
TD-20	3.2	-60	-65	-71
TD-30	4.2	-60	-65	-71

The surprising feature in this table is the temperature independence of the  $\gamma$  relaxation with respect to oxyethylene content. This effect was also observed by Bohn and by Park.<sup>92,95</sup> Park reported that the magnitude of the  $\gamma$  loss peak, measured at 100 Hz and located at about -60°C, was also independent of oxyethylene content and of thermal history, in contrast to McCrum's observations and to the results of this work which show an increase in the magnitude of the transition with a decrease in density or an increase in oxyethylene content (Figure 16).<sup>90</sup> As further evidence, in favor of the dynamic mechanical results shown in Figure 16, the dielectric behavior of these copolymers exhibits a similar trend.

Historically, the  $\gamma$  loss in polyoxymethylene has been assigned to short range segmental motions in the disordered regions of the polymer including those associated with lattice defects.<sup>90,91</sup> Recently, Boyd and Porter showed that, based on dielectric measurements of the  $\gamma$  relaxation, the fractional relaxation strength in solid polyoxymethylene compared to the melt is larger than the amorphous volume fraction in

the solid from density measurements.<sup>142</sup> This indicates that there is probably a contribution to the  $\gamma$  process in the solid from the crystalline phase. The agreement between the experimental static dielectric constants of polyoxymethylene and those calculated theoretically, assuming a preferential population of gauche over trans states, further suggests that the  $\gamma$  transition is better interpreted in terms of rotational rearrangements than the local torsional mode model.<sup>143, 144</sup> These rotational rearrangements are pictured as flip-flop motions of three bond segments on the polymer chain.



These structures, as in polyethylene, may be crankshaftlike, i.e. bonds 1 and 5 are parallel and approximately colinear. Flip-flop motions about bonds 1 and 5 would occur in such a fashion that the volume swept out by the bonds during the conformational change is small enough to be energetically feasible in an amorphous matrix.<sup>145, 146</sup>

A contribution to the  $\gamma$  process may also arise from the destruction and reformation of crystalline defects by the twisting of two chain halves, around the chain axis, against each other.<sup>142, 147</sup> These defects (or kinks) are incorporated into the crystal lattice as a result of bonds 1 and 5 being brought into crystallographic register by steric distortion.<sup>147</sup>

The independence of  $T_{\max}$  for the  $\gamma$  process on oxyethylene content may be explained by the replacement of flip-flop motions due to structure

A with the flip-flop motions of structures B and C, which would involve roughly the same energetics. The increase in the magnitude of the  $\gamma$  relaxation with oxyethylene content implies that the motions of structures B and C are the major contributors to the  $\gamma$  process in the copolymers. This increase is not a linear function of oxyethylene content (Figure 16), suggesting that motions due to structures A, B and C, trapped in the crystalline regions, are also minor contributors to the  $\gamma$  relaxation.

The  $T_{\max}$  for the broad Delrin  $\beta$  relaxation process in Figure 16 shifts to lower temperature in TD-10 and then increases slightly with an increase in oxyethylene content in the copolymers. The magnitude of the  $\beta$  loss process increases and the breadth decreases as the oxyethylene content is increased. Both of these results are corroborated by Park's dynamic mechanical studies on trioxane-ethylene oxide copolymers.<sup>95</sup> The  $T_{\max}$ 's for the  $\beta$  process in the trioxane-dioxolane copolymers and the activation energies calculated from plots of log frequency vs. the reciprocal of  $T_{\max}$ , in  $^{\circ}\text{K}$ , are tabulated in Table 24.

Table 24

Characteristics of the  $\beta$  ( $\tan \delta$ ) Relaxation  
of Trioxane-Dioxolane Copolymers

Sample Designation	Moles $\text{CH}_2\text{CH}_2\text{O}/$ 100 Moles $\text{CH}_2\text{O}$	$T_{\max}$ (110 Hz) ( $^{\circ}\text{C}$ )	$T_{\max}$ (11 Hz) ( $^{\circ}\text{C}$ )	$T_{\max}$ (3.5 Hz) ( $^{\circ}\text{C}$ )
TD-10	2.2	0	-6	-7
TD-20	3.2	4	-3	-6
TD-30	4.2	6	0	-4



Table 24, continued

<u>Sample Designation</u>	<u><math>E_a</math> kcal/mole</u>
TD-10	64
TD 20	52
TD-30	47

$T_{\max}$  for Delrin could not be calculated accurately, due to the broad nature of the relaxation. In Figure 16, the  $\beta$  relaxation for the homopolymer begins to peak at about 20°C (110 Hz).

Inasmuch as the mechanical activation energies were obtained on the basis of only three frequencies, caution must be exercised in any conclusions drawn from the data. Furthermore, the determination of  $T_{\max}$  is subject to some error especially for the broader relaxations. Finally, if the dependency of  $1/T_{\max}$  on  $\log f$  is non-linear, then the slope of the best line through three points would not be an accurate representation of the nature of the relaxation process being described. The values of  $E_a$ , calculated in this work, should therefore be treated more as rough approximations of the activation energy for the process.

Many investigators have ascribed the  $\beta$  relaxation to main chain micro-Brownian motions in the disordered interlamellar regions of polyoxymethylene, as assignment which implies that the  $\beta$  process may be related to the "glass transition".<sup>123</sup> In line with this interpretation, the difference between the  $T_{\max}$  observed for the homopolymer and that observed for the copolymers as well as the roughly linear increase in the magnitude of the  $\beta$  peak with an increase in oxyethylene content suggest that this



process takes place predominantly in the amorphous regions of the copolymer and that it must involve motions of main chain segments containing the oxyethylene unit. A more detailed description of the structure involved in this intermediate temperature relaxation process for trioxane-dioxolane copolymers will be presented in the discussion of the dielectric behavior of these copolymers.

Table 25 summarizes the  $T_{\max}$ 's and corresponding activation energy parameters determined for the  $\alpha$  mechanical relaxation process of TD-10 and TD-30 (Figure 16). The  $\alpha$  process for TD-20 was so undefined that accurate  $T_{\max}$  values could not be determined from plots of  $\tan \delta$  vs. temperature at different frequencies.

Table 25

Characteristics of the  $\alpha$  ( $\tan \delta$ ) Relaxation  
of Trioxane-Dioxolane Copolymers

Sample Designation	Oxyethylene Content (Mole %)	$T_{\max}$ ( $^{\circ}\text{C}$ )			$E_a$ kcal/mole
		(110 Hz)	(11 Hz)	(3.5 Hz)	
TD-10	2.2	144	136	134	76
TD-30	4.2	123	113	110	87

The  $T_{\max}$  for the  $\alpha$  relaxation was seen to decrease in temperature but increase in magnitude with a decrease in frequency. This phenomenon was also reported by Read and Williams, who studied the dynamic mechanical properties of polyoxymethylene at frequencies ranging from 0.08 to 0.42 Hz.<sup>91</sup> A similar trend was observed in the mechanical  $\alpha$  of STG 7 and of the TED 5 ester.

As the oxyethylene content in the copolymer increases, the

relaxation shifts to lower temperatures, its magnitude decreases and the activation energy increases. The absolute values of the activation energies compare well with the activation energies estimated by Read and Williams (between 65 and 92 kcal/mole) determined at frequencies between about 0.08 and 0.42.<sup>91</sup> The mechanical results of Thurn are also consistent with a very high activation energy, since according to his data, the  $\alpha$  peak becomes essentially independent of temperature at frequencies above about 100 Hz.<sup>148</sup>

It now seems fairly generally accepted that the  $\alpha$  mechanism in polyoxymethylene, as in the case of polyethylene, is in some way associated with the crystalline phase.<sup>123</sup> Recently, Boyd and Biliyar observed the effect of melting on the mechanical  $\alpha$  relaxation of polyoxymethylene at frequencies accessible to the ultrasonic pulse technique ( $\sim 10$  MHz).<sup>149</sup> It was apparent from a discontinuity in the sound velocity and internal friction vs. temperature plots and from the results of supercooling experiments that the loss process in polyoxymethylene must be assigned an origin in the crystal lattice. In agreement with these interpretations and those of other investigators, the shift of the  $\alpha$  relaxation to lower temperatures and the decrease in its magnitude with a corresponding increase in oxyethylene content is indicative of motions of the molecular helix within the crystalline phase.<sup>89, 95, 150, 151</sup>

## 2. TED 5 Ester Terpolymer

The dynamic mechanical relaxations of this terpolymer are shown in Figure 17. Again, three distinct relaxations are observed for this polymer, which are labeled  $\alpha$ ,  $\beta$ , and  $\gamma$  in order of decreasing temperature.

The  $T_{\max}$  values for the  $\gamma$  relaxation are reported in Table 26.

Table 26

$T_{\max}$  for the  $\gamma$  ( $\tan \delta$ ) Relaxation  
of a TED Ester Terpolymer

Sample Designation	Mole % E <sup>a</sup>	Mole % D <sup>b</sup>	$T_{\max}$ (110 Hz) (°C)	$T_{\max}$ (11 Hz) (°C)	$T_{\max}$ (3.5 Hz) (°C)
Delrin	0	0	-60	-65	-71
TED 5 Ester	0.9	1.2	-57	-63	-69

<sup>a</sup>Moles  $\text{CH}_2\text{CH}(\text{COOC}_2\text{H}_5)$ /100 moles  $\text{CH}_2\text{O}$ .

<sup>b</sup>Moles  $\text{CH}_2\text{CH}_2\text{O}$ /100 moles  $\text{CH}_2\text{O}$ .

The TED  $\gamma$  loss has a slightly higher  $T_{\max}$  than those of Delrin homopolymer and of the trioxane-dioxolane copolymers (Table 26 vs. Table 23). This indicates that a new process which is slightly more energetic contributes to the  $\gamma$  relaxation in the TED ester terpolymer in addition to the motions described for the  $\gamma$  relaxation of trioxane-dioxolane copolymers. This new process is assigned to the motion of the ethyl ester carbonyl side chains in the amorphous phase. This assignment is analogous to the interpretation of the dielectric and mechanical  $\gamma$  relaxations in ethyl-acrylic and ethylene-methacrylic acid copolymers.<sup>152</sup>

The  $T_{\max}$ 's and activation energy for the  $\gamma$  relaxation of the TED terpolymer are shown in Table 27.

Table 27  
 Characteristics of the  $\beta$  ( $\tan \delta$ ) Relaxation  
 of a TED Ester Terpolymer

<u>Mole % E<sup>a</sup></u>	<u>Mole % D<sup>b</sup></u>	<u>T<sub>max</sub>(110 Hz) (°C)</u>	<u>T<sub>max</sub>(11 Hz) (°C)</u>	<u>T<sub>max</sub>(3.5 Hz) (°C)</u>	<u>E<sub>a</sub> kcal/mole</u>
0.9	1.2	0	-5	-7	65

<sup>a</sup>Moles CH<sub>2</sub>CH(COOC<sub>2</sub>H<sub>5</sub>)O/100 moles CH<sub>2</sub>O.

<sup>b</sup>Moles CH<sub>2</sub>CH<sub>2</sub>O/100 moles CH<sub>2</sub>O.

Assuming this process is exclusively due to motions of backbone segments which contain the oxyethylene unit then one would expect a smaller magnitude and a lower temperature for the process due to the lower concentration of oxyethylene units in the terpolymer. Indeed, a smaller magnitude is observed. The reason why the energetics of the process are higher than expected is believed to be due to an added restriction introduced by the termonomer units on chain mobility in the amorphous regions of the polymer. Therefore, the thermal energy required for the  $\beta$  relaxation to occur, in the terpolymer, is greater than that required for the corresponding copolymer. This explanation is in agreement with Park's interpretation of a shift in the temperature of the  $\beta$  process of a trioxane-ethylene oxide copolymer to a higher temperature in a trioxane-ethylene oxide terpolymer containing a small amount of a rigid non-crystallizable termonomer.<sup>95</sup> The motions of the carbonyl ester side chain are not believed to contribute to the  $\beta$  relaxation on the basis of the above discussion and the ensuing dielectric results. The mechanical  $\beta$  transition in the TED terpolymer is therefore ascribed to the motions of



main chain segments, containing the oxyethylene unit, in the amorphous regions.

Figure 18 illustrates the dependence of the  $\alpha$  transition on frequency in the TED ester terpolymer. As in the trioxane-dioxolane systems, the relaxation increases in magnitude and decreases in temperature with a corresponding decrease in frequency. The  $T_{\max}$  and activation energy for this process are listed in Table 28

Table 28

Characteristics of the  $\alpha$  ( $\tan \delta$ ) Relaxation  
of a TED Ester Terpolymer

Mole % E <sup>a</sup>	Mole % D <sup>b</sup>	$T_{\max}$ (110 Hz) (°C)	$T_{\max}$ (11 Hz) (°C)	$T_{\max}$ (3.5 Hz) (°C)	$E_a$ kcal/mole
0.9	1.2	140	129	124	76

<sup>a</sup>Moles  $\text{CH}_2\text{CH}(\text{COOC}_2\text{H}_5)\text{O}/100$  moles  $\text{CH}_2\text{O}$ .

<sup>b</sup>Moles  $\text{CH}_2\text{CH}_2\text{O}/100$  moles  $\text{CH}_2\text{O}$ .

### 3. STG Copolymers

The dynamic mechanical relaxations of the STG copolymers at 110 Hz are shown in Figure 19. Two relaxations are prominent in all copolymers except for STG 7 which shows an additional peak at higher temperature. These relaxations are labeled  $\alpha$ ,  $\alpha'$  and  $\gamma$  in order of decreasing temperature. The mechanical  $\beta$  process, observed in the trioxane-dioxolane and trioxane-ethyl glycidate-dioxolane systems and in Delrin, is either absent or as weak as in Delrin.

Table 29 summarizes the  $T_{\max}$  values for the  $\gamma$  process in these polymers.

Table 29  
 $T_{\max}$  for the  $\gamma$  ( $\tan \delta$ ) Relaxations  
 of the STG Copolymers

Sample Designation	Moles STG/ 100 Moles $\text{CH}_2\text{O}$	$T_{\max}$ (110 Hz) ( $^{\circ}\text{C}$ )	$T_{\max}$ (11 Hz) ( $^{\circ}\text{C}$ )	$T_{\max}$ (3.5 Hz) ( $^{\circ}\text{C}$ )
Delrin	0	-60	-65	-71
STG 7	1.3	-60	-65	-71
STG 2	2.9	-61	-69	-73
STG 9	4.5	-62	-71	-75
STG 23	6.5	-68	-79	-83

As more ionic comonomer units are incorporated into the polymer, the  $\gamma$  peak shifts to lower temperatures and becomes broader. This behavior serves to reinforce the conclusion that the  $\gamma$  relaxation in polyoxymethylene and its derivatives, as in polyethylene, arises from motions occurring in both the amorphous and crystalline phases.<sup>142,153</sup> The crystalline  $\gamma$  relaxation occurs at lower temperatures than the amorphous relaxation and the salt groups do not take part in the molecular motion responsible for the amorphous relaxation. A similar assignment was made for the  $\gamma$  process in polyethylene ionomers.<sup>101</sup> The crystalline and amorphous mechanical relaxations, in the STG copolymers are therefore assigned to the same processes responsible for the  $\gamma$  relaxations in trioxane-dioxolane copolymers and Delrin.

No significant  $\beta$  relaxation is observed in the STG systems. The absence of this transition, in these copolymers, reinforces the conclusion that the  $\beta$  process in the TD copolymers and TED ester terpolymer

arises from motions of main chain segments containing oxyethylene units.

The  $\alpha'$  relaxation, located between 60 and 110°C in Figure 19, increases in magnitude (and becomes narrower) as the content of sodium thioglycolate units in the copolymer increases. The  $T_{\max}$ 's and activation energies for this process are reported in Table 30.

Table 30

$T_{\max}$  for the  $\alpha'$  ( $\tan \delta$ ) Relaxations  
of the STG Copolymers

Sample Designation	Moles STG/ 100 Moles $\text{CH}_2\text{O}$	$T_{\max}$ (°C)			$E_a$ kcal/mole
		(110 Hz)	(11 Hz)	(3.5 Hz)	
STG 7	1.3	85	--	--	--
STG 2	2.9	87	81	78	93
STG 9	4.5	90	83	69	80
STG 23	6.5	100	90	86	64

The  $T_{\max}$ 's at 11 and 3.5 Hz and, therefore,  $E_a$  in the STG 7 sample could not be resolved from Figure 19 due to the increased overlap between  $\alpha'$  and the higher temperature  $\alpha$  process, at the lower frequencies.  $T_{\max}$  for  $\alpha'$  increases and  $E_a$  decreases with a corresponding increase in the content of ionic comonomer. This is in direct contrast with the behavior of the  $\alpha$  process in the TD and TED systems.

Figure 20 illustrates the frequency dependence of the  $\alpha'$  process. It is exactly opposite to that observed for the  $\alpha$  relaxation (Figure 18), i.e., the magnitude of  $\alpha'$  increases with increasing frequency.

The clearcut differences in the behavior of  $\alpha$  and  $\alpha'$  and their distinct presence in the STG 7 sample indicate that the two relaxations

arise from different mechanical relaxation processes.

Very interestingly, there is an exact parallel between the behavior of the  $\alpha'$  mechanical relaxation observed in the STG systems and the behavior of the dielectric  $\alpha$  relaxation process observed in the salts of ethylene-methacrylic acid copolymers.<sup>103</sup> The high activation energy, which decreased with increasing neutralization, and the temperature increase of the relaxation with increasing ionization were also observed in the polyethylene ionomers.<sup>103</sup> On the basis of X-ray studies, the relaxation in those systems was assigned to the breakup of large ionic regions into smaller clusters which were then very stable.<sup>154</sup> The  $\alpha'$  loss peak in the STG copolymers is therefore tentatively assigned to motions occurring in the ionic phase. This is the first direct experimental evidence of microphase separation in ionomers based on polyoxymethylene.

An ethylene-phosphonic acid copolymer, apparently exhibits microphase separation at high phosphonic acid contents, even without ionization as shown by the appearance of new prominent peak at 50°C.<sup>103, 110, 111</sup> In this case, the dispersed phase consists of hydrogen bonded aggregates of phosphonic acid groups.

The mechanical  $\alpha$  relaxation in STG 7 decreased in temperature from 143°C to 114°C as the frequency was lowered from 110 to 3.5 Hz. The resulting activation energy for this process was 64 kcal/mole.

#### D. Dielectric Studies

##### 1. Trioxane-Dioxolane Copolymers

The dielectric behavior of TD-10, TD-20, TD-30, and Delrin is



shown in Figure 21. Only one prominent relaxation is observed at low temperatures. The absence of an intermediate  $\beta$  process assumes a great deal of significance in light of the dynamic mechanical data on the same systems.  $\tan \delta_\epsilon$  begins to increase at temperatures higher than 60°C. Beyond this temperature, the data is not plotted because it contains d.c. conductivity effects and probably contributions from an ion double layer impurity which cannot be extracted out of the contribution from dipolar reorientation processes, if any.

$T_{\max}$ 's and activation energies for the  $\gamma$  dielectric process are summarized in Table 31.

Table 31  
Characteristics of the  $\gamma$  ( $\tan \delta_\epsilon$ ) Relaxation  
of Trioxane-Dioxolane Copolymers

Sample Designation	$T_{\max}, ^\circ\text{C}$ (10 kHz)	$T_{\max}, ^\circ\text{C}$ (5 kHz)	$T_{\max}, ^\circ\text{C}$ (1 kHz)	$T_{\max}, ^\circ\text{C}$ (0.5 kHz)	$T_{\max}, ^\circ\text{C}$ (0.2 kHz)	$E_a^c$ kcal/mole	$E_a^b$
Delrin	-52	-55	-60	-63	-65	16	29
TD-10 (2.2) <sup>a</sup>	-47	-50	-56	-58	-60	5	-
TD-20 (3.2) <sup>a</sup>	-42	-45	-52	-54	-56	5	-
TD-30 (4.2) <sup>a</sup>	-44	-48	-54	-55	-57	7	-

<sup>a</sup>Moles  $\text{CH}_2\text{CH}_2\text{O}/100$  moles  $\text{CH}_2\text{O}$ .

<sup>b</sup>From  $T_{\max}$  curve.

<sup>c</sup>From  $f_{\max}$  curve.

In contrast to the dynamic mechanical results which showed no differences (Table 23), the dielectric data exhibit an increase in the

$T_{\max}$ 's for the copolymers over that of Delrin. Comparison of Figure 21 with Figure 16 demonstrates that the mechanical relaxations, although larger in magnitude, are somewhat broader than the corresponding dielectric relaxations.

The trends in  $T_{\max}$  for the mechanical and dielectric  $\gamma$  process should be viewed with some reservation in light of the observed broadening of the relaxation spectra with decreasing temperature.<sup>123</sup> Nevertheless, the slight discrepancy between the results from the two measurements may also be due to the fact that the dielectric measurement is more selective as to the nature of the dipolar reorientation process observed. For example, structures A, B, and C described in Section C, part 1 of Chapter III and believed to be responsible for the mechanical  $\gamma$  process, have different dipole moments and therefore a larger contribution from one of these structures will give rise to a somewhat narrower dielectric relaxation process. The shift of  $T_{\max}$  to a higher temperature could be indicative of a larger contribution from structure C to the dielectric process since it involves motions about a carbon-carbon bond and a carbon-oxygen bond which are slightly more energetic than motions about two carbon-oxygen bonds (structures A and B). A slight decrease in the  $T_{\max}$  of TD-30 with respect to that of TD-20 may reflect an added contribution from structure B to the relaxation.

The activation energies for this process are relatively low. Nevertheless, if one draws the parallel with polyethylene, the motions to which this dielectric relaxation process is assigned require only

a very small activation energy. The value for the activation energy of the  $\gamma$  process of polyethylene, calculated assuming flip-flop motions of three-bond crankshafts, was about 8 kcal/mole.<sup>145</sup> The analogy with polyethylene is somewhat justified by the agreement between the lower rotational barriers for polyoxymethylene ( $\sim 2$  kcal/mole) and those for polyethylene ( $\sim 3$  kcal/mole)<sup>155, 156</sup> Therefore, the dielectric  $\gamma$  relaxation in polyoxymethylene is assigned to the same process responsible for the mechanical  $\gamma$  relaxation, i.e. flip-flop motions of three bond segments on the main chain, located in the amorphous and crystalline regions in the polymer.

The observed divergence between the  $f_{\max}$  and  $T_{\max}$  curves (Figure 22) for the  $\gamma$  relaxation has been ascribed largely to a rapid broadening of the dielectric relaxation spectrum with decreasing temperature.<sup>91</sup> Similar master curves have been described by Mc Crum, Read and Williams for the dielectric  $\gamma$  process in polyoxymethylene.<sup>123</sup> From the slope and curvature of the  $T_{\max}$  curve for Delrin (dashed curve in Figure 22), it is clear that an apparent activation energy derived (erroneously) from this curve will be larger than the correct value at low temperatures and will appear to vary with temperature (Table 31).

The  $\beta$  relaxation observed mechanically in the trioxane-dioxolane copolymers (Figure 16) is completely absent in their dielectric spectra (Figure 21). Table 32 shows how the flat dielectric  $\tan \delta_{\epsilon}$  in this region does not result from offsetting contributions by the dielectric loss and the dielectric constant. The dielectric constant remains unchanged in region; therefore the dielectric loss behaves in a similar fashion to  $\tan \delta_{\epsilon}$ .

Table 32  
Behavior of the 200 Hz Dielectric Parameters for TD-30  
in the Mechanical  $\beta$  Region

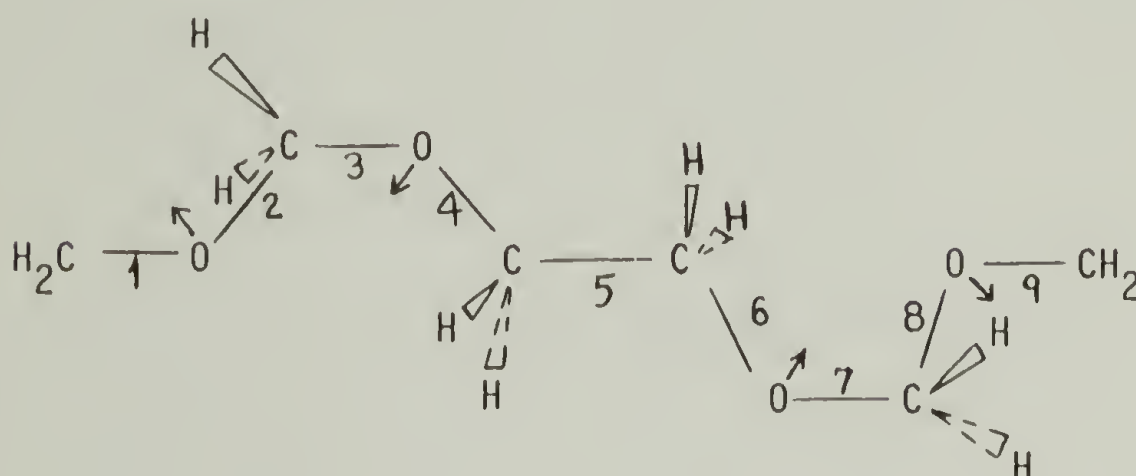
<u>Temperature (<math>^{\circ}\text{C}</math>)</u>	<u><math>\tan \delta_f</math></u>	<u><math>\epsilon'</math></u>	<u><math>\epsilon''</math></u>
-23	$1.82 \times 10^{-2}$	2.54	$4.63 \times 10^{-2}$
-8	$1.52 \times 10^{-2}$	2.54	$3.86 \times 10^{-2}$
4	$1.48 \times 10^{-2}$	2.55	$3.77 \times 10^{-2}$
15	$1.46 \times 10^{-2}$	2.55	$3.72 \times 10^{-2}$
28	$1.52 \times 10^{-2}$	2.54	$3.86 \times 10^{-2}$

The absence of a dielectric loss process in a temperature region where a prominent mechanical loss process is observed means that the motion which gives rise to the mechanical loss process does not involve a dipolar reorientation. This phenomenon is observed when the moving segment or structure has no dipole moment. An example of this type of mechanically active and dielectrically inactive relaxation is the motion of long alkyl side chains in polydodec-1-ene and higher homologs which influence the behavior of the mechanical  $\alpha$  process.<sup>123</sup> Another possibility is that a cooperative motion of two segments, each exhibiting a dipole moment, takes place such that the dipolar reorientation associated with the motion of one segment effectively cancels out that associated with the motion of the other segment.

Due to the polar nature of the chain, even the smallest segment in trioxane-dioxolane copolymers exhibits a dipole moment. Therefore, in this case, the first explanation may be excluded. In order to test the second hypothesis, molecular models of the chain were constructed and



examined. Again, due to the nature of the chain, no cooperative motion involving a net cancellation of dipole moments could be visualized for the oxymethylene homopolymer. However, the presence of an isolated oxyethylene unit along the backbone gives rise to an energetically favorable symmetrical structure which may be represented by the following configuration:



The dipole moments in this structure are aligned parallel to each other and in exactly opposite directions. They also possess the same magnitude and therefore effectively cancel each other out. In light of this model, the motion responsible for the mechanical  $\beta$  relaxation in the trioxane-dioxolane copolymers is assigned to the cooperative rotation about the three colinear bonds 1, 5, and 9 in the manner of a crankshaft. The colinearity between bonds is achievable if there are intervening carbon-oxygen atoms, on the assumption of tetrahedral valence angles and a rotational isomeric state model.

Further refinement of this model envisions these rotations as simultaneous clockwise or counterclockwise flip-flop motions of three bond

segments 2, 3 and 4 and 6, 7 and 8 about bonds 1, 5 and 9. It is not necessary for the segments to rotate a full  $360^\circ$  as long as the motions are simultaneous and in the same direction. This refinement dispenses with the argument that a large swept out volume, and therefore more energy, are required for those motions to take place. The matrix surrounding this structure must be sufficiently homogeneous so that the symmetry elements in the crankshaft can interact to the same extent with identical non-bonded nearest neighbors.

This kind of structure is less likely to exist in the crystalline array of helical polyoxymethylene chains unless it represents a defect (or kink) in the lattice.<sup>147</sup> Also, as mentioned previously, the oxyethylene units are less inclined to incorporate into the crystalline lattice.<sup>82</sup> Thus, contributions from the crystalline regions to this mechanical process although possible are highly improbable. These rotational isomers are, therefore, believed to exist predominantly in the amorphous regions of the copolymers.

The magnitude of the mechanical  $\beta$  relaxation should increase with the concentration of these rotational isomers in the amorphous phase. This is observed experimentally (Figure 16).

The rotational isomeric state model has already been invoked, successfully, to account for different experimental observations made on the polyoxymethylene system. A statistical mechanical calculation of the static dielectric constant of the polyoxymethylene melt based on the rotational isomeric state model was in good agreement with experiment.<sup>143</sup>

The rotational isomeric state scheme was shown to be adequate for the calculation of the average intramolecular conformational energy of polyoxymethylene, if the torsional oscillation about skeletal bonds is taken into account in the harmonic approximation.<sup>155</sup> The appearance of "surplus" bands in the infrared spectrum of polyoxymethylene was believed to be due to rotational isomerism in the chain and not to the disturbance of the selection laws operating in an isolated molecule due to its going over to the crystal lattice of the polymer.<sup>157-159</sup>

## 2. TED Ester and Salt Terpolymers

The dielectric relaxations of the ester and salt terpolymers of trioxane, ethyl glycidate and dioxolane at 200 Hz are shown in Figures 23 and 24. A low temperature relaxation is observed in all cases, whereas an intermediate temperature relaxation is observed at higher concentrations of ester groups in the polymer but not in the corresponding salts.

The  $T_{\max}$  values and activation energies for the low temperature dielectric relaxation in these systems are reported in Table 33.

Table 33  
 Characteristics of the  $\gamma$  ( $\tan \delta_\epsilon$ ) Relaxations  
 of Trioxane-Ethyl Glycidate-Dioxolane Terpolymers

Sample Designation	$T_{\max}, ^\circ\text{C}$ (10 kHz)	$T_{\max}, ^\circ\text{C}$ (5 kHz)	$T_{\max}, ^\circ\text{C}$ (1 kHz)	$T_{\max}, ^\circ\text{C}$ (0.5 kHz)	$T_{\max}, ^\circ\text{C}$ (0.2 kHz)	$E_a$ kcal/mole
Delrin	-55	-55	-60	-63	-65	16
TED Ester(0.9) <sup>a</sup> (1.2) <sup>b</sup>	-44	-48	-56	-58	-64	6
TED Ester(1.7) <sup>a</sup> (1.2) <sup>b</sup>	-44	-49	-57	-60	-64	5
TED Ester(2.0) <sup>a</sup> (1.2) <sup>b</sup>	-44	-48	-56	-60	-66	7
TED Salt(0.9) <sup>c</sup> (1.2) <sup>b</sup>	-48	-51	-57	-60	-68	11
TED Salt(1.7) <sup>c</sup> (1.2) <sup>b</sup>	-47	-51	-58	-61	-68	11
TED Salt(2.0) <sup>c</sup> (1.2) <sup>b</sup>	-47	-52	-58	-61	-69	10

<sup>a</sup>Moles  $\text{CH}_2\text{CH}(\text{COOC}_2\text{H}_5)_0/100$  moles  $\text{CH}_2\text{O}$ .

<sup>b</sup>Moles  $\text{CH}_2\text{CH}_2\text{O}/100$  moles  $\text{CH}_2\text{O}$ .

<sup>c</sup>Moles  $\text{CH}_2\text{CH}(\text{COO}^\ominus \oplus \text{Na})_0/100$  moles  $\text{CH}_2\text{O}$ .

The  $\gamma$  relaxation in these systems is assigned to the same motions responsible for the dielectric and mechanical  $\gamma$  relaxations of trioxane-dioxolane copolymers, i.e., flip-flop motions of three bond segments in the crystalline and amorphous regions of the polymer. The magnitude of the  $\gamma$  process in the ester terpolymers varies as a function of composition while the breadth of the relaxation remains unchanged (Figure 23). These variations cannot be accounted for only by motions of segments containing oxyethylene units since the concentration of oxyethylene units in these



systems is relatively constant, according to NMR analysis. Therefore, as in the mechanical case, an additional contribution to the  $\gamma$  process is believed to be due to the motions of ester carbonyl side chains. On the other hand, both the magnitude and the breadth of the  $\gamma$  relaxation in the salt systems remain relatively constant despite an increase in the concentration of salt groups. These results imply that the salt groups do not participate in the motions responsible for this relaxation, possibly because they are segregated into clusters. The presence of these clusters may nevertheless hinder these motions causing the slightly higher activation energy observed in the salt systems vs. that of the corresponding esters.

At higher concentrations of ester groups (and constant concentration of oxyethylene units) an intermediate temperature relaxation appears in the dielectric spectrum which grows in magnitude as the concentration of ester groups increases. This dielectric peak is absent in the ester terpolymer containing 0.9 mole % of the ester groups, although a mechanical peak is observed, at intermediate temperatures, in the same system (Figure 17). The activation energy for this intermediate temperature dielectric and mechanical relaxations (and their  $T_{\max}$ 's measured at approximately the same frequencies) are significantly different from each other to suggest that two separate relaxation processes are going on. On the basis of these results, the mechanical  $\beta$  relaxation in the TED ester (0.9 mole % ester groups) is assigned to the motion of rotational isomers containing oxyethylene units. The dielectrically active  $\beta'$  relaxation is assigned to the

motions of the ester carbonyl side chains.

Table 34 lists the  $T_{\max}$ 's and activation energy of the intermediate  $\beta'$  temperature relaxation in the TED ester terpolymers.

Table 34

Characteristics of the Intermediate Temperature

Dielectric Relaxation in the TED Ester Terpolymer (2.0)<sup>a</sup> (1.2)<sup>b</sup>

$T_{\max}$ (5 kHz) (°C)	$T_{\max}$ (1 kHz) (°C)	$T_{\max}$ (0.5 kHz) (°C)	$T_{\max}$ (0.2 kHz) (°C)	$E_a$ kcal/mole
-6	-10	-12	-16	42

<sup>a</sup>Moles  $\text{CH}_2\text{CH}(\text{COOC}_2\text{H}_5)\text{O}/100$  moles  $\text{CH}_2\text{O}$ .

<sup>b</sup>Moles  $\text{CH}_2\text{CH}_2\text{O}/100$  moles  $\text{CH}_2\text{O}$ .

The absence of the  $\beta$  peak in the corresponding salts (Figure 23) is further indication that the salt groups are not free to move even at intermediate temperatures because they are grouped into microphase separated clusters which retain their integrity to higher temperatures in the solid.

## C H A P T E R IV

## CONCLUSIONS

Ethyl glycidate, unlike dioxolane, is very reluctant to copolymerize, cationically, with trioxane. This reluctance is reflected by the low yield, high percent of base unstable fraction and low molecular weight of the products obtained in the gas phase, in bulk or in solution. Chain transfer reactions (to ethyl glycidate) are believed to be responsible for the low tendency of the monomer to copolymerize with trioxane.

The preparation of a cesium salt of a polyoxymethylene derivative is reported for the first time. Polyoxymethylene ionomers based on monovalent cations have also been obtained.

Trifluoromethane sulfonic acid is a highly efficient initiator for the copolymerization of trioxane with dioxolane. Products exhibiting high molecular weights and a low content of base unstable fraction were obtained in high yields, using much lower concentrations of trifluoromethane sulfonic acid than with  $\text{BF}_3$  or its complexes. This efficiency is controlled in part by the macroester  $\rightleftharpoons$  macroion equilibrium believed to exist during this polymerization.<sup>45</sup>

Calorimetric and relaxation studies provide evidence for a three phase model in the STG copolymers. This model consists of a crystalline phase composed entirely of oxymethylene units, an amorphous phase of mixed composition and a third phase comprised of small ionic clusters randomly distributed throughout the amorphous phase. The melt recrystallized trioxane-dioxolane copolymers fit a two phase model with an oxymethylene-rich crystalline phase, containing a small fraction of

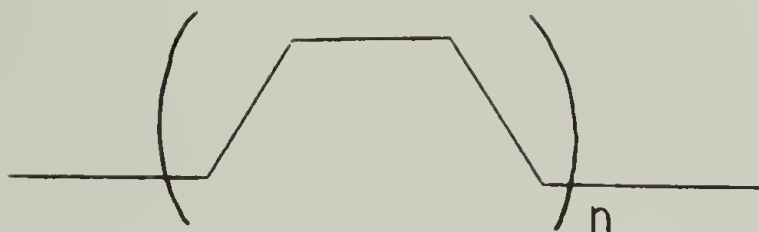
oxyethylene units, and an amorphous phase of mixed composition. The kinetic theory of crystallization of random copolymers, proposed by Sanchez and Eby, is applicable, in principle, to both of these systems.<sup>160</sup> The crystallization behavior of the ionic STG copolymers is different from that of the unionized trioxane copolymers, suggesting that the ionic clusters slow down the rate of crystallization in these systems.

The mechanical and dielectric  $\gamma$  transition arises from flip-flop motions of three bond segments on the main chain, located in the amorphous and crystalline regions of the polymers. An additional contribution is observed, in the trioxane-ethyl glycidate-dioxolane terpolymers, from motions of the carbonyl side chains in the amorphous regions.

Flip-flop motions of a specific rotational isomer, containing the oxyethylene unit and located in the amorphous regions, are responsible for the mechanical  $\beta$  transition observed in the trioxane-dioxolane copolymers. This crankshaft model accounts for the absence of the corresponding dielectric process.

The assignments for the  $\gamma$  and  $\beta$  transitions fit the general scheme proposed by Boyer, who states that all polymers tend to have three amorphous transitions,  $T_{g,g}$ ,  $T_G$  and  $T_{l,l}$ , involving motion around the chain axis in the crankshaft model:





where  $n$  assumes values of ,  $1 < n < 10$  and  $10 < n < \infty$ .

Experimental evidence for  $T_{1,1}$  in polyoxymethylene is provided by the high frequency dielectric experiments by Boyd<sup>143</sup> who showed that what appeared to be a single loss region in the solid<sup>91</sup> and whose center moves above 8 GHz, at higher temperatures, becomes two regions in the melt. He postulated that the  $\gamma$  region in the solid moved abruptly to higher frequency, upon melting and a new  $\alpha$  mechanism appeared at somewhat lower frequency. This  $\alpha$  peak in the melt, presumably has little relation molecularly to the crystalline  $\alpha$  peak observed in the solid, mechanically.<sup>91</sup>

The dielectric  $\beta'$  transition is assigned to motions of carbonyl side chains in the amorphous regions of the trioxane-ethyl glycidate-dioxolane terpolymers.

The mechanical  $\alpha'$  transition in copolymers containing sodium thioglycolate groups, arises from motions within microphase segregated ionic clusters. Indirect evidence for the presence of these clusters is provided by calorimetric studies and by a water uptake experiment (Table 9). The amount of water uptake increases with increasing ion concentration. Wissbrun also observed a reasonably linear increase in the moisture vapor transmission, weight gain and length expansion with increasing ionic content, after exposure of these copolymers to a 90% relative humidity atmosphere.<sup>4</sup> A less dramatic but still pronounced increase of water

absorption was also found for polyolefin ionomers.<sup>98, 99, 127</sup> This increased moisture sensitivity, in the polyolefin ionic systems, is attributed to the presence of ionic clusters which create regions of high dielectric constant that are favorable for water.<sup>127</sup> In the polyoxymethylene ionomers, these results are rationalized in light of the chemical structure of the oxymethylene chain with its large proportion of oxygen available for hydrogen bonding once the polymer crystal structure is disrupted by the ionic clusters present.<sup>4</sup>

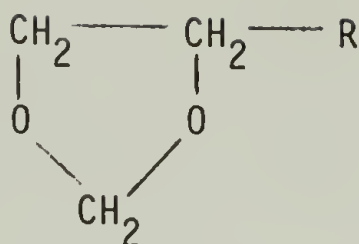
The mechanical  $\alpha$  transition is ascribed to motions of the molecular helix within the crystalline phase.

## CHAPTER V

### SUGGESTIONS FOR FURTHER WORK

The main objective of this investigation was to prepare ionomers based on polyoxymethylene and study their physical properties. This task was partially accomplished by the preparation and subsequent characterization of derivatives of trioxane-ethyl glycidate copolymers and of trioxane-ethyl glycidate-dioxolane terpolymers. A high content of base unstable fraction in the polymers and low molecular weight of all the polymers indicated that the ionic monomer units were not distributed randomly throughout the polymer chains. Consequently, the resulting ionomer films did not have adequate mechanical strength which prevented extensive measurements of mechanical properties. Both of these requirements, had they been met, would have simplified considerably the task of characterizing the properties of the ionomers as a function of only one variable, the ionic content. In addition, difficulty in incorporating the monomer, ethyl glycidate, into trioxane polymers proved a real stumbling block throughout the entire investigation.

A different method to prepare the same oxymethylene polymers with high molecular weights and random distribution of the ionic comonomer throughout the polymer chain is proposed. The copolymerization of trioxane with a substituted dioxolane,



where  $R = \text{COOC}_2\text{H}_5$  or  $\text{COOCH}_3$  has been reported.<sup>6, 161</sup> The polymeric ester could then be converted to the corresponding sodium salt.

This substituted monomer has been synthesized from the ethyl ester of glyceric acid in the presence of paraformaldehyde and p-toluene sulfonic acid.<sup>6</sup> Heat resistant polyoxymethylenes with ionizable side chains have been claimed by polymerizing trioxane with up to 25 weight percent of the substituted dioxolane, at 60°C, in the presence of  $\text{BF}_3\text{Bu}_2\text{O}$ .<sup>161</sup>

In view of the results of this work, a random polymer with excellent mechanical properties might be achieved by solution copolymerization of trioxane with the substituted dioxolane in the presence of trifluoromethane sulfonic acid. This polymer could then be converted to the corresponding ionomer by solution hydrolysis with sodium hydroxide, in methanol at about 160°C and 250 psi pressure.

One of the conclusions of this investigation was that the cesium salt of polyoxymethylene derivatives can be obtained in a straightforward way from the corresponding sodium salt. In analogy to the studies on the cesium salts of ethylene-methacrylic acid copolymers, characterization of the cesium salts of the oxymethylene copolymers with thioglycolate groups by low angle and wide-angle x-ray scattering techniques would provide direct evidence for the presence of clusters as well as information as to their size and shape.<sup>108, 154, 162</sup>



Further evidence in support of the microphase separated structural model may be obtained by determination of the static and dynamic strain optical coefficient as a function of temperature and cation concentration, by X-ray diffraction and infrared dichroism studies of the relaxation of polyoxymethylene ionomers and their unionized precursors, and by investigating the behavior of the mechanical  $\alpha'$  peak with increasing water content in the polymers. Similar studies have been carried out on ethylene-methacrylic acid copolymers and their salts.<sup>105,107,163</sup>

Additional experimental evidence for the presence of rotational isomers in polyoxymethylene is available in literature.<sup>143,155,157-159</sup> Considerable insight on the conformations and molecular structure of trioxane-dioxolane copolymer chains may be gained by temperature dependent spectroscopic studies such as the ones carried out by Snyder on liquid n-paraffins and molten polyethylene. Tadokoro, Enikolopyan and co-workers conducted similar studies on polyoxymethylene, polydioxolane, and their oligomers,<sup>157-159, 164-170</sup> and actually calculated the possible isomeric structures of the molecules  $\text{CH}_3\text{-O-(CH}_2\text{O)}_n\text{CH}_3$  ( $n=3-8$ ).<sup>167,168</sup>

## REFERENCES

1. K.V. Martin and O. Vogl (to DuPont de Nemours Co.)  
U.S. Patent 3,284,411 (1966).
2. K.V. Martin (to DuPont de Nemours Co.) U.S. Patent  
3,316,218 (1968).
3. K. Weissermel, E. Fischer, K.H. Hafner and H. Cherdron,  
Angew. Makromol. Chem., 4/5, 168 (1968).
4. K.F. Wissbrun, Makromol. Chem., 118, 211 (1968).
5. K.F. Wissbrun, F.M. Berardinelli, and M.B. Price  
(to Celanese Research Co.) U.S. Patent 3,488,322 (1970).
6. Perstorp AB, French Patent 2,064,881 (1971).
7. R.N. MacDonald (to DuPont de Nemours Co.) French Patent  
1,082,519 (1954).
8. R.N. MacDonald (to DuPont de Nemours Co.) British Patent  
748,836 (1956).
9. R.N. MacDonald (to DuPont de Nemours Co.) U.S. Patent  
2,768,994 (1957).
10. C. Walling, F. Brown and K.W. Bartz (to Celanese Research Co.)  
U.S. Patent 3,027,352 (1962).
11. DuPont de Nemours Co., British Patent 796,862 (1958).
12. W. Kern, Chem. Z., 88, 623 (1964).
13. E. Kunzel, A. Gieffer and W. Kern, Makromol. Chem., 96, 17 (1966).
14. R.E. Gee, J.B. Gray, P.R. Hippely, H.A. O'Hern Jr. and  
J.B. Thompson (to DuPont de Nemours Co.) U.S. Patent 3,172,736 (1965).
15. S. DalNogare and J.O. Punderson (to DuPont de Nemours Co.)  
U.S. Patent 2,998,409 (1961).

16. J.O. Punderson (to DuPont de Nemours Co.) British Patent 880,737 (1960).
17. Montedison, Belgian Patent 596,750 (1959).
18. A.L.J. Raum and J.M. Barton (to Distillers Co.) British Patent 1,039,979 (1962).
19. Degussa, Belgian Patent 606,723 (1960).
20. Houilleres du Basin du Nord, Belgian Patent 580,339 (1958).
21. W. Kern, E. Eberius and V. Jaacks, Makromol. Chem., 141, 63 (1971).
22. O. Vogl, Makromol. Chem., 175, 1281 (1974).
23. O. Vogl, J. Macromol Sci. (Revs.), C 12 (1), 109 (1975).
24. T.E. Carruthers and R.G.W. Norrish, Trans. Faraday Soc., 32, 195 (1934).
25. J.C. Bevington and R.G.W. Norrish, Proc. Roy. Soc., A 205, 516 (1951).
26. V. Jaacks, K. Boehlke and E. Eberius, Makromol Chem., 118, 354 (1968).
27. K. Boehlke and V. Jaacks, Makromol Chem., 142, 189 (1971).
28. H. Staudinger, Die Hochmolekularen Organischen Verbindungen, Springer, Berlin (1932).
29. N. Brown, J. Macromol. Sci. (Chem.), A 1, 209 (1967).
30. H. Gudgeon and R.J. Marklow (to Imperial Chemical Industries Ltd.) British Patent 1,035,891 (1966).
31. H. Sidi (to Tenneco Chemicals Inc.) U.S. Patent 3,293,222 (1966).
32. W.P. Baker (to DuPont de Nemours Co.) U.S. Patent 3,225,121 (1965).

33. T. Eguchi and J. Yamauchi (to Kurashiki Rayon Co.)  
U.S. Patent 3,346,540 (1967).
34. G.W. Halek, F.M. Berardinelli, C.M. Hendry and W.J. Roberts  
(to Celanese Research Co.) U.S. Patent 3,317,475 (1967).
35. S. Kawasumi, K. Maemoto and M. Onishi (to Sumitomo Chemical Co.)  
U.S. Patent 3,326,857 (1967).
36. M. Ragazzini, M. Modena, E. Gallinella and G. Ceridalli,  
J. Polymer Sci., A 2, 5203 (1964).
37. G.J. Mantell and D. Rankin (to Gulf Oil Co.) U.S. Patent 3,265,665  
(1966).
38. S. Okamura, S. Nakashio and K. Hayashi, Doitai To Hoshasen,  
3, 242 (1960).
39. H. Yamoka, K. Hayashi and S. Okamura, Makromol. Chem., 76, 196 (1964).
40. C. Chachaty, M. Magat and L.T. Minassian, J. Polymer Sci., 48,  
139 (1960).
41. W. Kern and V. Jaacks, J. Polymer Sci., 48, 399 (1960).
42. V. Jaacks and W. Kern, Makromol Chem., 62, 1 (1963).
43. V. Jaacks, H. Frank, E. Grunberger and W. Kern, Makromol Chem.,  
115, 290 (1968).
44. B.A. Rosenberg, O.M. Chekhuta, E.B. Lyudvig, A.R. Gantmakher and  
S.S. Medvedev, Vysokomolekul. Soedin., 6, 2030 (1964).
45. S. Penczek, J. Fejgin, P. Kubisa, K. Matyjaszewski and  
M. Tomaszewicz, Makromol. Chem., 172, 243 (1973).
46. T. Miki, T. Higashimura and S. Okamura, Bull. Chem. Soc. Japan,  
39, 36 (1966).



47. B.A. Rosenberg, V.I. Irjak and N.S. Enikolopyan, Vysokomolekul. Soedin., 7, 2180 (1965).
48. T. Higashimura, T. Miki and S. Okamura, Bull. Chem. Soc. Japan, 39, 31 (1966).
49. N.S. Enikolopyan, V.J. Irzhak, I.P. Kravchuk, O.A. Plechova, G.V. Rakova, L.M. Romanov and G.P. Savushkina, J. Polymer Sci., C 16, 2453 (1965).
50. T. Miki, T. Higashimura and S. Okamura, J. Polymer Sci., A 1 (5), 95 (1967).
51. T. Miki, T. Higashimura and S. Okamura, J. Polymer Sci., A 1 (6), 3031 (1968).
52. S. Rosinger (to Farbwerke Hoechst A.-G.) German Patent 1,157,783 (1960).
53. S. Rosinger, H. Herman and K. Weissermel, J. Polymer Sci., A 1 (5), 183 (1967).
54. S. Okamura, K. Hayashi, S. Nakashio and I. Sakurada, Isotopes and Radiation (Tokyo), 3, 242 (1959).
55. S.E. Jamison and H.D. Noether, J. Polymer Sci., B 1, 51 (1963).
56. E.V. Prut and N.S. Enikolopyan, Vysokomolekul. Soedin., 8, 1905 (1966).
57. T.R. Steadman and F. Jaffe (to W.R. Grace and Co.) U.S. Patent 3,115,480 (1963).
58. W. Wilson and H. May (to Brit. Industrial Plastics Ltd.) U.S. Patent 3,296,210 (1967).
59. W. Wilson and H. May (to Brit. Industrial Plastics Ltd.) U.S. Patent 3,317,477 (1967).
60. I. Rosen (to Diamond Alkali Co.) U.S. Patent 3,344,120 (1967).

61. C.N. Wolf (to Ethyl Corp.) U.S. Patent 3,356,649 (1967).
62. K. Weissermel, E. Fischer, K. Gutweiler, H.D. Hermann and H. Cherdron, Angew. Chem., 79, 512 (1967).
63. Farbwerke Hoechst A.-G., Belgian Patent 624,203 (1963).
64. A.K. Schneider (to DuPont de Nemours Co.) U.S. Patent 2,795,571 (1957).
65. J.E. Wall, E.T. Smith and G.J. Fisher (to Celanese Research Co.) U.S. Patent 3,174,948 (1965).
66. K.J. Saunders, Organic Polymer Chemistry, Chapman and Hall Ltd., London (1973).
67. J. Brandrup and E.H. Immergut, Polymer Handbook, Wiley Interscience, 2nd Edition (1975).
68. W.H. Stockmayer and L.L. Chan, Polymer Preprints, 6, 333 (1965).
69. H.L. Wagner and K.F. Wissbrun, Makromol. Chem., 81, 14 (1965).
70. V. Kokle and F.W. Billmeyer, Jr., J. Polymer Sci., B 3, 47 (1965).
71. G. Allen, R. Warren and K.G. Taylor, Chem. and Ind., 623, (1964).
72. Von R. Boltze, J. Brunn, K. Doerffel, W. Hobold and G. Opitz, J. prakt. Chemie, 312, 596 (1970).
73. E.G. Brame, Jr. and O. Vogl, J. Macromol. Sci. (Chem.), A 1 (2), 277 (1967).
74. D. Fleischer and R.C. Schultz, Makromol. Chem., 152, 311 (1972).
75. H. Wilski, Makromol. Chem., 150, 209 (1971).
76. L. Mortillaro, G. Galiazzo and S. Brezzi, Gazz. Chim. Ital., 94, 109 (1964).
77. L. Leese and M.W. Baumber, Polymer, 6 (5), 269 (1965).

78. K. O'Leary and P.H. Geil, J. Macromol. Sci. (Phys.), B 1 (1), 147 (1967).
79. A. Peterlin and C. Reinhold, J. Polymer Sci., A 3, 2801 (1965).
80. Y. Aoki, A. Nobuta, A. Chiba and M. Kaneko, Polymer J., 2 (4), 502 (1971).
81. R. Mateva, G. Wegner and G. Lieser, J. Polymer Sci. (Lett.), 11, 369 (1973).
82. M. Droscher, G. Lieser, H. Reimann and G. Wegner, Polymer, 16, 497 (1975).
83. W. Glenz, H.G. Kilian and F.H. Muller, Kolloid - Z.u.Z. Polymere, 206, 104 (1966).
84. A. Nobuta, A. Chiba and M. Kaneko, Rep. Progr. Polym. Phys. Japan, 12, 137 (1969).
85. E.W. Fischer, F. Kloos and G. Lieser, J. Polymer Sci., B 7, 845 (1969).
86. F.S. Dainton, D.M. Evans, F.E. Hoare and T.P. Melia, Polymer, 3, 263 (1962).
87. W.H. Linton, Trans. Plast. Inst. London, 28, 131 (1960).
88. G. Kortleve and C.G. Vonk, Kolloid - Z.u.Z. Polymere, 225, 124 (1968).
89. M. Takayanagi, Mem. Fac. Eng. Kyushu Univ., 23 (1), 1 (1963).
90. N. McCrum, J. Polymer Sci., 54, 561 (1961).
91. B. Read and G. Williams, Polymer, 2, 239 (1961).
92. L. Bohn, Kolloid - Z.u.Z. Polymere, 201, 20 (1965).
93. Y. Ishida, M. Matsuo, H. Ito, M. Yoshino F. Irie and M. Takayanagi, Kolloid - Z.u.Z. Polymere, 174, 162 (1961).

94. K. Arisawa, K. Tsuge and V. Wada, Rep. Prog. Polymer Phys., 6, 151 (1963).
95. I.K. Park, Makromol. Chem., 118, 375 (1968).
96. K. Miki, S. Yamane and M. Kaneko, Proc. of the Fifth Congress on Rheology, Univ. of Tokyo Press, 3, 335 (1970).
97. R.W. Rees (to DuPont de Nemours Co.) British Patent 1,011,981 (1966).
98. R.W. Rees and D.J. Vaughan, Polymer Preprints, 6, 287 (1965).
99. R.W. Rees and D.J. Vaughan, Polymer Preprints, 6, 296 (1965).
100. W.J. MacKnight, T. Kajiyama and L. McKenna, Polym. Eng. Sci., 8 (4), 267 (1968).
101. L.W. McKenna, T. Kajiyama and W.J. MacKnight, Macromolecules, 2, 58 (1969).
102. L.W. McKenna, Ph.D. Thesis, Univ. of Massachusetts (1971).
103. P.J. Phillips and W.J. MacKnight, J. Polymer Sci., A 2 (8), 727 (1970).
104. K. Sakamoto, W.J. MacKnight and R.S. Porter, J. Polymer Sci., A 2 (8), 277 (1970).
105. T. Kajiyama, T. Oda, R.S. Stein and W.J. MacKnight, Macromolecules, 4, 198 (1971).
106. Y. Uemura, R.S. Stein and W.J. MacKnight, Macromolecules, 4, 490 (1971).
107. W.J. MacKnight in Colloidal and Morphological Behavior of Block and Graft Copolymers, Ed. G.E. Molau, Plenum Press, 131 (1971).
108. J. Kao, R.S. Stein, W.J. MacKnight, W.P. Taggart and G.S. Cargill III, Macromolecules, 7, 95 (1974).
109. W.P. Taggart, Ph.D. Thesis, Univ. of Massachusetts (1973).



110. P.J. Phillips, F.A. Emerson and W.J. MacKnight, Macromolecules, 3, 767 (1970).
111. P.J. Phillips, F.A. Emerson and W.J. MacKnight, Macromolecules, 3, 771 (1970).
112. P.J. Phillips and W.J. MacKnight, Polymer Letters, 8, 87 (1970).
113. F.A. Emerson, Ph.D. Thesis, Univ. of Massachusetts (1971).
114. R. Weiss, Ph.D. Thesis, Univ. of Massachusetts (1975).
115. K. Sanui, R.W. Lenz and W.J. MacKnight, J. Polymer Sci., 12, 1965 (1974).
116. L.P. DeMejo, W.J. MacKnight and O. Vogl, Canadian High Polymer Forum Communication, Paper # 17 (1975).
117. W.D. Emmons and A.S. Pagano, J. Am. Chem. Soc., 77, 89 (1955).
118. H.Y. Aboul-Enein, Synth. Comm., 4 (5), 255 (1974).
119. A.M. Muldajhmetov, A.V. Schelkunov and A.K. Shokanov, Tr. Khim. Met. Inst. Akad. Nauk. Kaz. SSR., 2, 176 (1968).
120. E.S. Watson, M.J. O'Neill, J. Justin and N. Brenner, Anal. Chem., 36, 1233 (1964).
121. B. Wunderlich and C. Cormier, J. Polymer Sci., A 2 (5), 987 (1967).
122. Encyclopedia of Chem. Tech., 2nd Ed., Interscience, New York, 11, 581 (1966).
123. N.G. McCrum, B.E. Read and G. Williams, Anelastic and Dielectric Effects in Polymeric Solids, Wiley Interscience, New York (1967).
124. C.H. Porter, J.H.L. Lawler and R.H. Boyd, Macromolecules, 3 (3), 309 (1970).
125. C.H. Porter and R.H. Boyd, Macromolecules, 4 (5), 589 (1971).
126. R.M. Neumann and W.J. MacKnight, Polymer Preprints, 17 (2), 178 (1976).

127. A. Eisenberg and M. Navratil, Macromolecules, 6 (4), 604 (1973).
128. K.F. Wissbrun and M.J. Hannon, J. Polymer Sci. (Phys.), 13, 223 (1975).
129. K. Weissermel, E. Fischer, K. Gutweiler and H.D. Hermann, Kunststoffe, 54, 410 (1964).
130. I. Penczek and S. Penczek, Makromol. Chem., 67, 203 (1963).
131. S. Slomkowski and S. Penczek, Chem. Comm., 1347 (1970).
132. S. Slomkowski, Ph.D. Thesis, Polish Academy of Sciences, Lodz (1963).
133. S. Penczek, Symposium on Cationic Polymerization, Akron, Abstract # VII/2 (1976).
134. T. Saegusa, Symposium on Cationic Polymerization, Akron, Abstract # VII/1 (1976).
135. S. Penczek, J. Fejgin, W. Sadowska and M. Tomaszewics, Makromol. Chem., 116, 203 (1968).
136. A. Stolarczyk, P. Kubisa and S. Penczek, Bull. Acad. Pol. Sci., Ser. Sci. Chim., 22 (5), 431 (1974).
137. J.V. Crivello, private communication.
138. H. Bohnsack, Riechst. Aromen. Koerperpflagem., 16 (12), 512 (1966).
139. V. Jaacks, H. Baader and W. Kern, Makromol. Chem., 83, 56 (1965).
140. R. Silverstein and G. Bassler, Spectrometric Identification of Organic Compounds, John Wiley & Sons Inc., 2nd Ed. (1967).
141. M. Inoue, J. Appl. Polymer Sci., 8, 2225 (1964).
142. R.H. Boyd and C.H. Porter, Polymer Preprints, 12 (1), 135 (1971).
143. C.H. Porter, J.H.L. Lawler and R.H. Boyd, Macromolecules, 3 (3), 308 (1970).

144. K. Yamafuji and Y. Ishida, Kolloid Z., 183, 15 (1962).
145. R.H. Boyd and S.M. Breitling, Macromolecules, 7 (6), 855 (1974).
146. R.F. Boyer, Rubber Chem Tech., 34, 1303 (1963).
147. Von B. Stoll, W. Pechold and S. Blasenbrey, Kolloid - Z.u.Z. Polymere, 250, 1111 (1972).
148. H. Thurn, Kolloid Z., 173, 72 (1960).
149. R.H. Boyd and K. Biliyar, Polymer Preprints, 14 (1), 329 (1973).
150. N. Yamada, Z. Orito and S. Minami, J. Polymer Sci., A 3, 4173 (1965).
151. K. Hikichi and J. Furuichi, J. Polymer Sci., A 3, 3003 (1965).
152. W.J. MacKnight and F.A. Emerson in Dielectric Properties of Polymers, F.E. Karasz ed., Plenum Press, New York, 237 (1972).
153. J.D. Hoffman, G. Williams and E. Passaglia, J. Polymer Sci., C 14, 173 (1966).
154. B.W. Delf and W.J. MacKnight, Macromolecules, 2, 309 (1969).
155. G. Allegra, M. Calligaris and L. Randaccio, Macromolecules, 6 (3), 390 (1970).
156. G. Allegra and A. Immirzi, Makromol. Chem., 124, 70 (1969).
157. E.F. Oleinik, Vysokomol. soyed., 6, 2103 (1964).
158. E.F. Oleinik and N.S. Enikolopyan, Vysokomol. soyed., 8 (4), 583 (1966).
159. E.F. Oleinik and N.S. Enikolopyan, J. Polymer Sci., C 16, 3677 (1968).

160. I.C. Sanchez and R.K. Eby, J. Res. Nat. Bur. of Standards, A - Phys. and Chem., 77 A (3), 353 (1973).
161. Perstorp AB, French Patent 2,077,359 (1971).
162. W.J. MacKnight, W.P. Taggart and R.S. Stein, J. Polymer Sci., Symp. # 45, 113 (1974).
163. T. Kajiyama, R.S. Stein and W.J. MacKnight, J. Appl. Phys., 41, 4361 (1970).
164. R.G. Snyder, J. Chem. Phys., 47 (4), 1316 (1967).
165. H. Tadokoro, M. Kobayashi, Y. Kawaguchi, A. Kobayashi and S. Murahashi, J. Chem. Phys., 38 (3), 703 (1963).
166. E.F. Oleinik and N.S. Enikolopyan, Vysokomol. soedin. Ser. A, 9 (12), 2609 (1967).
167. E.F. Oleinik and V.Z. Kompaniets, New Advances in Methods of Polymer Investigation, Izd. "Mir" (1968).
168. E.F. Oleinik, V.Z. Kompaniets, V.P. Volkov and N.S. Enikolopyan, 2nd Mater. Konf. Vop. Str. Reakts. Sposobnosti Atsetalei, 26 (1970).
169. V.Z. Kompaniets, E.F. Oleinik and N.S. Enikolopyan, Vysokomol. soedin. Ser. A, 14 (3), 669 (1972).
170. E.F. Oleinik, A.L. Bugachenko and E.V. Anufrieva, New in Life, Science and Technology - Chemistry Series, # 7 : Spectroscopic Methods for Studying Polymers (1975).



## PMR SPECTRUM OF ETHYL GLYCIDATE

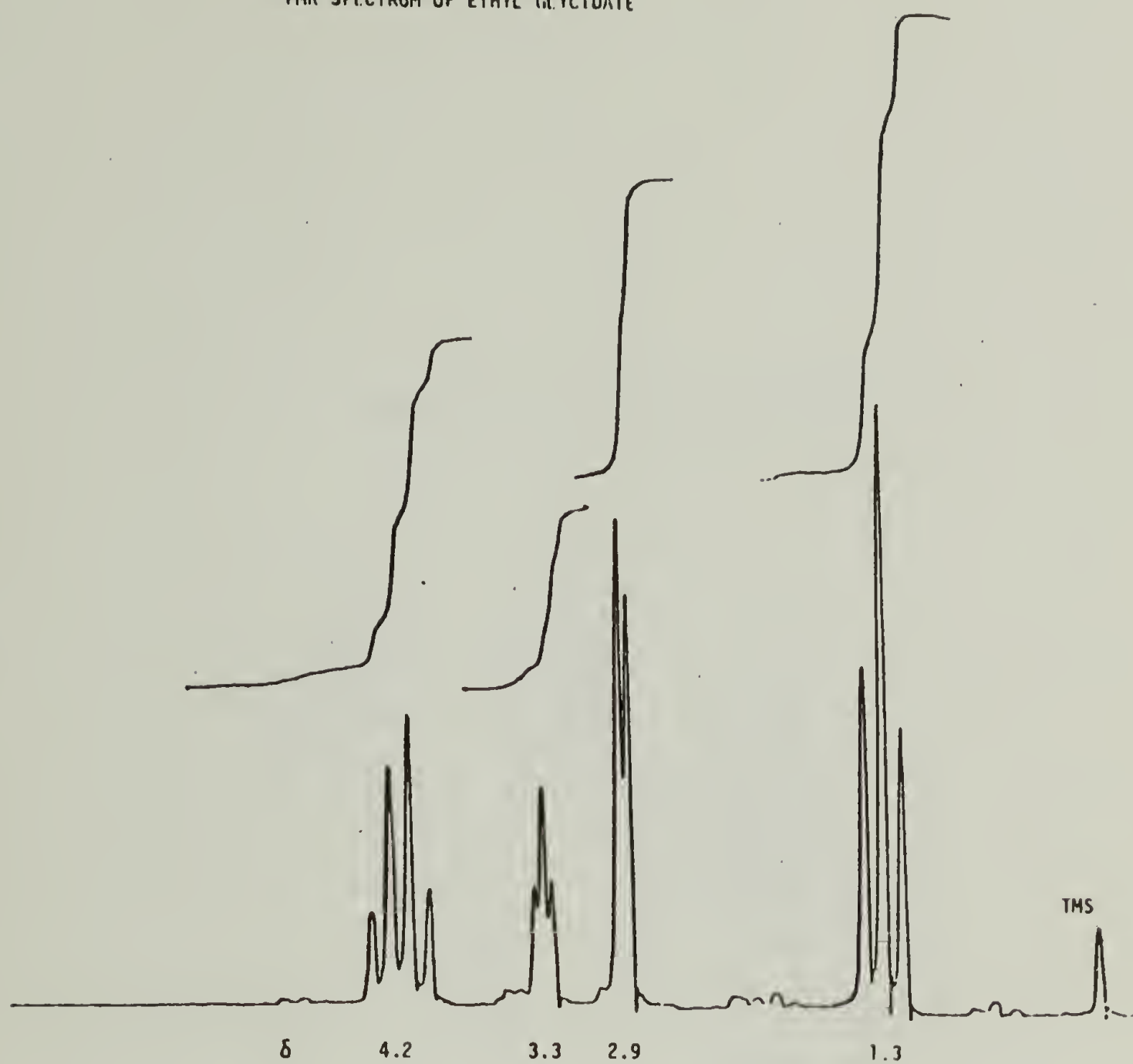


FIGURE 1

## INFRARED SPECTRA OF POM DERIVATIVES

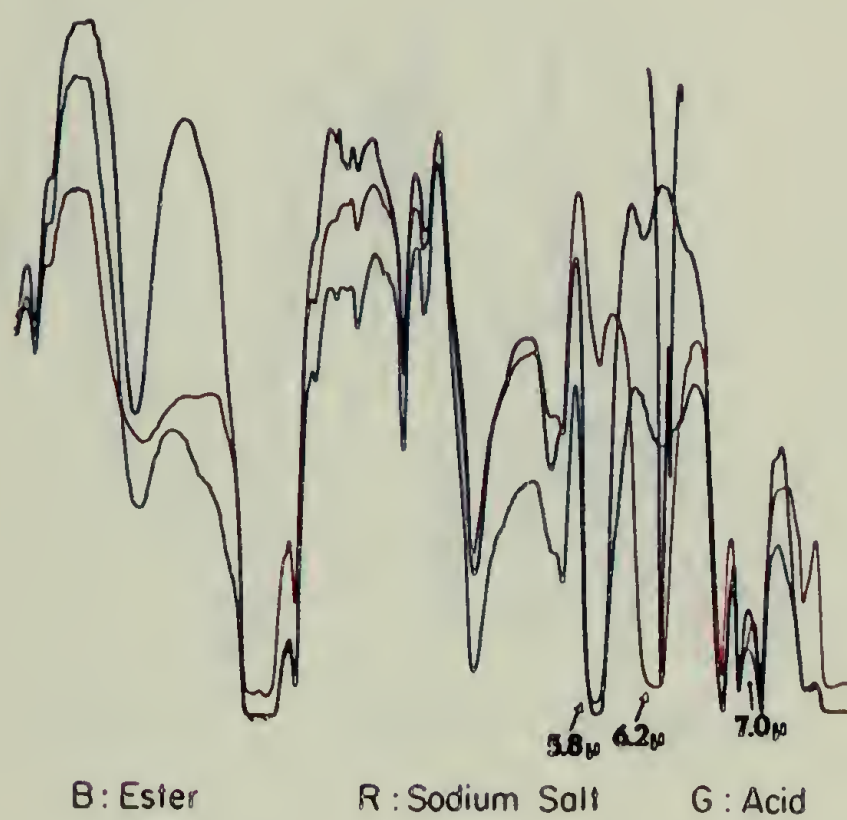


FIGURE 2

## INFRARED SPECTRA OF POM CARBOXYLATES

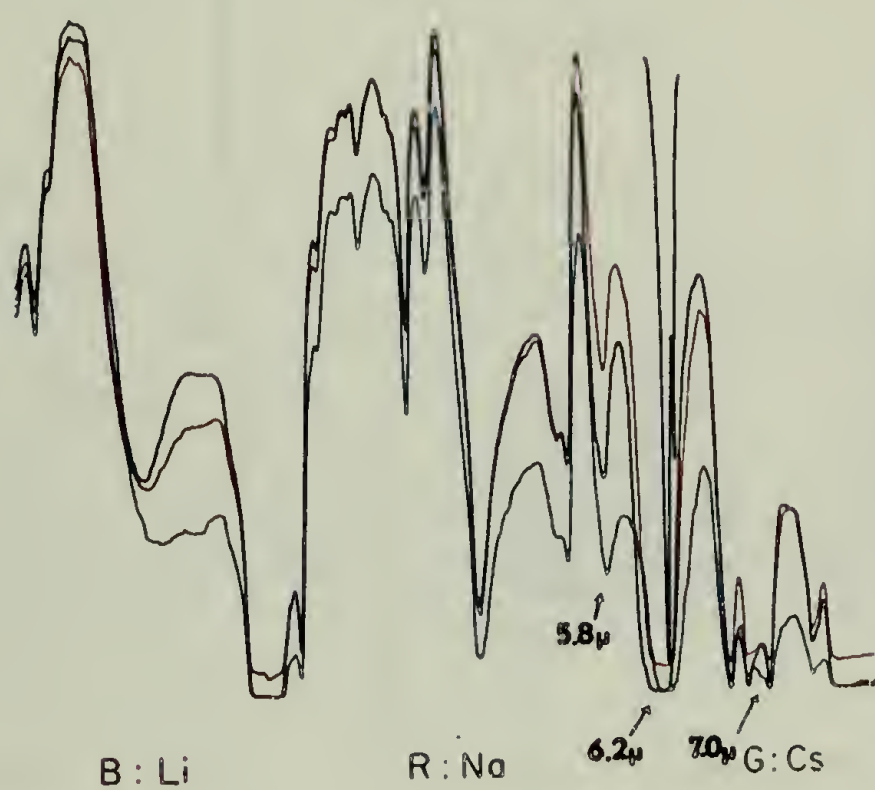


FIGURE 3

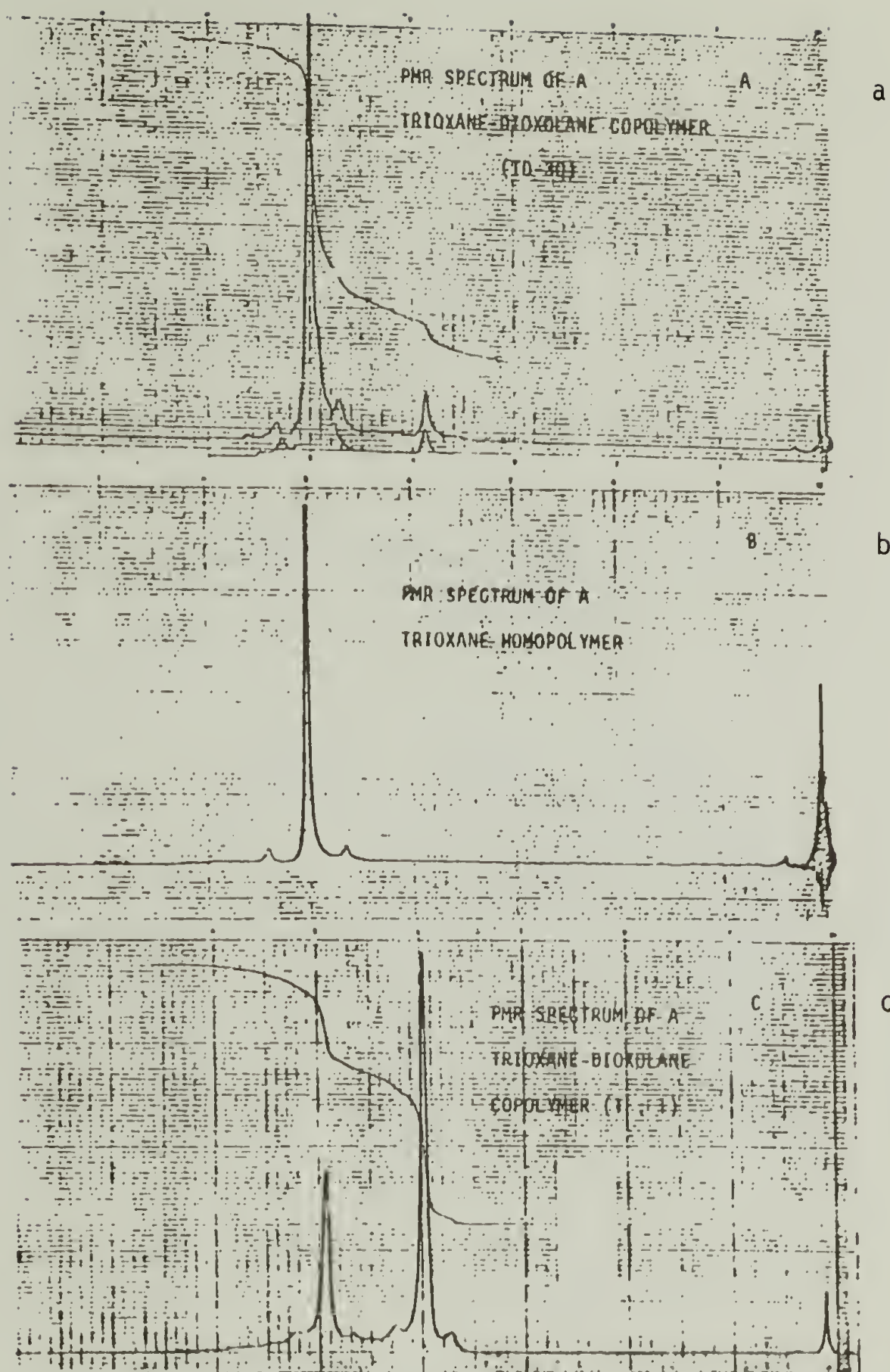


FIGURE 4



INFRARED SPECTRA OF TRIOXANE - DIOXOLANE  
COPOLYMERS

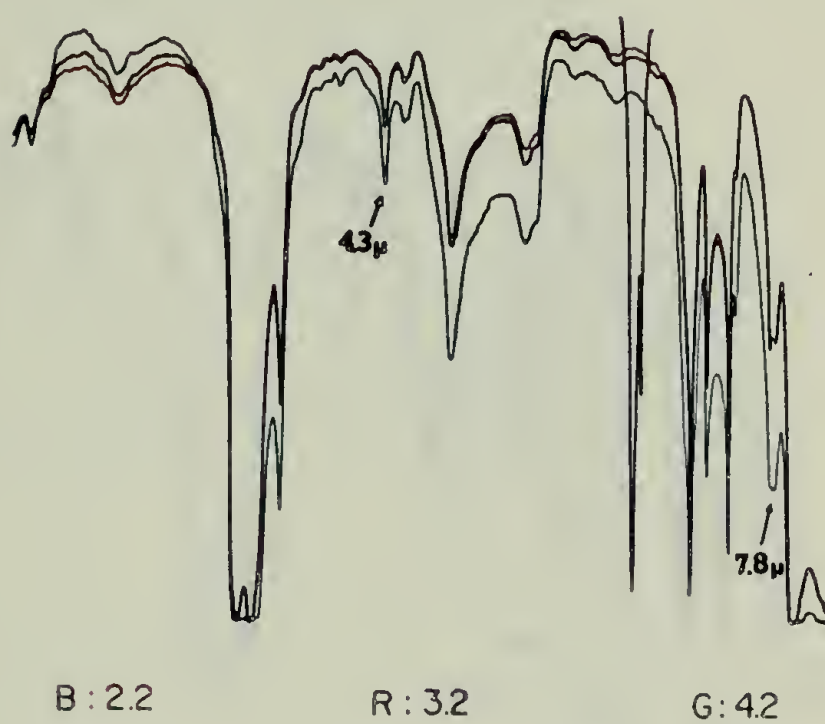


FIGURE 5

## INFRARED SPECTRA OF POM DERIVATIVES

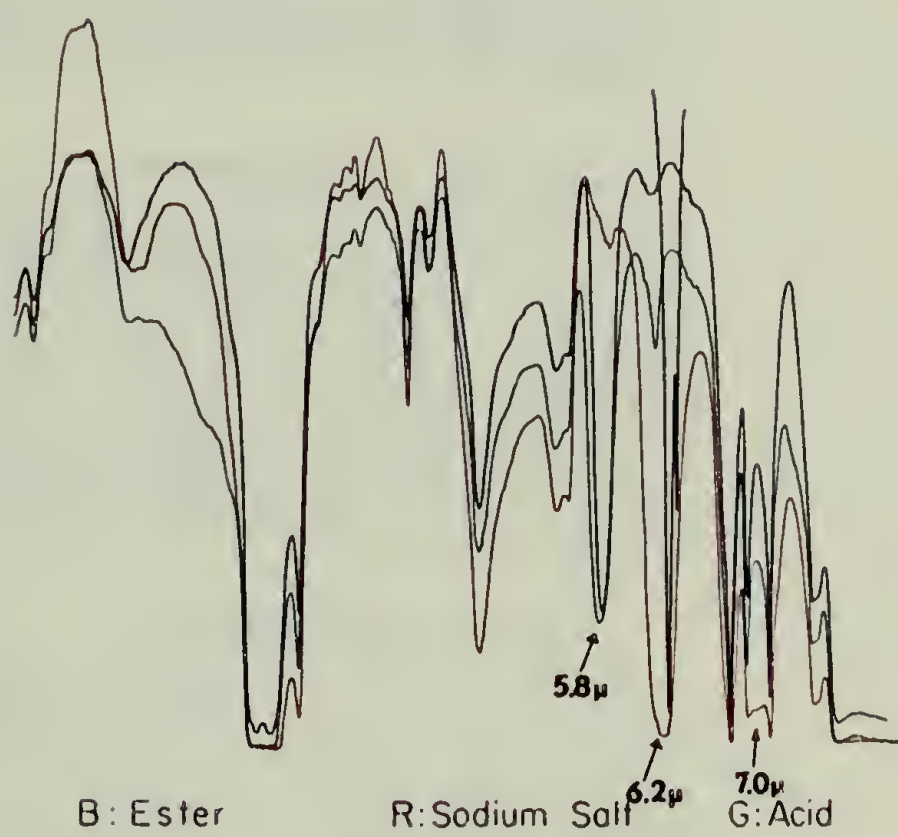
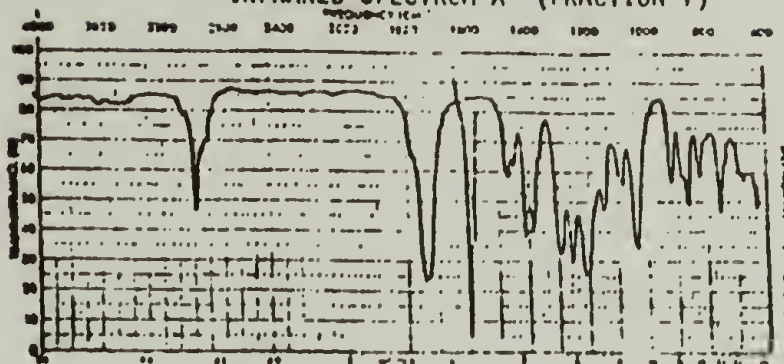


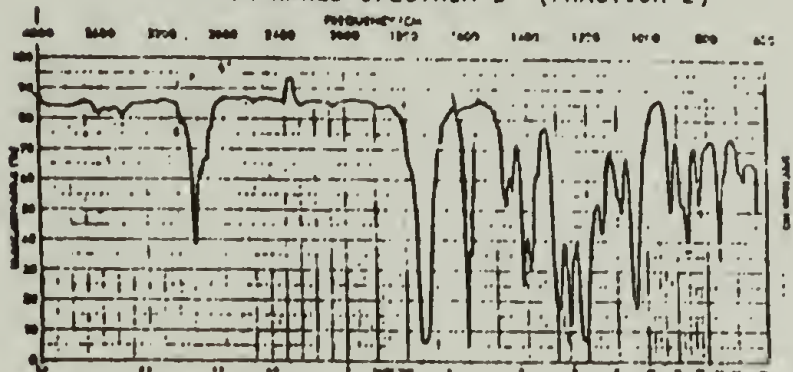
FIGURE 6

## ETHYL GLYCIDATE DISTILLATION

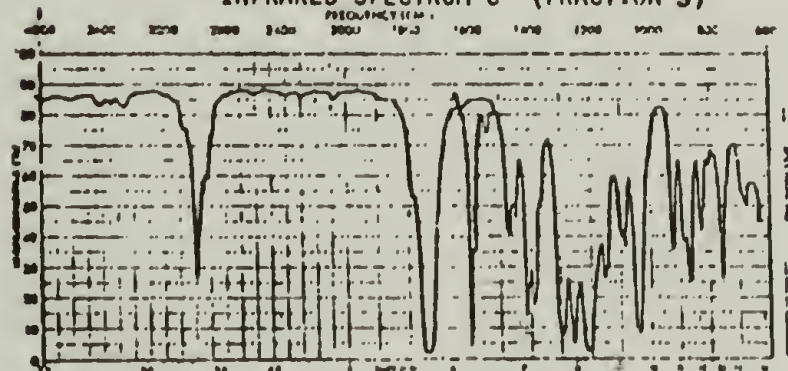
## INFRARED SPECTRUM A (FRACTION 1)



## INFRARED SPECTRUM B (FRACTION 2)



## INFRARED SPECTRUM C (FRACTION 3)



## INFRARED SPECTRUM D (FRACTION 4)

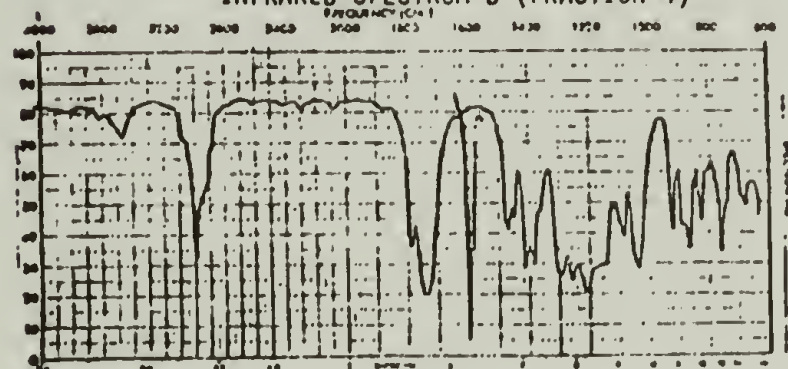


FIGURE 7

INFRARED OF TRIOXANE HOMOPOLYMER

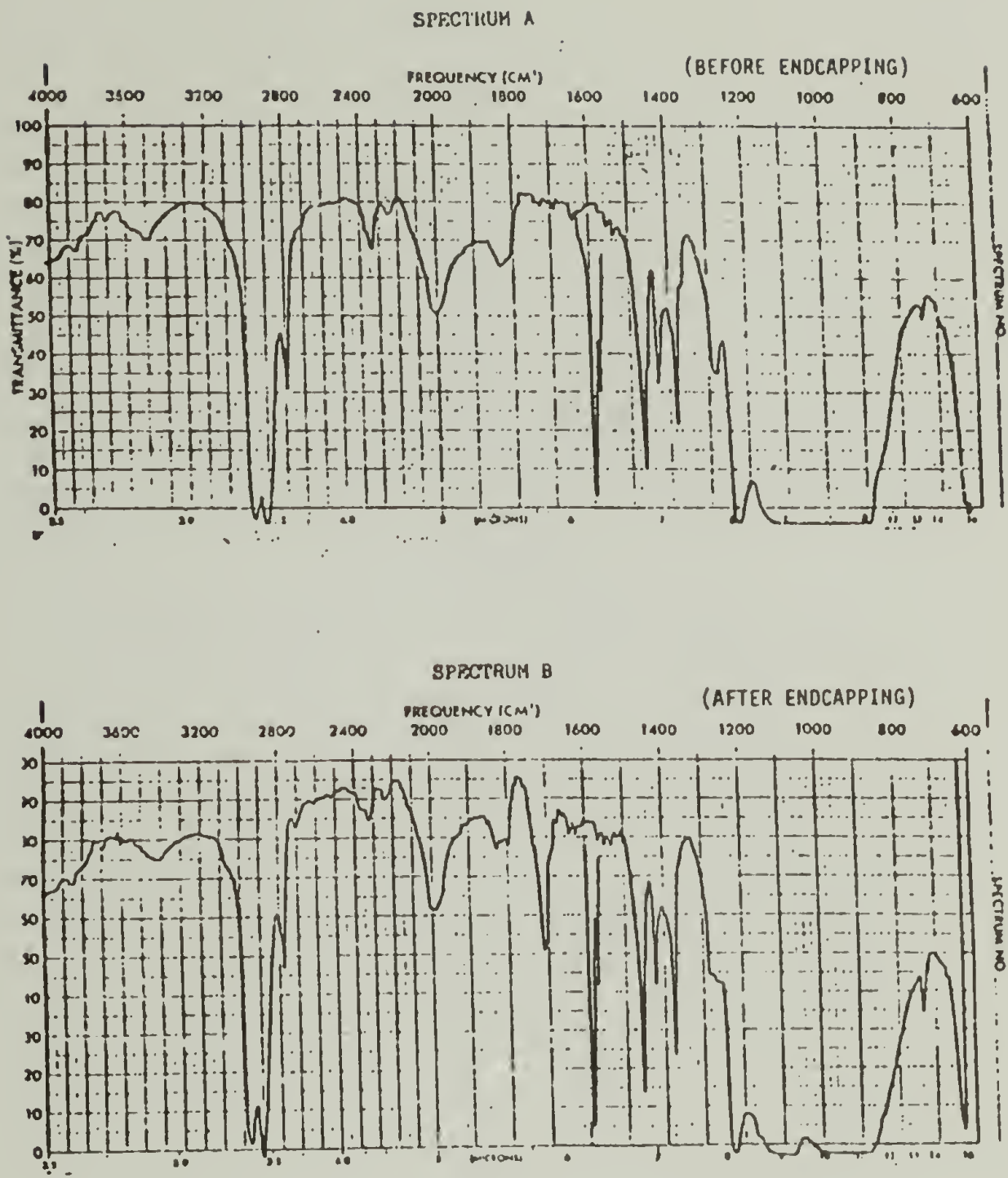
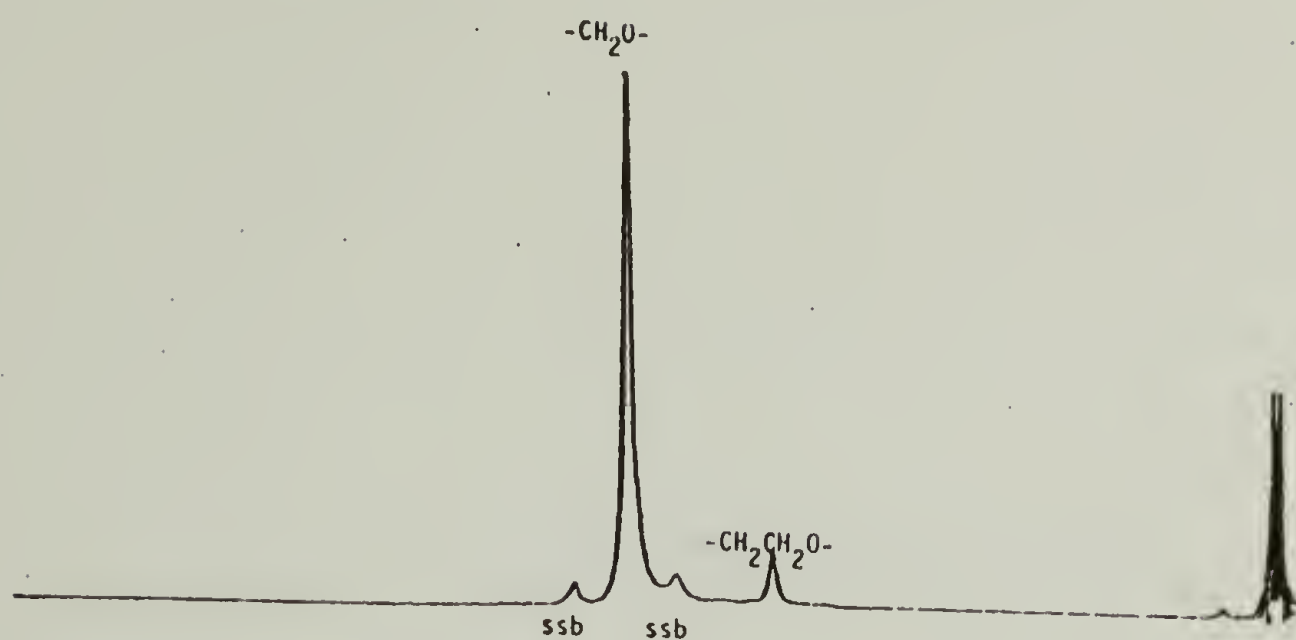


FIGURE 8



SPECTRUM A

PMR SPECTRUM OF A POM COPOLYMER



SPECTRUM B

PMR SPECTRUM OF A POM TERPOLYMER

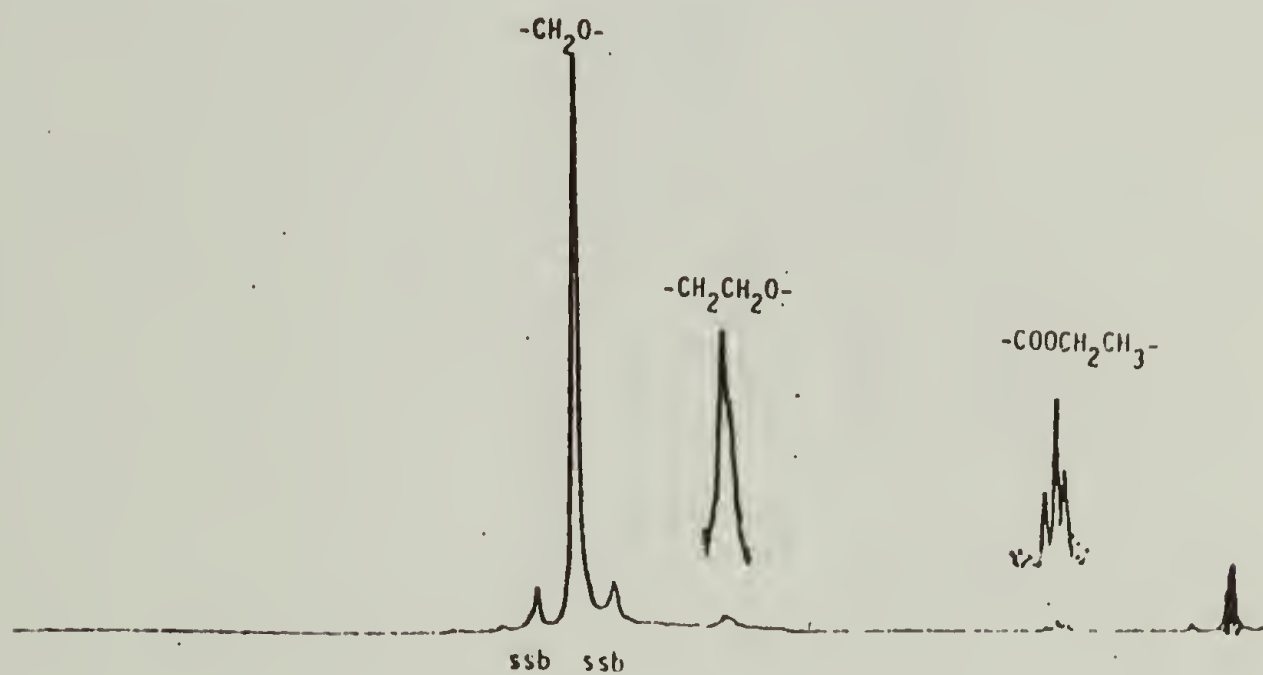
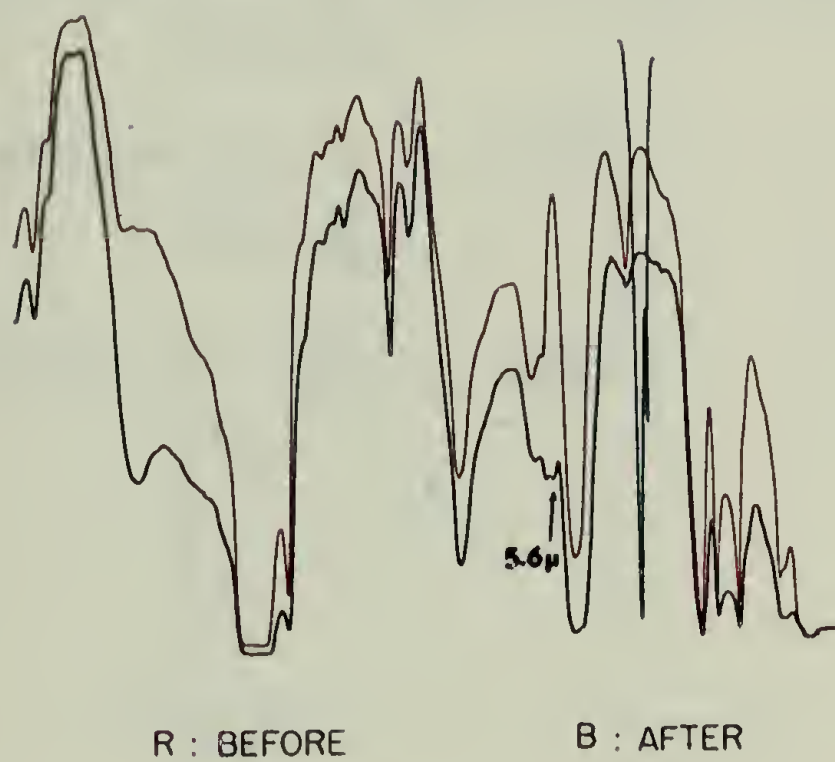


FIGURE 9

INFRARED SPECTRA OF POM ACID  
BEFORE AND AFTER HEAT TREATMENT



F I G U R E    10

## OXYMETHYLENE COPOLYMERS AND TERPOLYMERS

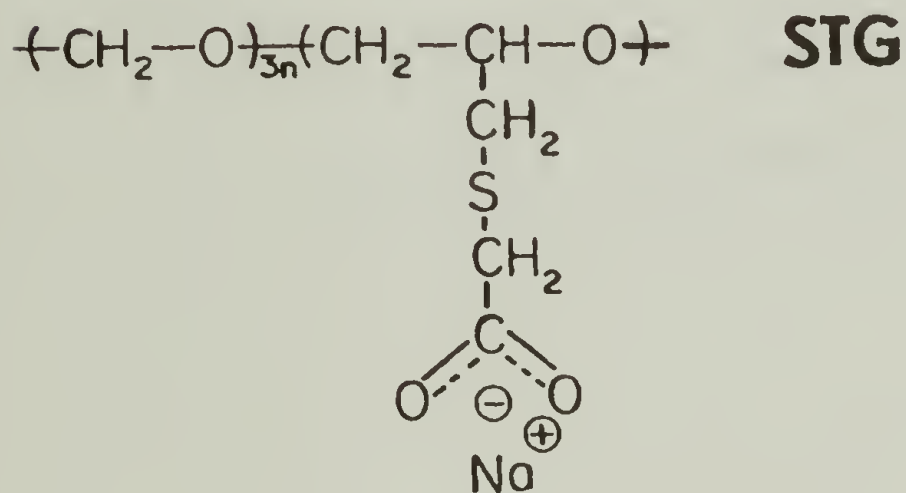
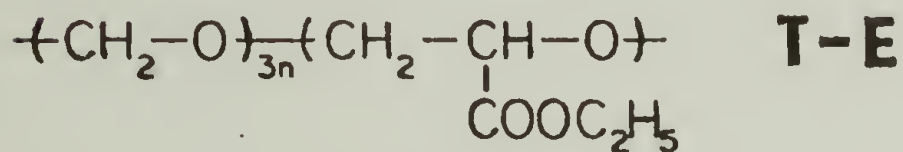
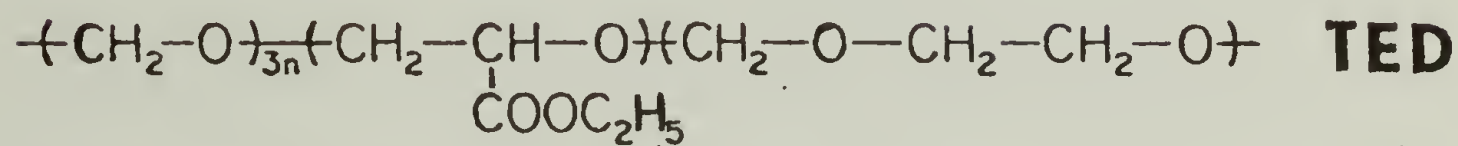


FIGURE 11

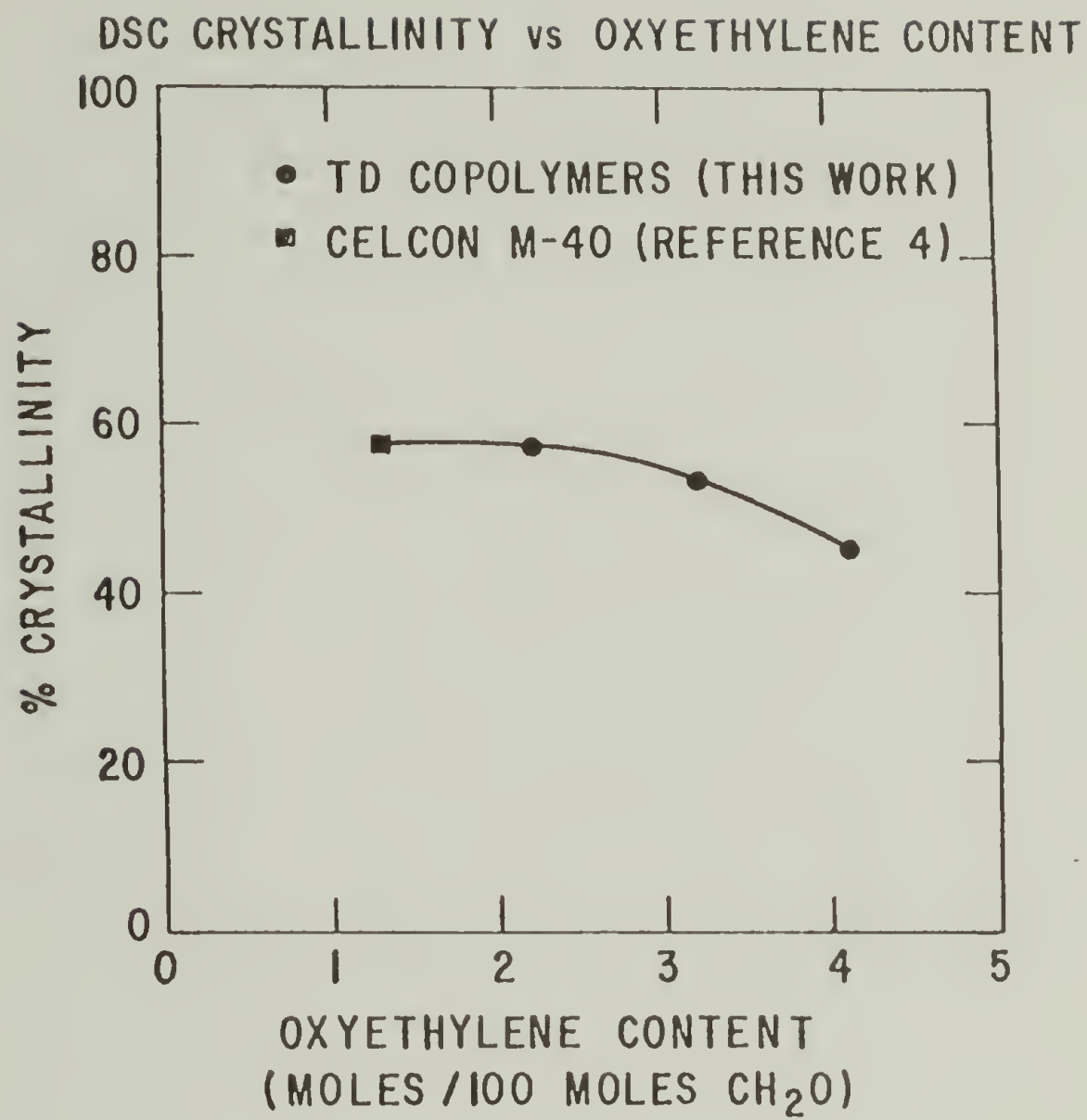


FIGURE 12



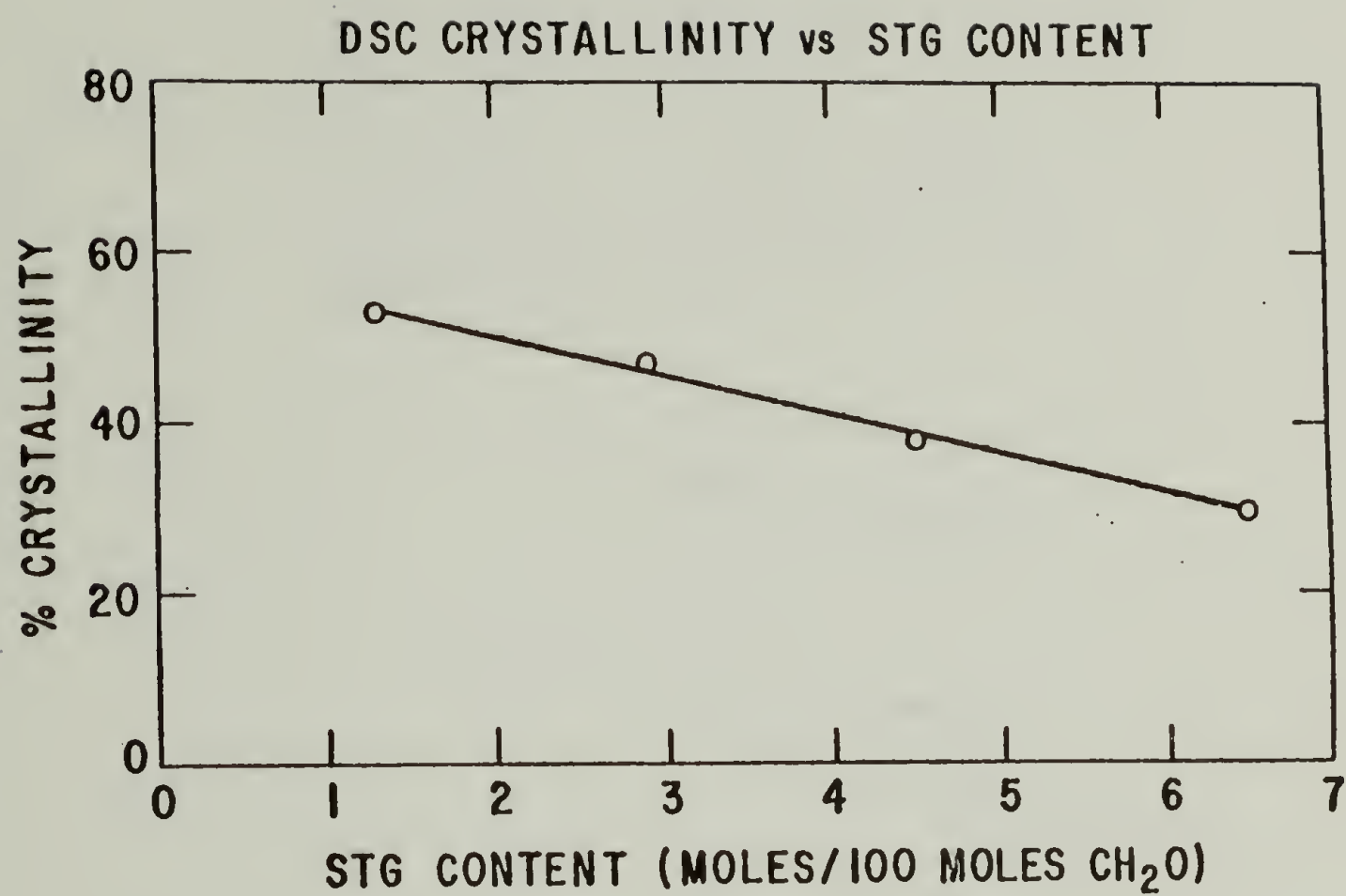


FIGURE 13

# MELTING AND CRYSTALLIZATION OF IONIC AND NON-IONIC COPOLYMERS

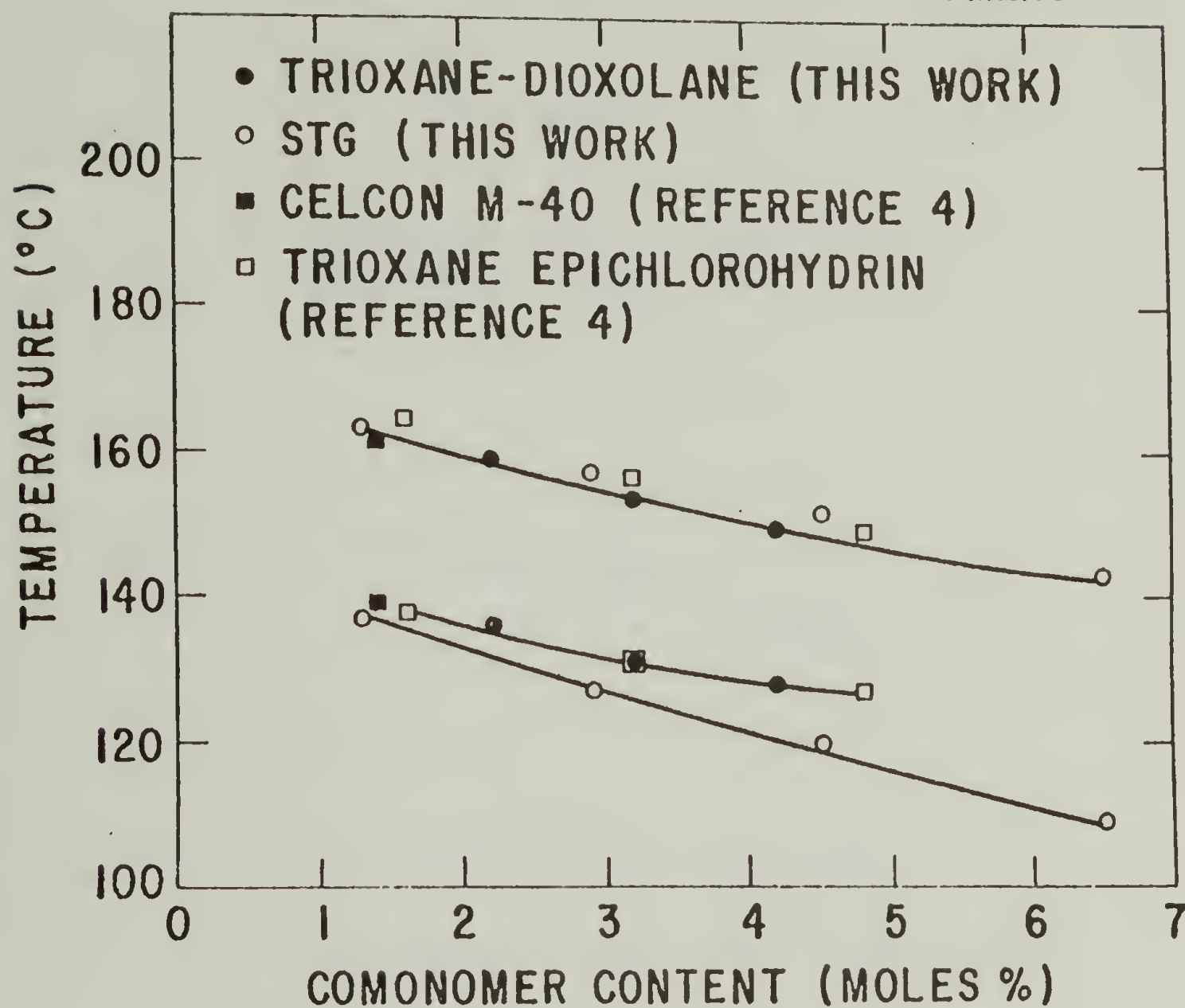


FIGURE 14

# ONSET OF CRYSTALLIZATION IN IONIC AND NON-IONIC COPOLYMERS

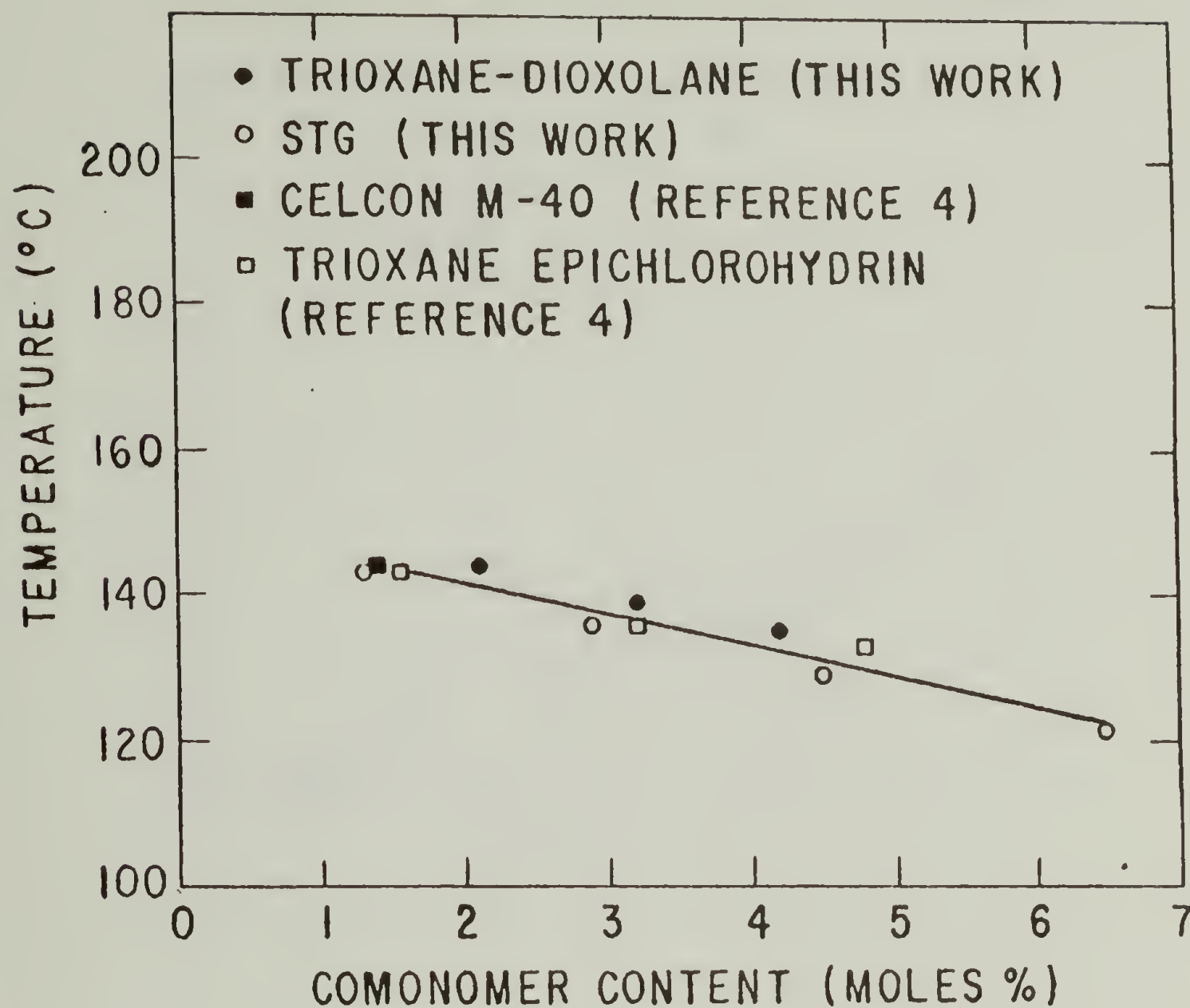


FIGURE 15

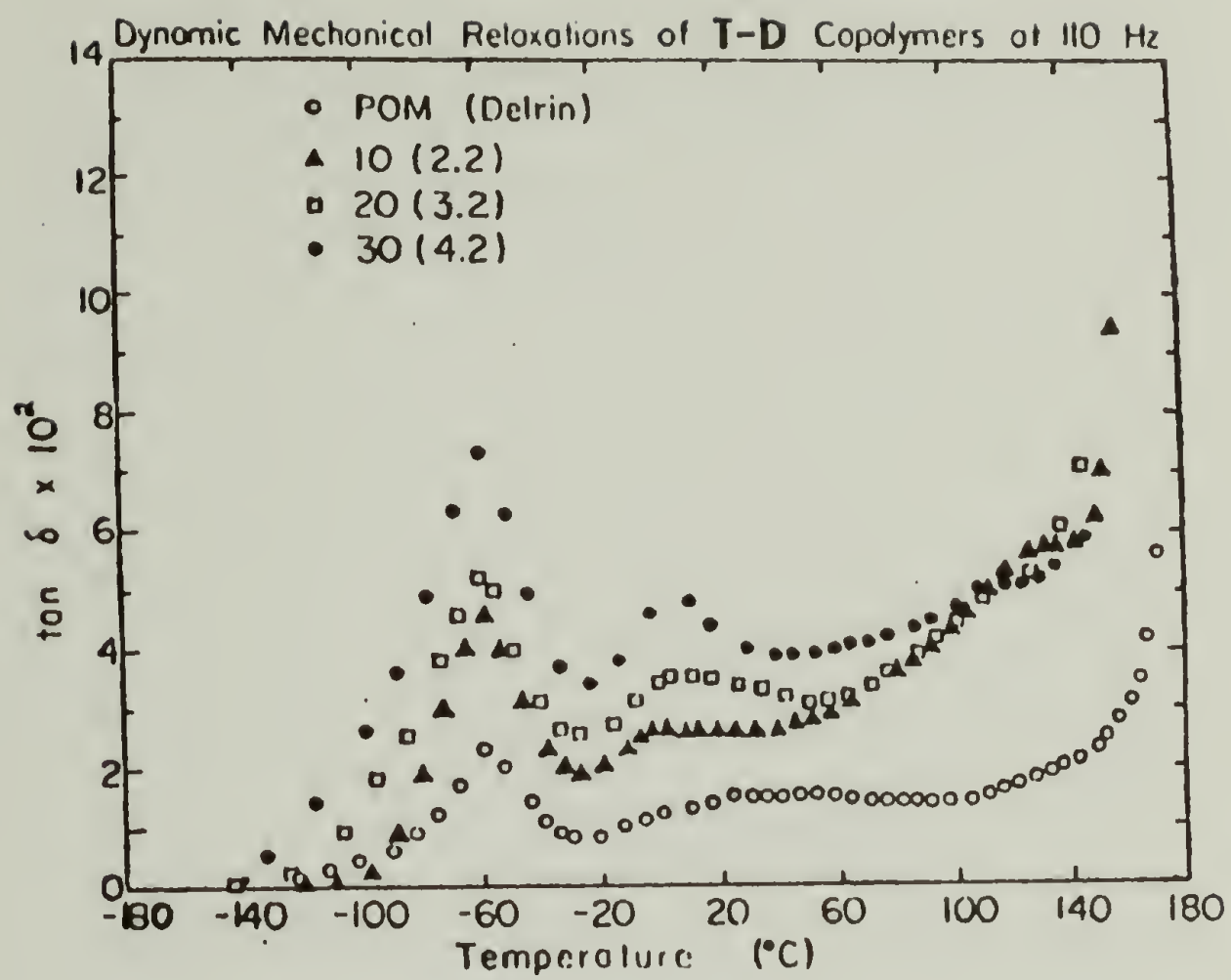


FIGURE 16



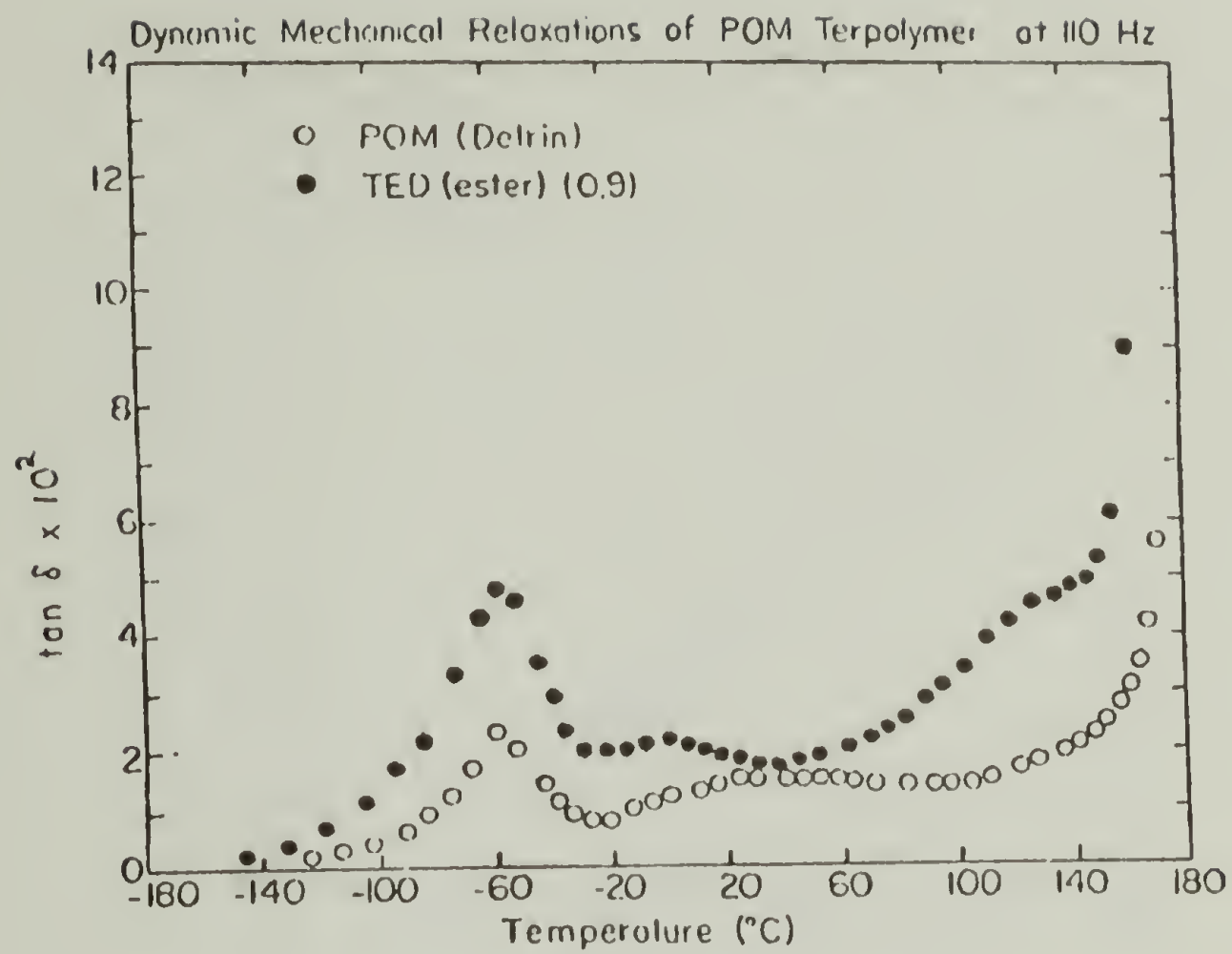


FIGURE 17

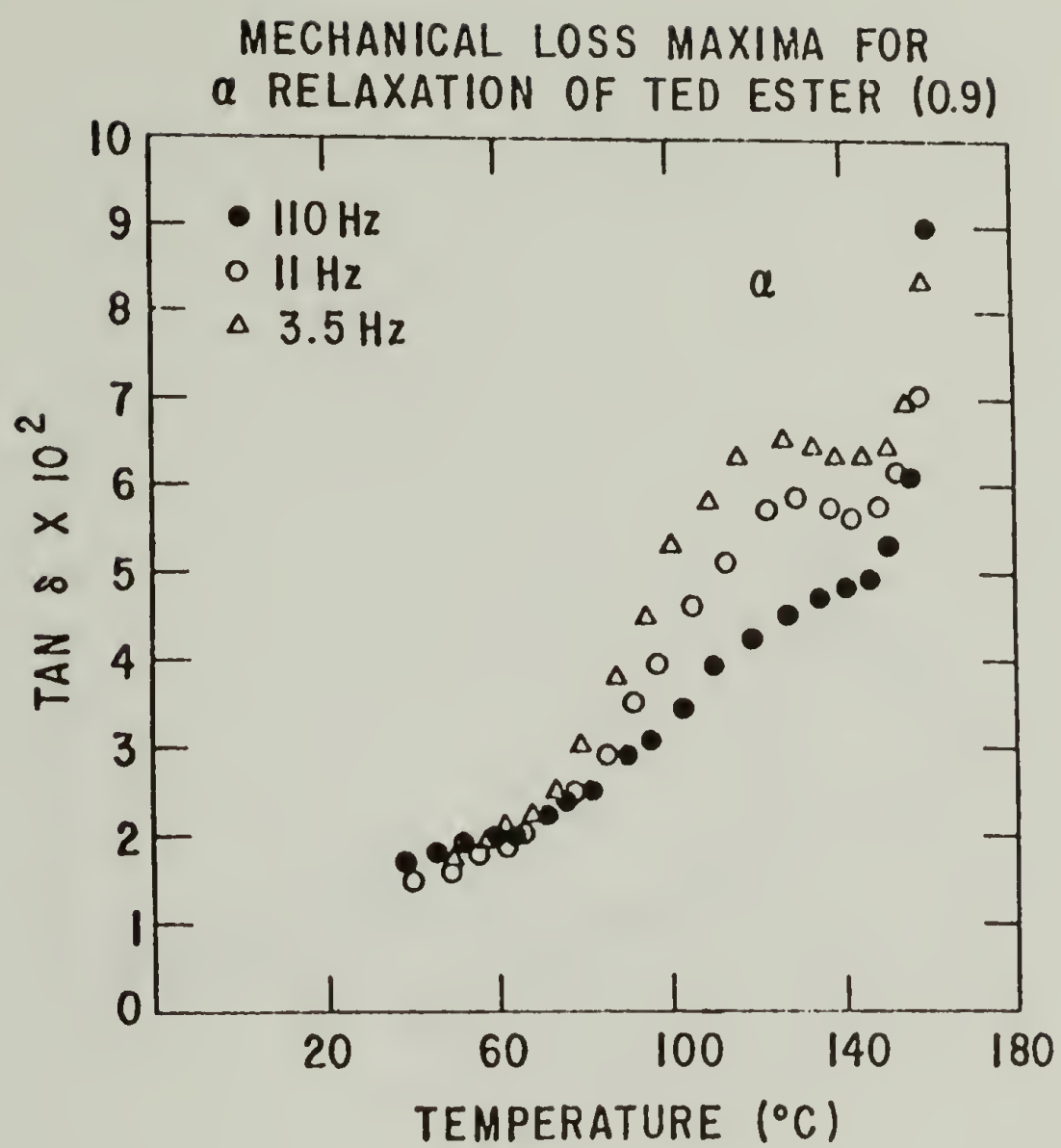


FIGURE 18

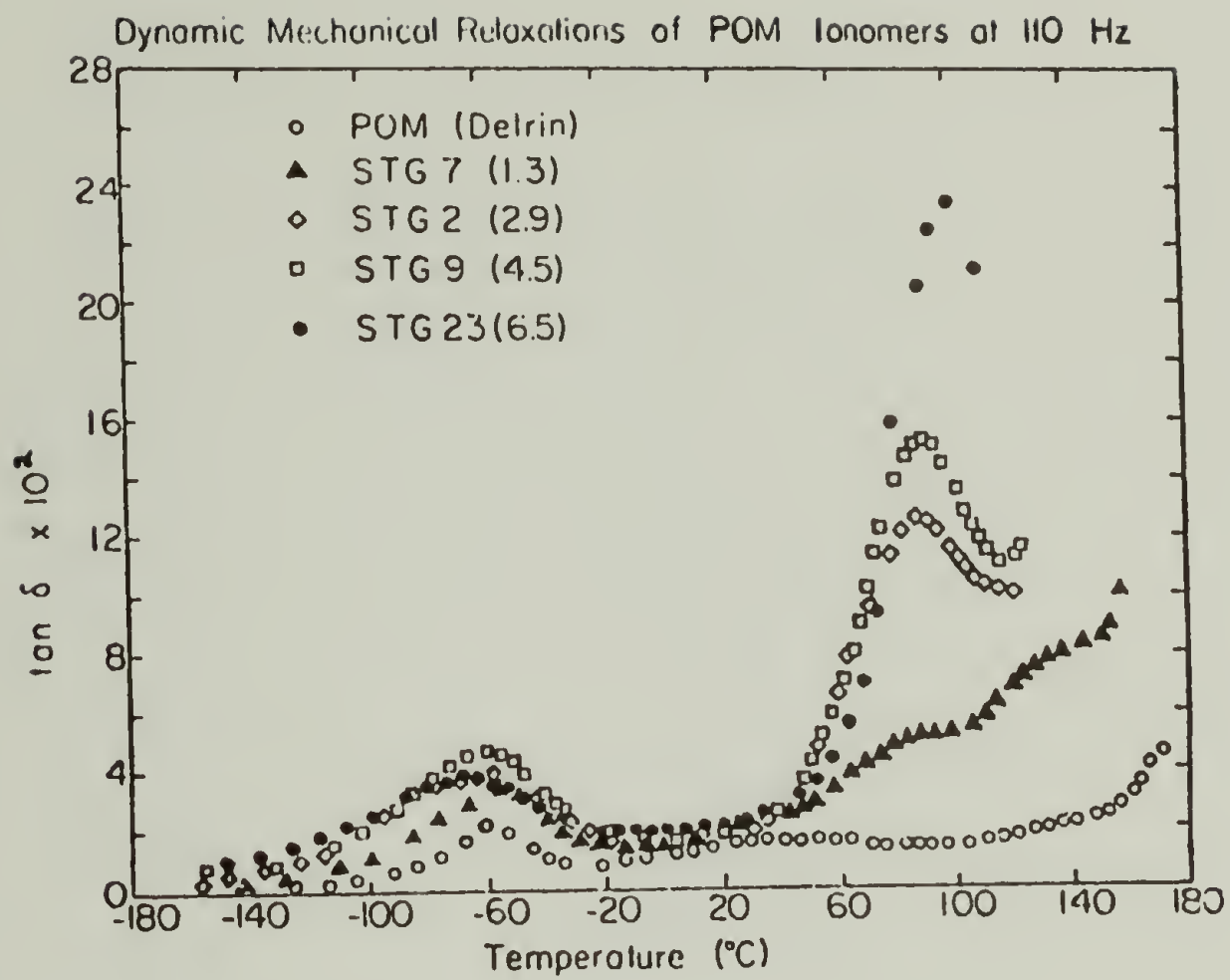


FIGURE 19

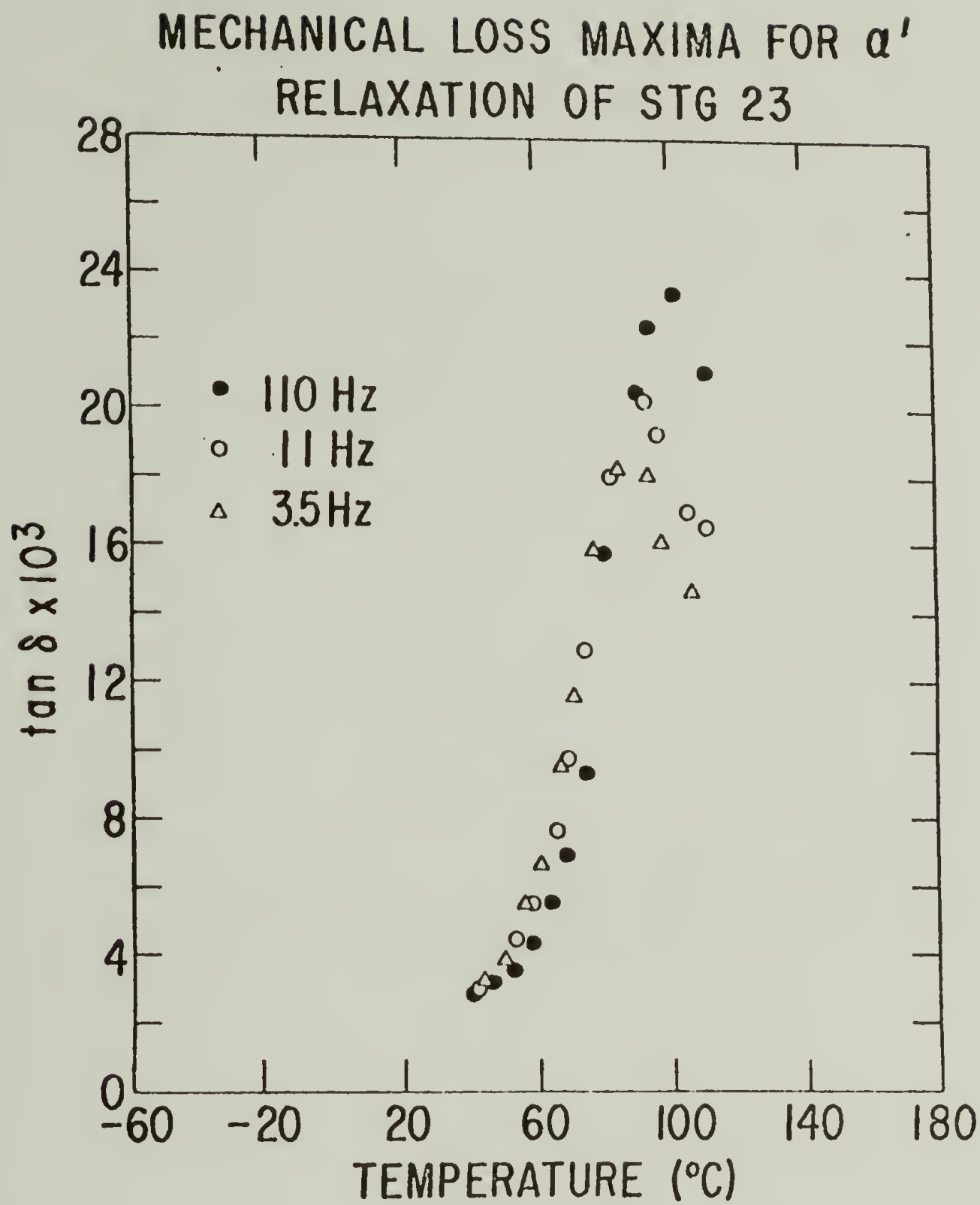


FIGURE 20



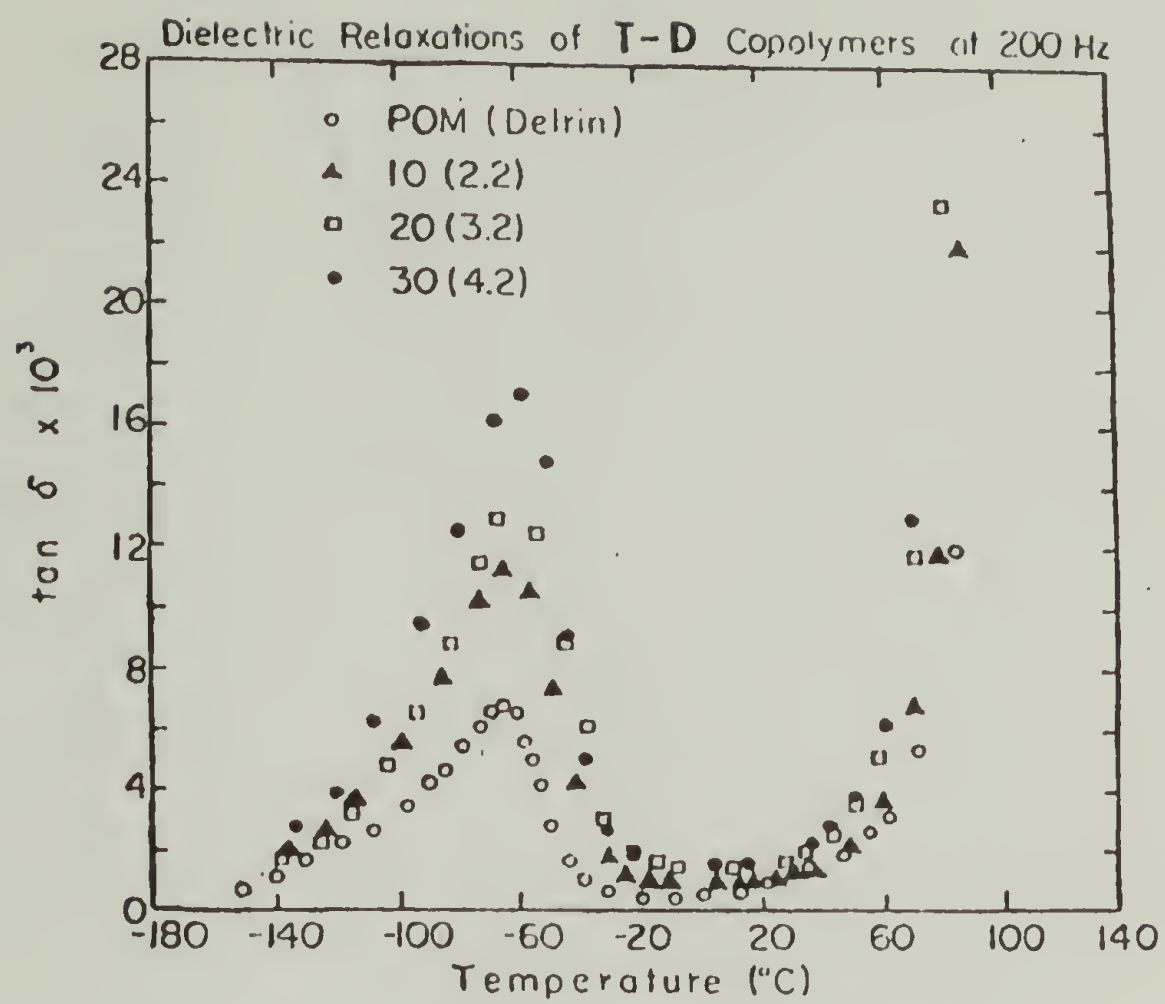


FIGURE 21

# DIELECTRIC LOSS MAXIMA FOR $\gamma$ RELAXATION OF OXYMETHYLENE POLYMERS

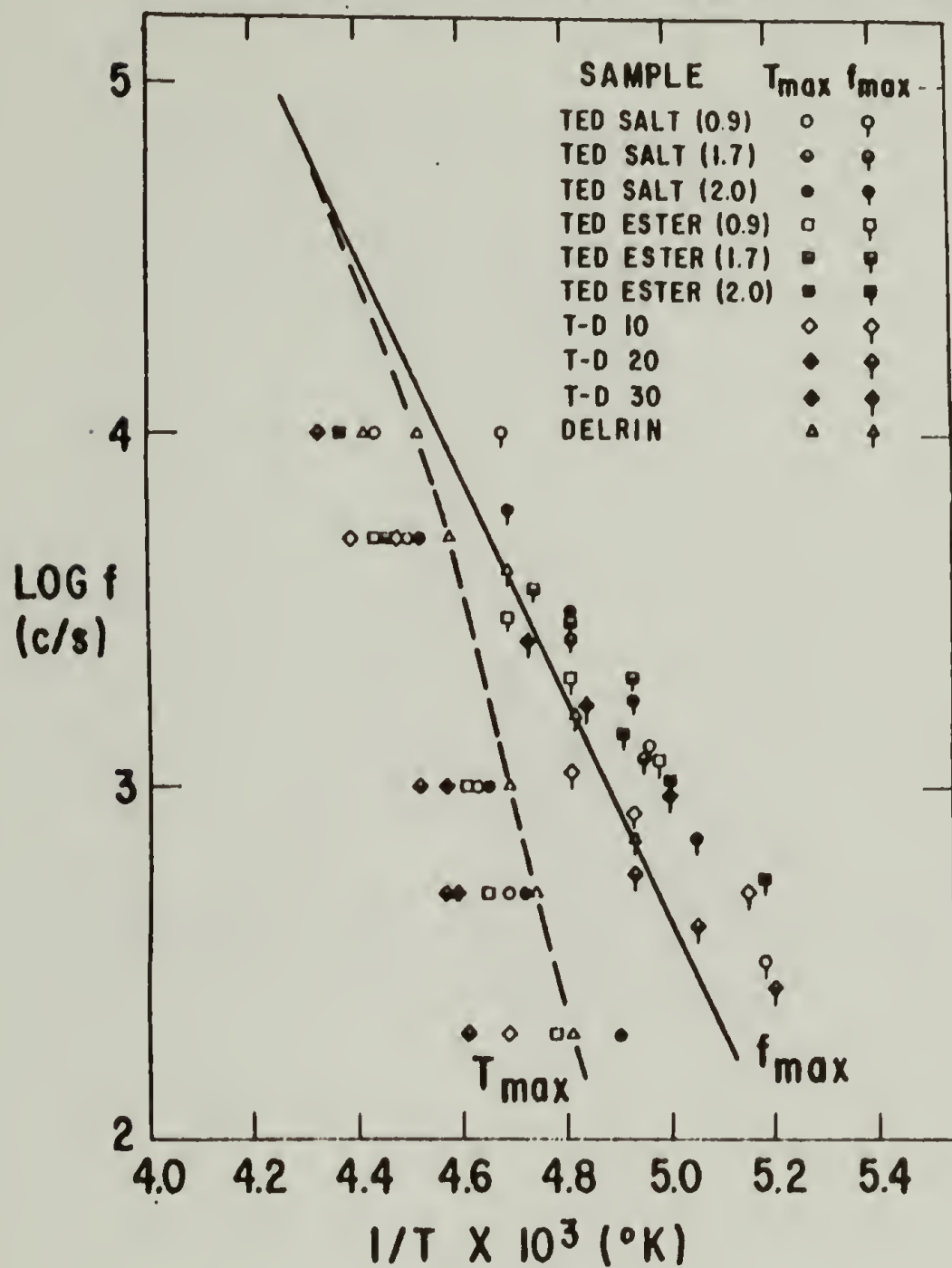


FIGURE 22

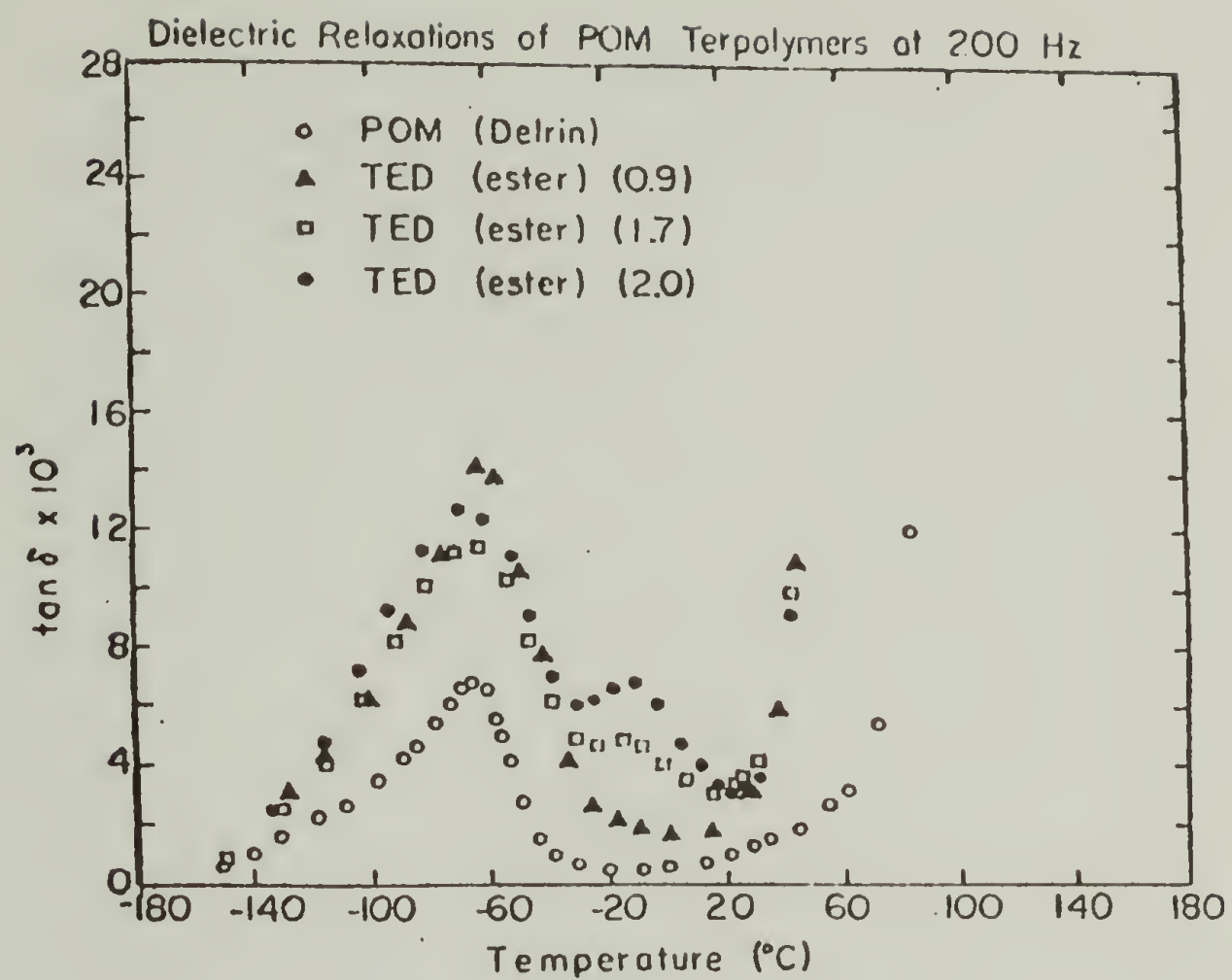


FIGURE 23

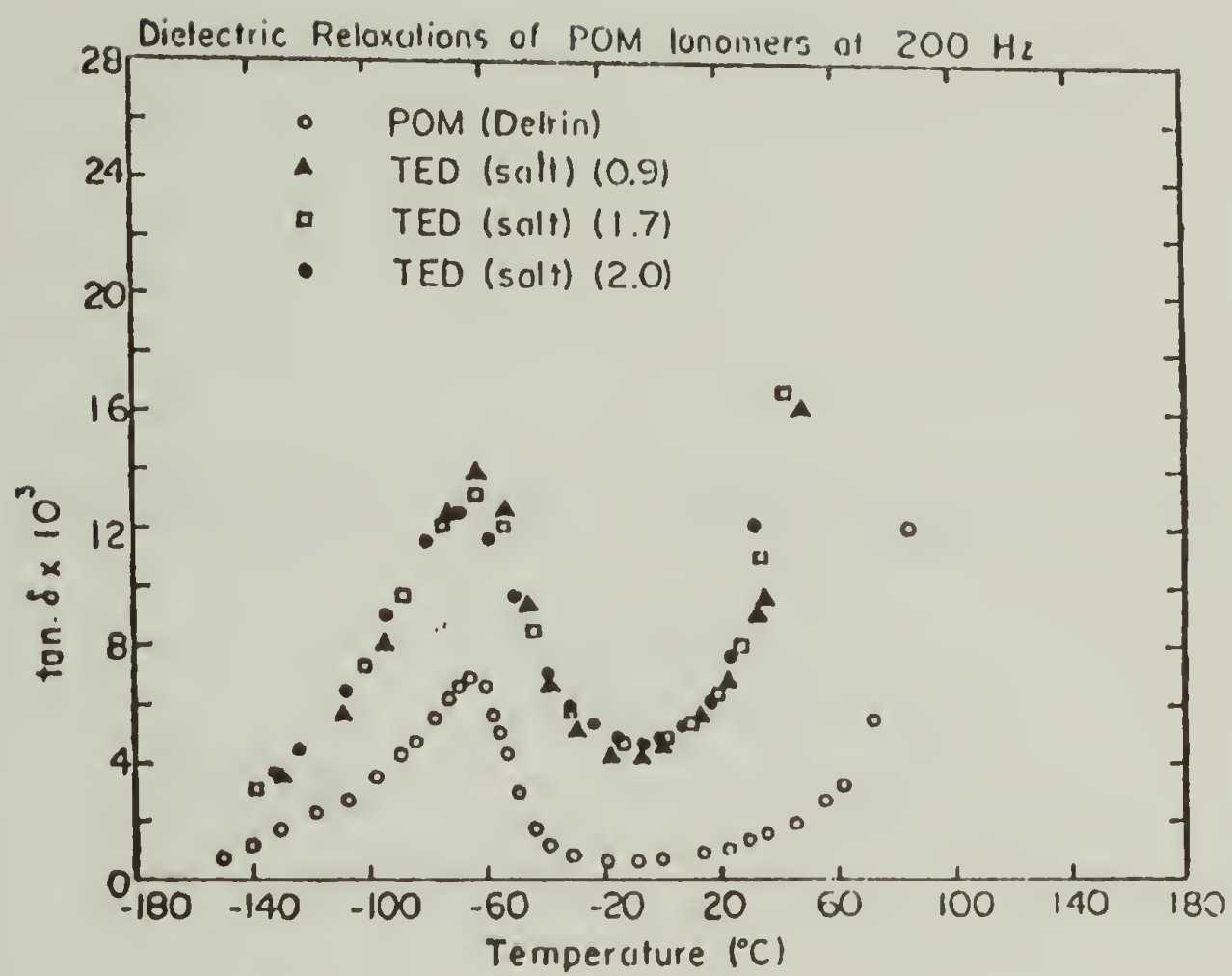
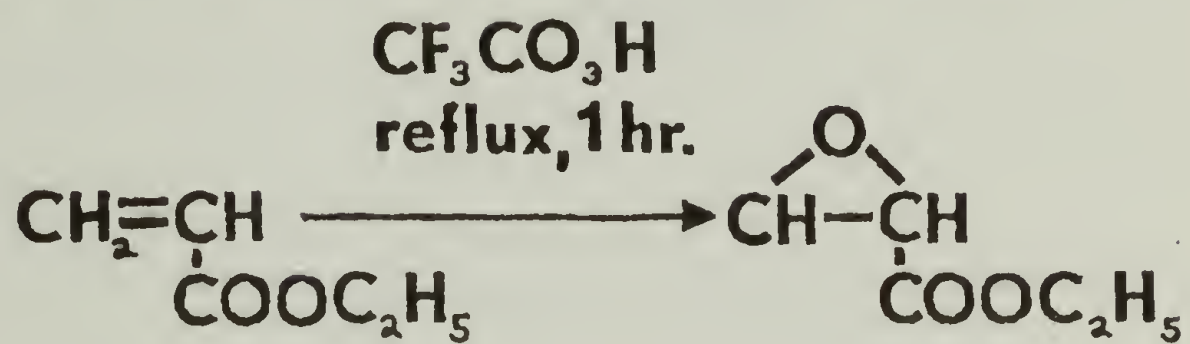


FIGURE 24

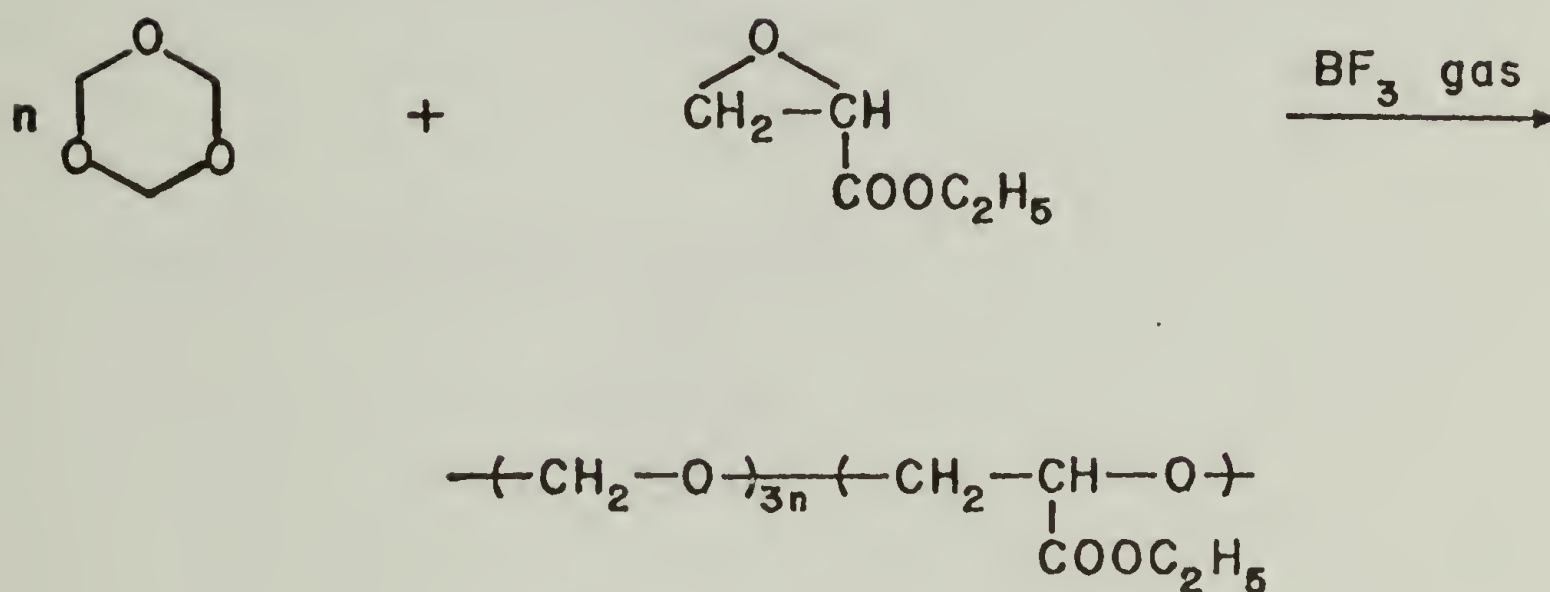


## SYNTHESIS OF ETHYL GLYCIDATE



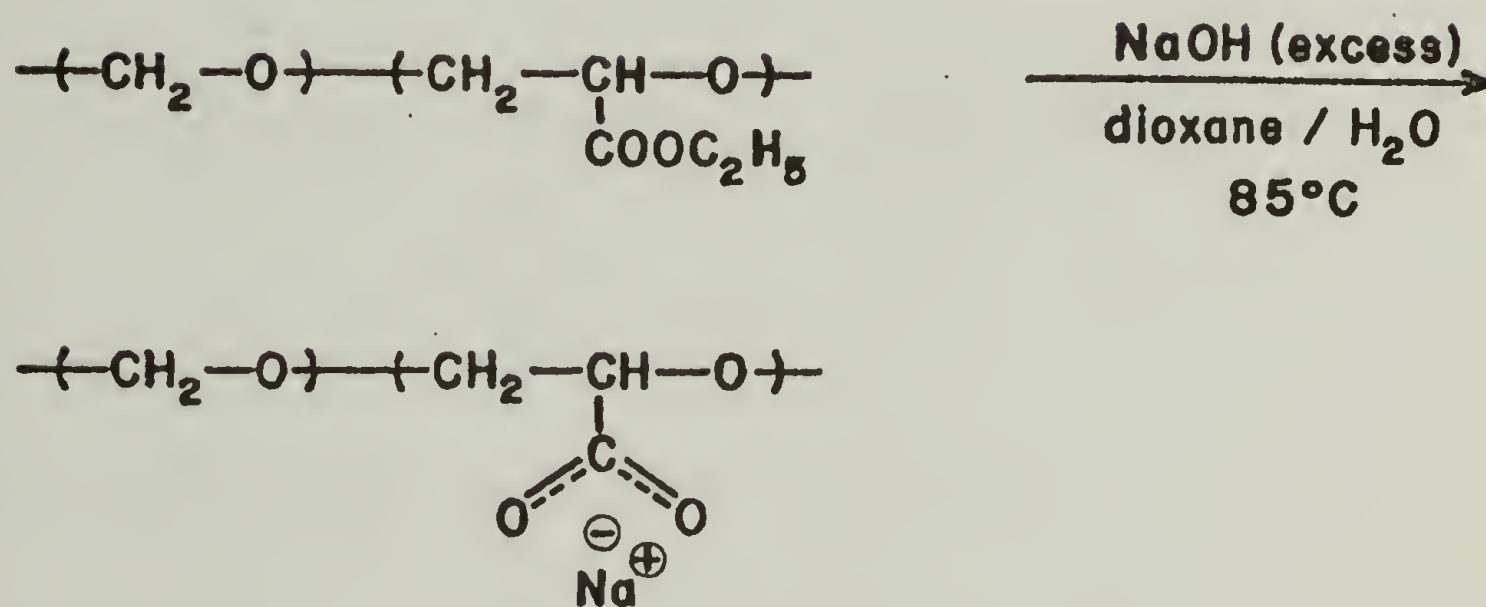
EQUATION 1

# VAPOR PHASE COPOLYMERIZATION OF TRIOXANE WITH ETHYL GLYCIDATE



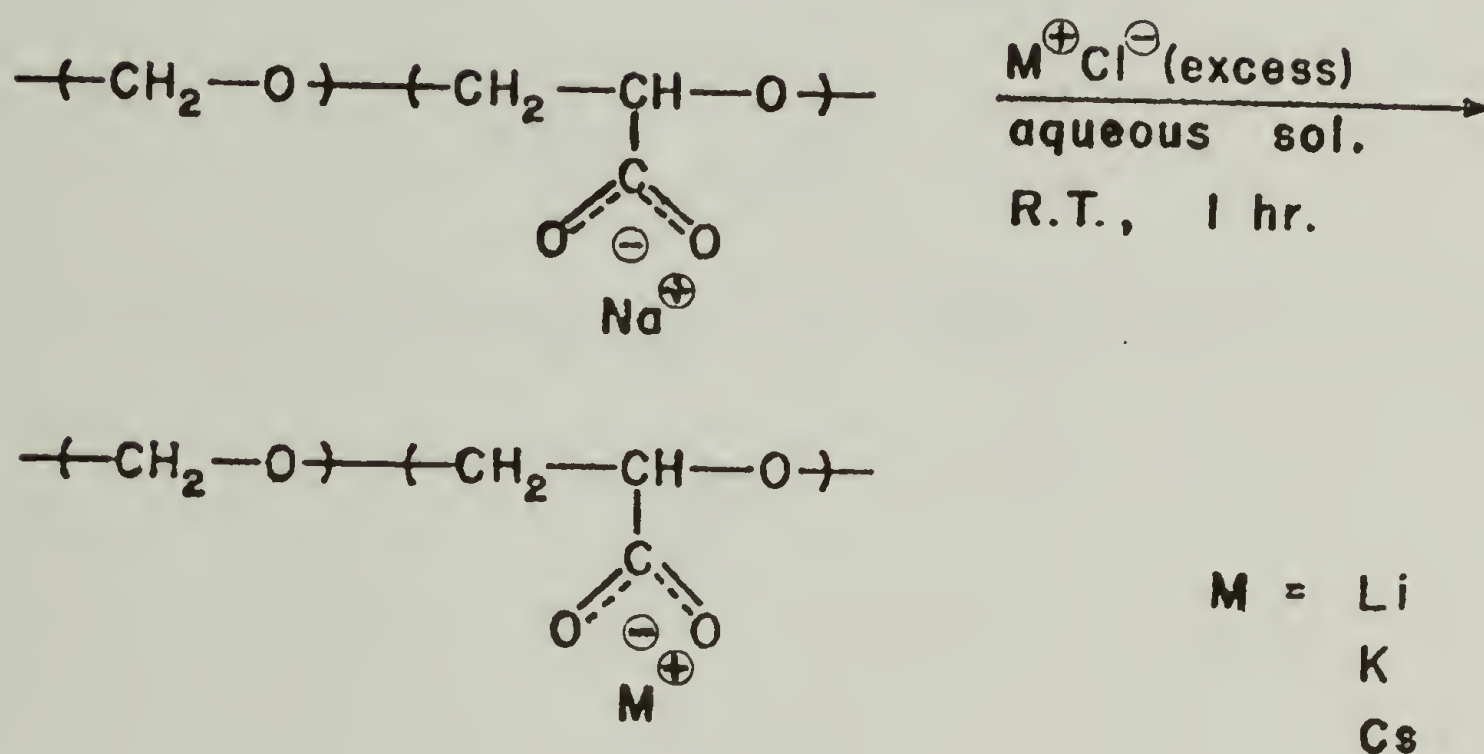
EQUATION 2

# HYDROLYSIS OF POLYMERIC ESTER TO Na SALT



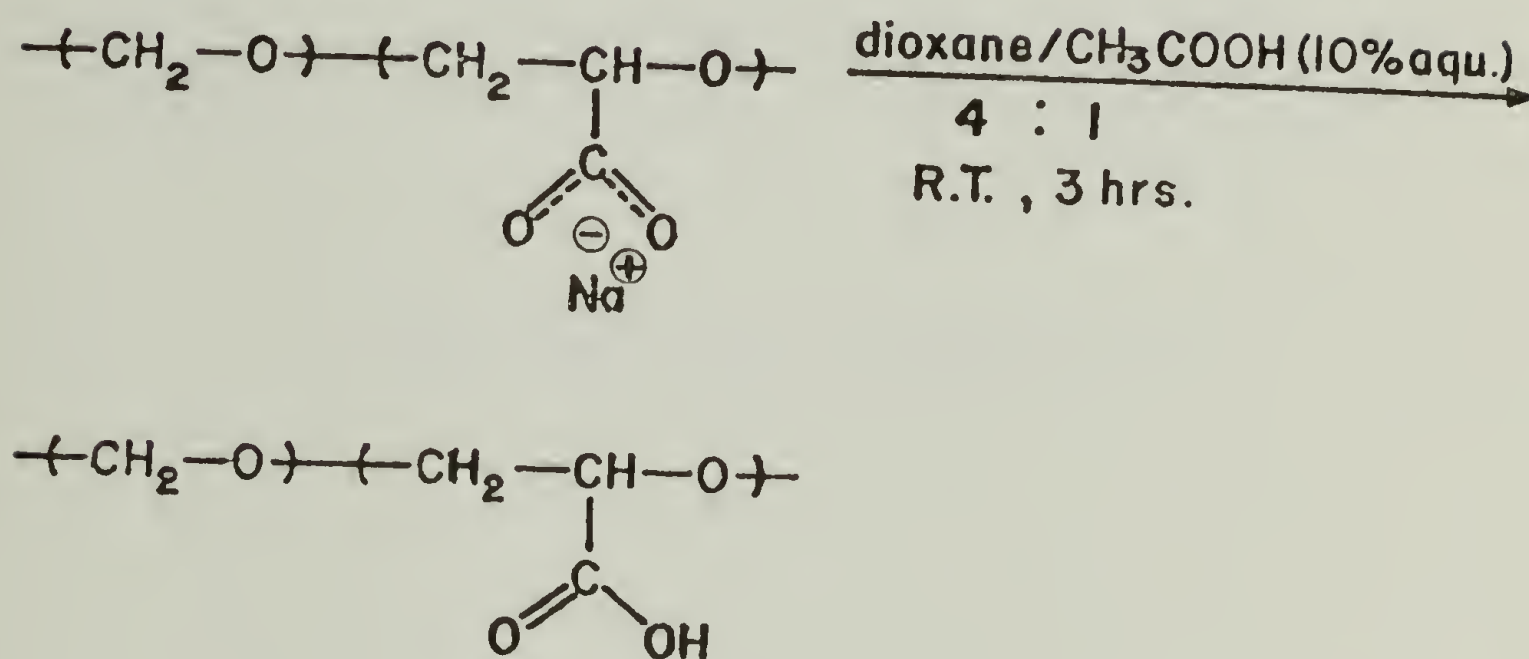
EQUATION 3

# EXCHANGE OF ALKALI METAL CATIONS



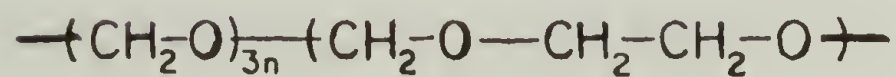
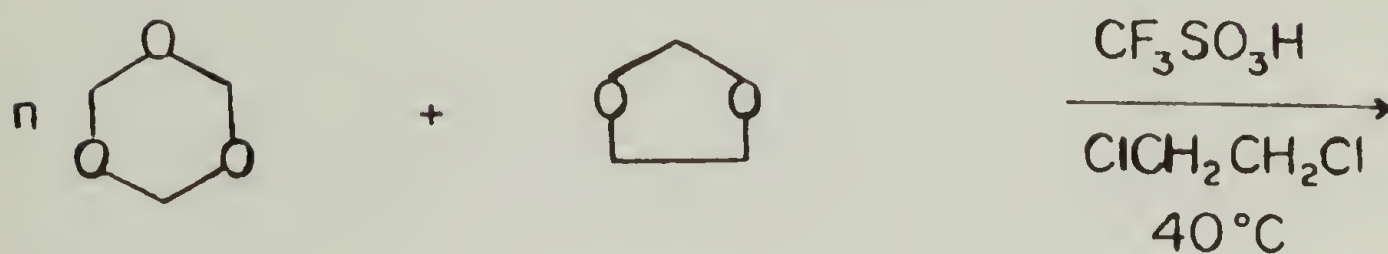


CONVERSION OF POLYMERIC SALT  
TO FREE ACID



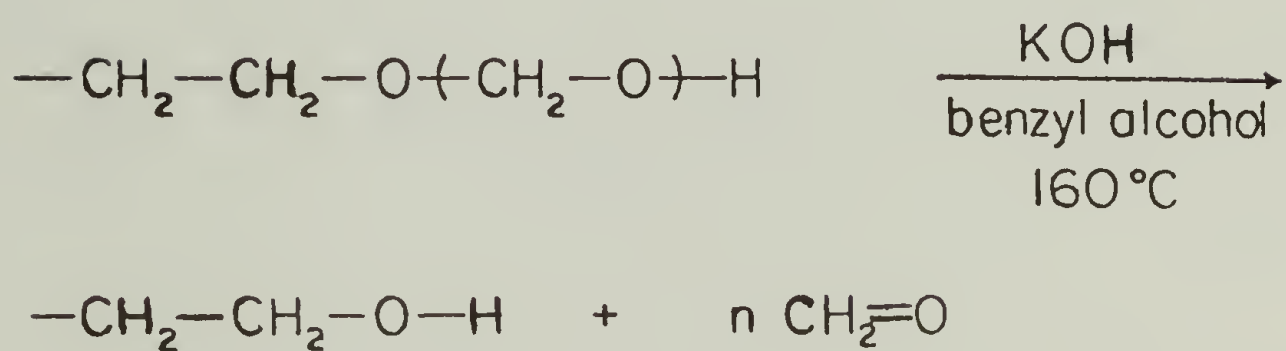
EQUATION 5

SOLUTION COPOLYMERIZATION OF  
TRIOXANE WITH DIOXOLANE



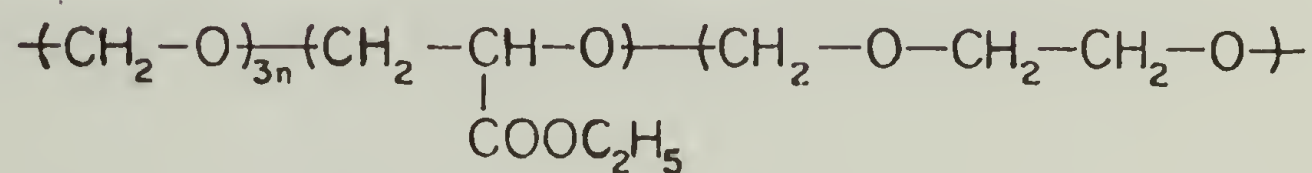
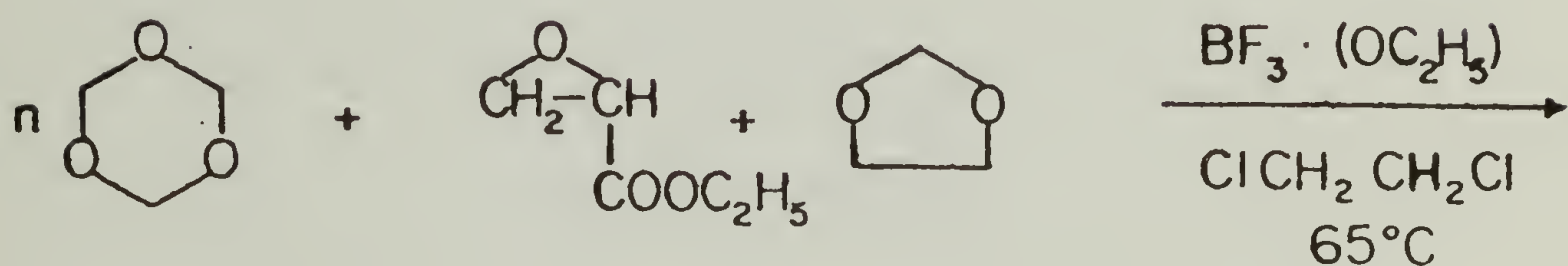
EQUATION 6

BASE STABILIZATION OF  
TRIOXANE-DIOXOLANE COPOLYMERS



EQUATION 7

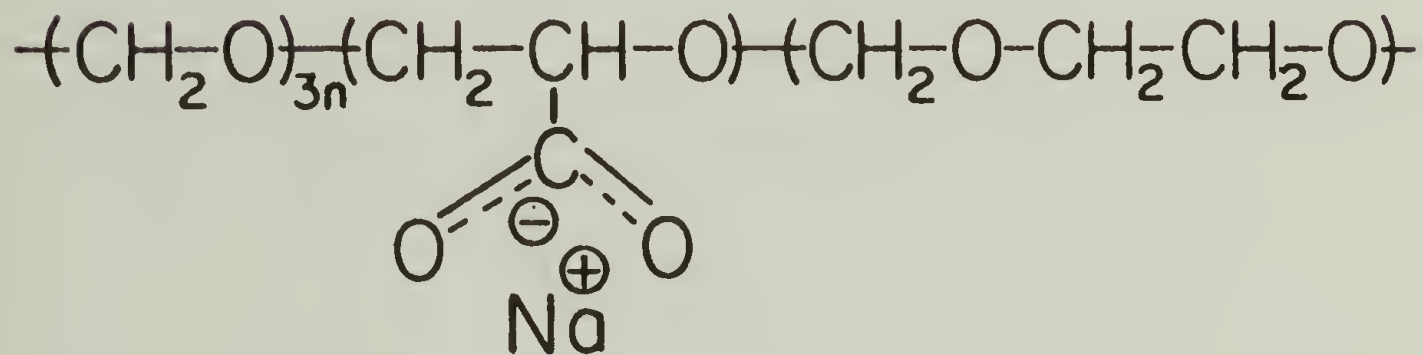
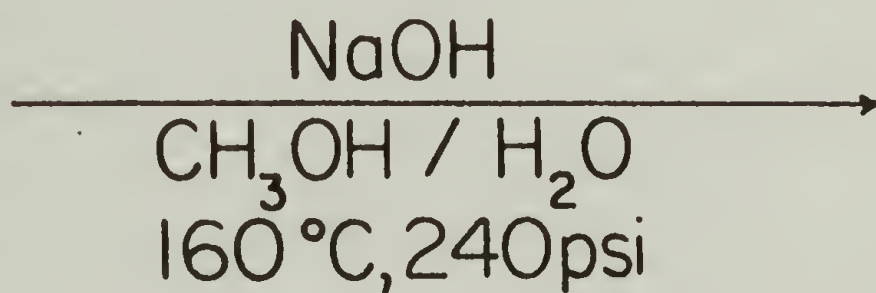
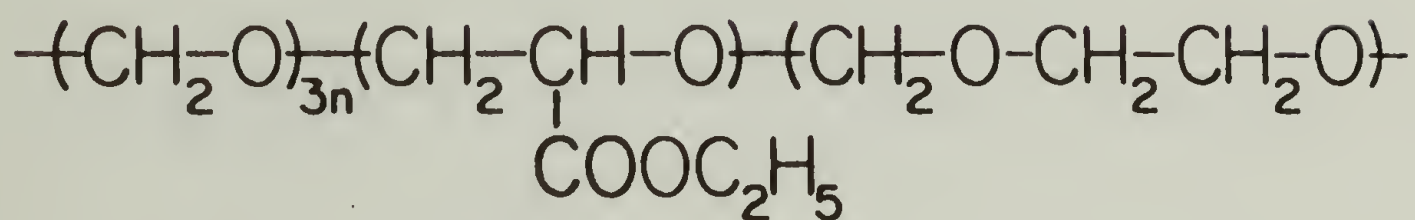
SOLUTION POLYMERIZATION OF TRIOXANE  
WITH ETHYL GLYCIDATE AND DIOXOLANE



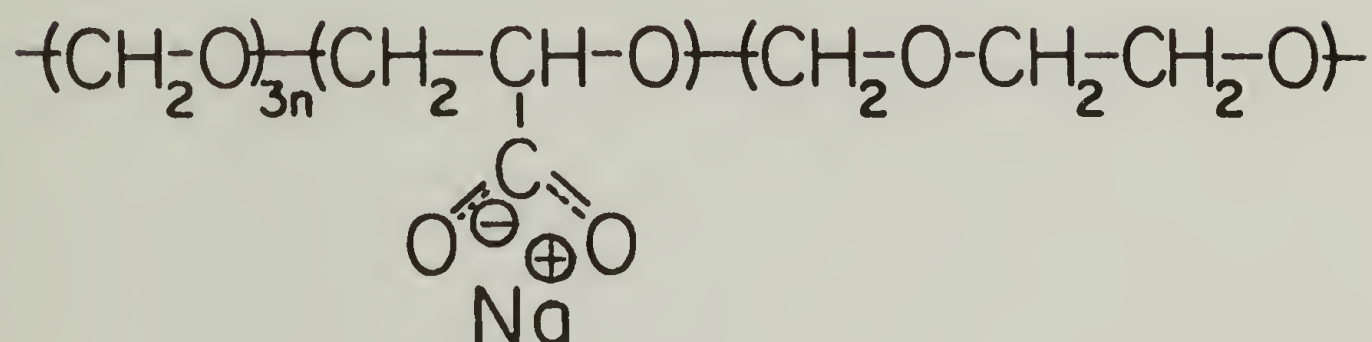
EQUATION 8



# HYDROLYSIS OF POLYMERIC ESTER TO Na SALT



# CONVERSION OF POLYMERIC SALT TO FREE ACID



(10% aqu.)  
dioxane/CH<sub>3</sub>COOH 4/1

Room Temperature, 3 hrs.

